THE UNIVERSITY OF MANITOBA

THERMODYNAMIC INVESTIGATIONS ON MOLTEN SALT MIXTURES:

THE SYSTEM $LiClO_3$-$LiNO_3$

A THESIS PRESENTED TO THE
FACULTY OF GRADUATE STUDY AND RESEARCH
UNIVERSITY OF MANITOBA,
IN PARTIAL FULFILMENT OF THE REQUIREMENTS
FOR THE DEGREE OF DOCTOR OF PHILOSOPHY

By

MADUKKARAI KRISHNA NAGARAJAN

Winnipeg, Manitoba

August 1963

TO MY BELOVED PARENTS

ACKNOWLEDGEMENTS

ABSTRACT

Salts with unsymmetrical complex anions are generally low melting and are known to give rise to strongly covalent melts. Such melts provide an interesting basis for a thermodynamic study of their nature and constitution. Because of its abnormally low melting point (127.9°C), lithium chlorate was chosen for such a study. Densities and relative viscosities of pure molten lithium chlorate were determined by methods capable of high precision. The molar volume and viscosity changes with temperature were interpreted with a view to obtain useful information on the lithium chlorate melt. Heat of fusion and molar heat capacities of solid and liquid lithium nitrate were determined by suitable calorimetric techniques. The heat of transition α LiCLO$_3$ - β LiCLO$_3$, which occurs at 99.1°C, was determined as the difference between the heats of solution of the two forms of lithium chlorate. The thermal data proved very useful in understanding the structural changes taking place during the process of fusion.

A study of thermodynamic properties of mixtures, generally, provides information on the constitution of the pure components and on any possible interaction between the constituents of the mixtures. Densities and relative viscosities of mixtures of lithium chlorate and lithium nitrate were, therefore, determined. From the dependence of these properties on temperature and composition, the structural entities present

in the melts and interactions between the constituents, were postulated. Heats of fusion and molar heat capacities of mixtures of lithium chlorate and lithium nitrate provided additional support for the model of molten lithium nitrate deduced from volume and viscosity data. Derived quantities such as, enthalpies, free energies and entropies of mixing, provided a suitable basis for the interpretation of the different data obtained for the system lithium chlorate-lithium nitrate.

TABLE OF CONTENTS

TABLE OF SYMBOLS

α	Coefficient of thermal expansion
β	Compressibility
γ	Activity coefficient
ρ	Density
Λ	Equivalent conductance
η	Viscosity
η_g	'Geometric contribution' to change in viscosity
η_s	'Structural contribution' to change in viscosity
ω	Lattice interaction energy
a	Activity
C_p	Molar heat capacity
d	Distance between centres of two neighbouring ions
E	Potential
E_{vis}	Activation energy for viscous flow
E_Λ	Activation energy for electrical conductance
$\Delta \overline{F}_1$	Partial molar free energy of component 1
ΔF^M	Free energy of mixing
$\Delta \overline{H}_1$	Partial molar enthalpy of component 1
ΔH^M	Heat of mixing
ΔH_f	Heat of fusion
ΔH_{trans}	Heat of transition
ΔH_{soln}	Heat of solution
h	Amount of heat evoled

I	Current
m	Mass
M	Molecular weight
n	Mole fraction
R	Gas constant
r_+ , r_-	Ionic radii of cation and anion respectively
s	Specific heat
ΔS	Entropy change
$\overline{\Delta S_1}$	Partial molar entropy of component 1
ΔS^M	Entropy of mixing
ΔS_f	Entropy of fusion
ΔS_{trans}	Entropy of transition
T	Temperature in Absolute scale
T_f	Freezing point
V	Molar volume
V_g	'Geometric contribution' to change in molar volume
V_s	'Structural contribution' to change in molar volume

LIST OF TABLES

LIST OF FIGURES

Chapter I

GENERAL AND THEORETICAL INTRODUCTION

Early interest in the field of molten salts was, for the most part, restricted to the study of their physical properties. The field has been the subject of reviews by Lorenz[1], Goodwin and Mailey[2], Drossbach[3] and Antipin[4]. The interest in the field of molten salts has grown simultaneously with the advance of high temperature technology, especially with their application in the metallurgical processing[5] of aluminium, magnesium, sodium, titanium, zirconium, niobium, tantulum, cerium, uranium and thorium. Molten salts are among the largest known class of non-aqueous inorganic solvents and give rise to systems which are liquid upto $3000^{\circ}C$, with electrical conductivities ranging from zero to 500 times that of aqueous electrolytes and viscosities from less than 0.1 cp to 10^5 poise. Their thermal stability, inertness towards nuclear radiation, excellent solvent, conducting and heat transfer properties and usually low viscosities and vapour pressures, have led to their application in the atomic energy industry as fuel solvents and heat transfer media and in the recovery of spent fuels. They are also finding increased uses as reagents and solvents in synthetic inorganic chemistry. The thermoelectric properties of some molten salts suggest their future use in fuel cells for the generation of electric power. Current interest in this field has largely been stimulated by the needs of high temperature technology.

Ionic nature of molten salts: The values of some typical
physical properties of molten salts are of the same order
of magnitude as those of conventional non-polar liquids,
in spite of the wide disparity between the temperature
regions in which the above two classes of liquids exist.
The essential difference between molten salts and other
non-polar liquids is that the former are made up of at
least two oppositely charged ions, simple or complex, in
close proximity to one another. Again, unlike systems of
aqueous electrolytes, there is no solvent in the molten
salt systems to make the charge on the ion more diffuse.
The fact that Faraday's laws[6] of electrolysis are obeyed
quantitatively by molten salts makes it very probable
that such melts are, at least partially, ionised. In fact,
melts with different stages of dissociation, from ionic to
covalent types, are possible.

Free volume: It is probable that in molten salts, there
will be a tendency for the constituent ions to group
themselves so as to surround the cations by anions and vice-
versa, the ions of like sign arranging themselves as far
away as possible from each other. This results in an open
structure for molten salts which is much more marked than in
other classes of liquids. This is in agreement with the
observation that the increase of volume on melting is con-
siderably greater for solid salts than for that of other

classes of solids. (cf. Table A1, Appendix). Furthermore,
it is observed that the coordination numbers[7,8] and the
interionic distances[9,10] between ions of like sign,
decrease on melting. Levy et al[11] showed that, in general,
the average distances between ions of like sign are greater
in the liquid than in the solid, whereas those between ions
of unlike signs are less in the liquid than in the solid.
The increase in volume on melting and also the changes in
the average interionic distances, lead to the introduction
of the concept of empty space or free volume in the melt.

Theories of liquid state: Most of the vast literature on
the theories of liquid state is based on an attempted
explanation of the thermal, mechanical, transport and other
properties of liquids. Almost all of the theories are
attempts to adapt known structures of gaseous and crys-
talline matter, to the intermediate state of the liquid.
Liquids, not far above their freezing points, are generally
recognized as possessing short-range order as in the
crystalline state, but lacking in the long-range order. It
has been found, from x-ray diffraction studies on liquids[7-10],
that surrounding each reference ion there is a shell of
three to eleven other ions at much the same distance as in
the solid. Beyond this first coordination shell, the
ordering of the structure diminishes rapidly, although a

semblance of order is noticed in the second and the third
coordination shells. It may seem at first that the
representation of a liquid by a rigid lattice is grossly
in error, since the long-range Coulombic forces might be
expected to change radically from the solid to the liquid
state and vary greatly from one liquid to the other. It
is observed, however, that the heats of fusion of the salts
are not very large compared to the over-all lattice energy
(generally 3-5%). This must mean therefore that the largest
contribution to the over-all lattice energy, viz. Coulombic
energy, does not alter much on fusion, inspite of the large
decrease in the long-range order.

The ''Cell'' theory: The ''cell'' theory of the liquid
state, first put forward by Lennard-Jones and Devonshire[12],
is based on a model of the liquid in which a regular
lattice structure of ''cells'', each containing one particle,
is assumed. The particle located in the cell is assumed to
possess a greater freedom of movement, than in the solid,
within the boundaries imposed by its neighbours. Recent
rigorous analyses[13] of the Lennard Jones-Devonshire model
have considered configurations which allow multiple
occupancy of cells. The ''Cell'' or ''Cage'' model[14] for
liquids is essentially derived from an alloy type structure
of atomic or molecular structural units (''cells'') and

FIG·I CELL MODEL OF LIQUID STATE·
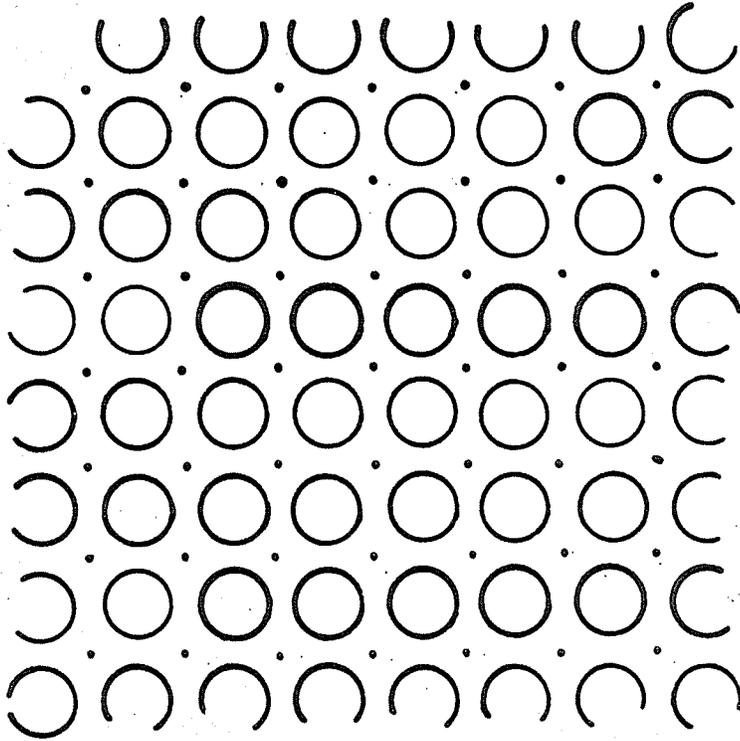
(a)
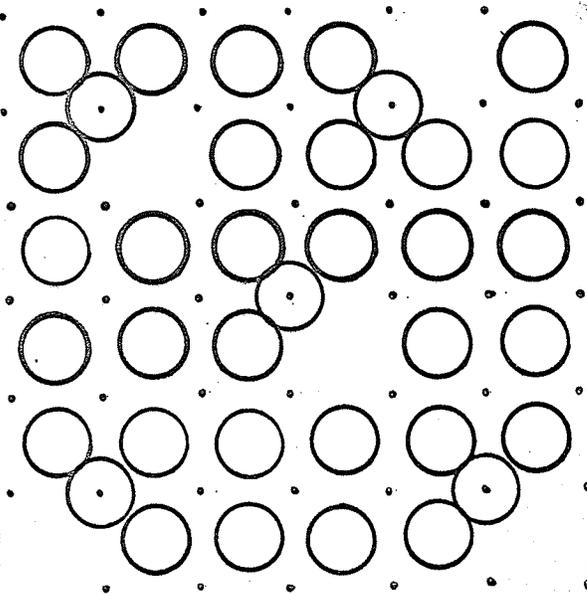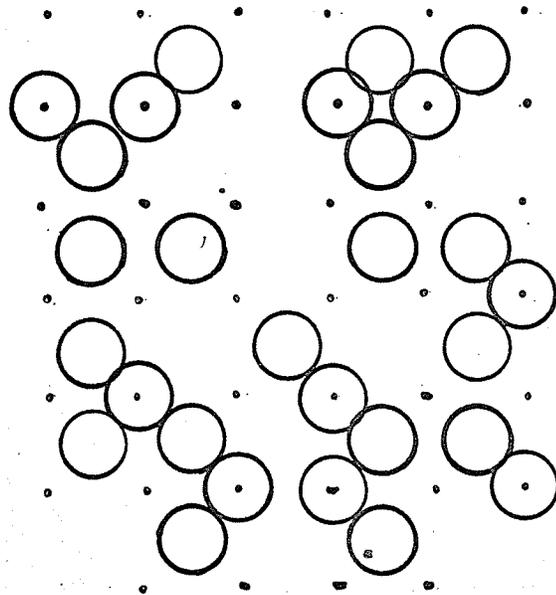
(b)   (c)

lattice defects and is schematically illustrated in Fig.1.
Fig. 1(a) shows a two dimensional array for one kind of
atoms only (''argon model''), at low temperatures. The
particles occupy all the available sites in a perfect
lattice and the lattice defects (shown as dots) occupy all
the available sites in a similar lattice interpenetrating
the first. During the process of fusion, local regions of
disorder interrupt the long-range order in the lattice.
This is shown in Fig. 1(b). The liquid state, represented
in Fig. 1(c), has local regions (''clusters'') of relatively
high order but has no long-range order. Unlike the solid
state, the particles are not localized in the ''clusters'',
but are assumed to interchange places continually. There-
fore, the particles can share the entire available volume
of the liquid. An interchange of a particle and a lattice
defect results in the migration of the former. The energy
for this process is a function of the whole volume.

It can be seen that the cell or cage model
requires a central particle to be surrounded by its neighbours,
''smeared'' over the surface of the spherical shell. In
molten salts, these conditions for the applicability of
L-JD theory are amply met, since it has been shown by
Stillinger, Kirkwood and Wojtowicz[15] that a given ion is
surrounded by concentric shells of alternating charge. In
so far as the application of the ''smeared-on the average''

concept is concerned, the cell model bears resemblance to the familiar Debye-Huckel theory[16] for aqueous electrolytes. The method of Stillinger et al[15] consists in the application of the theory of distribution functions to the molten state, on the basis of the cell model. An attempt[17] to apply the L-JD theory directly to fused salt systems, with an extension to include neighbours farther than the first has recently been made. Other workers[18] have set up the partition functions for the fused salt systems starting from the application of the Lennard Jones-Devonshire theory to such systems. One of the main drawbacks to the lattice theories is the restriction of rigidity i.e. of assigning fixed lattice sites to the ions. The explanation of entropy and volume effects on the basis of lattice theories, is therefore not very satisfactory.

The ''Hole'' theory: A ''hole'' model for the liquid state, proposed by Eyring[19], relaxed the restriction of the number of cells equal to the number of particles (as in cell theories) but maintained the restriction of single occupancy as a maximum. According to Eyring, the liquid state is composed of an equilibrium mixture of singly occupied cells and unoccupied cells (''holes'') in a regular lattice structure. Frenkel[20], Altar[21] and Furth[22] pictured the liquid to be a quasi-crystalline structure consisting of a

binary mixture of ions, each behaving as a linear harmonic oscillator, and ''holes'', distributed randomly in the lattice. The positions and the sizes of holes vary with the random fluctuations in the liquid due to thermal motion. The total volume of the holes is roughly equal to the volume increase on melting. The compressibility measurements of Bockris and Richards[23] showed the free volume or the ''fluctuation'' volume per mole to be about 2 percent of the molar volume. According to an ideal cell model, the increase in volume on melting (sometimes as much as 25%) could only be explained on the basis of 6-7 percent increase in the inter-ionic distances in the liquids. But as shown by Levy et al (loc. cit) there is actually a slight decrease in the average inter-ionic distances. This fact has been pointed out to be one of the strongest supports for the presence of holes in a liquid. Using the theory of Furth[22], Bockris and Richards[24] have further extended the scope of the hole theory, by advancing satisfactory equations for the volume of a hole, the mean number of holes and the energy of formation of a hole.

The hole theory has had much success[25] in explaining the transport properties, such as diffusion and electrical conductance, in melts. Employing the equations of statistical mechanics[13], many workers[26] have derived several approximations for the partition function of a

system. Mayer and coworkers[27] developed an independent
hole model and arrived at the partition functions for
melts. An extension, based on classical statistical
mechanics, of the hole theory to include the effect of all
configurations of particles and holes on the partition
function, has been given by Blomgren[28]. From an x-ray
diffraction study of molten alkali halides, Zarzycki[29]
arrives at a ''lacunar'' structure for molten halides and
makes an interesting suggestion that the holes are actually
''fluctuating cracks'' between ionic clusters grouping
1 - 2 ionic shells around a central ion.

Eyring's Theory of Significant structures: Eyring, Lee,
and Hirai[30] developed a method of significant structures
for the liquid state which consists in setting up the
individual partition functions for each one of the signi-
ficant structures. The partition function for the whole
system is then given as the product of the individual
partition functions. They recognize three significant
structures in the liquid state involving different types
of degrees of freedom:

1) Molecules with solid-like degrees of freedom, which
are bonded and restrained to an equilibrium position;

2) The degrees of freedom arising out of the possible
positional degeneracy due to the presence of dislocations

in the liquid;

3) Molecules which have escaped from fitting into the potential well formed by their neighbours, thus exhibiting gas-like degrees of freedom. A partition function for fused salts has been put forward[31], which is the product of all the individual partition functions and contains at least two parameters to be fitted to the experimental data. The general approach consists in the evaluation of these parameters in terms of at least one of the known physical properties of a liquid and subsequent computations leading to the other physical properties. The calculated and observed values of some of the properties of dense gases and liquids[32], molten metals[33], liquid chlorine[34] and fused alkali halides[31] agree very well over a wide range of temperature and pressure. This method also leads to a simple and surprisingly successful reduced equation of state for normal liquids. Though the method of significant structures has conceptual simplicity, the introduction of at least two parameters to be fitted to the experimental data, makes it a phenomenalogical approach rather than a fundamental one.

Other Theories: Apart from the three theories discussed above, other attempts at the elucidation of the structure of the liquid state have also been made. The mathematically more elegant kinetic multiple molecular contact model[35]

takes into account the effect of density perturbation on the free volume of the liquid state and gives rise to a whole spectral range of sizes for the holes in the liquid. A geometrical approach to the structure of the liquid state, totally different in its concept from the other theories, has recently been proposed by Bernal[36]. He treats the liquid state as homogeneous, and coherent, essentially an assemblage of irregular polyhedra, containing no holes large enough to admit another molecule. This theory, which assumes no regions of high coordination, has been developed for the liquids of the simplest spherical molecules. An extension[37] of this concept to the other types of liquids, such as molten salts, has met with a reasonable amount of success in the interpretation of the radial distribution curves obtained by x-ray and neutron diffraction in melts.

Ionic melts: The ''argon model'' for the liquids possessing one kind of atoms only (loc. cit.) can easily be extended to simple molten salts. A comparison of the entropies of fusion and volume changes on fusion (cf. Table Al, Appendix) for some of the simple salts and those of the rare gas solids, reveal interesting correlations. The entropies of fusion are found to be very nearly constant (2 - 3 e.u. per gm-atom) over a wide range of temperature and irrespective

of the type of the solid. An extension of the "argon model" to the ionic melts thus appears feasible, since the anions and the cations behave largely independently of each other, at least insofar as entropy considerations are concerned. This view is expressed in the "similitude rule"[38], that the randomization on melting is the same for crystals of similar structure. Based upon this observation and also from thermodynamic studies of molten salt mixtures, a model[39] for an ideal molten salt has been developed, which considers the anions and the cations to be randomly distributed among themselves, irrespective of valency, but that each anion is surrounded by cations and vice versa. A schematic illustration of this model, the Temkin model, is given in Fig. 2. It is seen that the molten salt consists of a semi-lattice of the larger anions with the smaller cations occupying the positions not very different from the crystalline state. This model has proved to be the most reasonable one for an explanation of the physical properties of molten salts and their mixtures - especially from a thermodynamic view point.

Experimental Methods: Underlying these theoretical advances are the experimental investigations on molten salts and their mixtures conducted during the past sixty years. The properties of molten salts that are most commonly investigated

FIG·2 TEMKIN MODEL OF MOLTEN SALTS
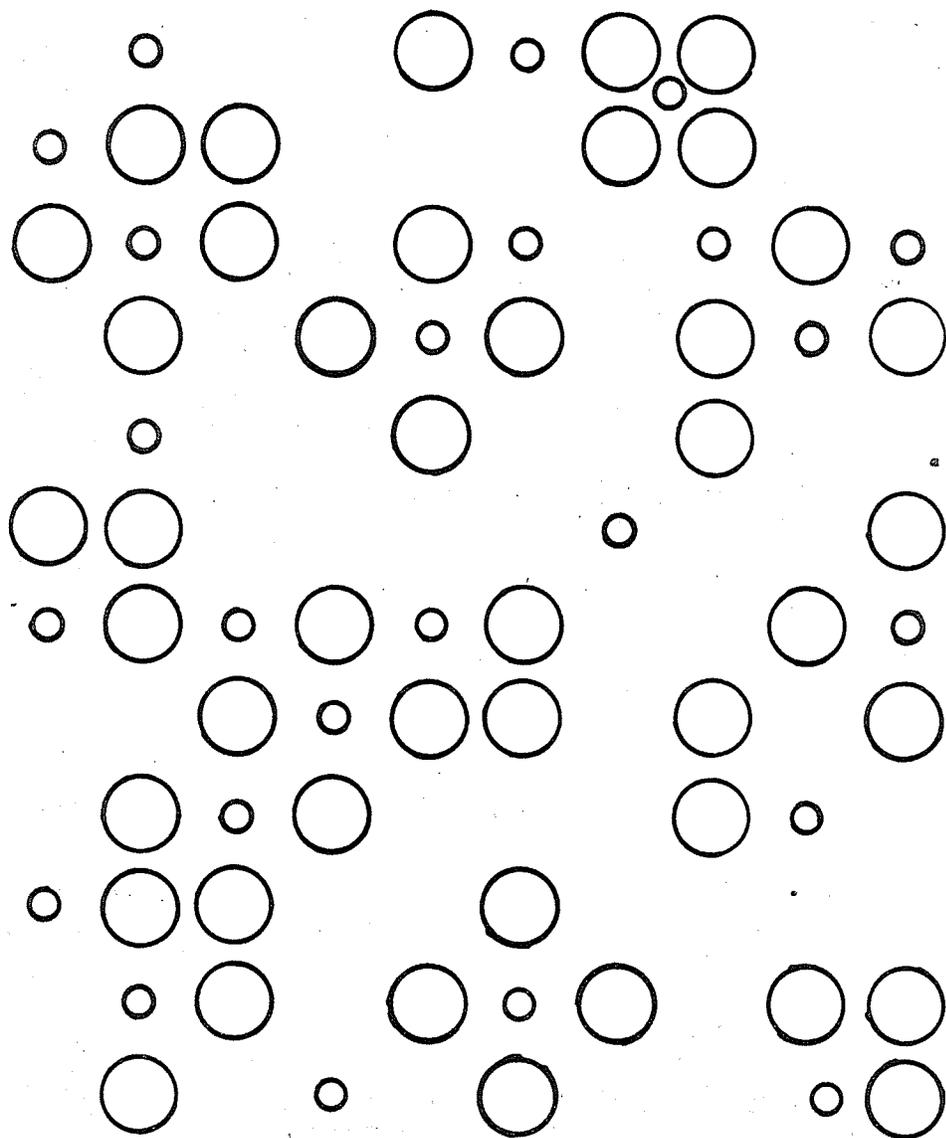
◯ anion   ○ cation

can be broadly be classified in three distinct types:
a) Transport properties, b) Spectroscopic studies and
c) Thermodynamic investigations. The determination of
transport properties (such as diffusion coefficients,
transport numbers, electrical conductivities, viscosities
and polarographic studies) in molten salts and in their
mixtures, offer a means of elucidating the structure of
the fluid, the processes of charge transport, the con-
figuration of the basic unit of flow, the extent of the
ionic character of the melt, the solute-solvent interactions,
the intensity of force fields and the energy barriers between
them and the kinetics of electrode reactions. Spectroscopic
techniques are undoubtedly among the most direct methods of
obtaining useful information on the structure of molten
salts. A knowledge of the time-average structure of the
molten salt, local orientations and association of ions,
the inter-play of inter-molecular forces and the environ-
mental influences, can be gained by spectroscopic studies,
e.g. Raman spectra, visible and ultraviolet absorption
spectroscopy, x-ray and neutron diffractions and nuclear
magnetic resonance.

Thermodynamic Properties: The application of thermodynamic
methods to molten salt systems yields valuable information
regarding the structural changes in the formation of molten

salt through the process of fusion. Many of the classical physiochemical techniques such as cryoscopy, densitometry, calorimetry, measurement of solubility, refractive indices, Cell EMF's, surface tensions, vapour pressures have been employed in the study of molten salts and their mixtures. The compressibility data, obtained from ultrasonic velocity technique[40], lead to important thermodynamic properties, a measure of the free volume and an equation of state for molten salts. Bockris and Richards[41] have developed a successful equation of state for molten salts, on the basis of which they have predicted a number of useful thermodynamic properties for liquids for which no such data are available. The observed dependence of partial molal volume on composition is closely linked with the structural theory assumed and therefore such studies contribute to our knowledge of the structural influences in molten salt systems. One of the main purposes of the application of thermodynamic methods to mixtures of molten salts is to gain information on the activity of the individual components in the melt. The observed deviation of the activity and quantities derived therefrom, from ''ideal'' behaviour can then be interpreted on the basis of the assumed structural model.

Thermodynamics and Structure: The entropy of a system provides the bridge between the structure of a liquid and thermodynamics, which chiefly concerns itself with the transformation

of energies. The values of the entropy of fusion vary by
less than one order of magnitude for nearly all substances
(cf. Table A1, Appendix). Since the free energy of a
system remains unaltered during the process of fusion, the
following relation holds:

$$T_f = \Delta H_f / \Delta S_f$$ where T_f, ΔH_f and ΔS_f denote

the temperature, enthalpy and entropy of fusion, respectively.
Ubbelohde[42] has classified the principal mechanisms con-
tributing to the randomization in melting as follows:
(a) increase in vibrational entropy due to looser packing
in the melt; (b) increase in the orientational randomization
due to the marked reduction of repulsion and barriers
accompanying the expansion in volume on melting; (c) increase
in positional disorder on melting; (d) randomization of
internal configuration of molecules or ions containing
flexible groups; (e) changes of association or chemical
bonding on melting. The over-all entropy change on fusion
can thus be written as:

$$\Delta S_f = \Delta S_{vib} + \Delta S_{orien} + \Delta S_{pos} + \Delta S_{conf} + \Delta S_{assoc}$$

For crystals containing monoatomic particles the postional
randomization is the principal contribution to ΔS_f. The
positional term is considered to be more or less a constant
for crystals having similar crystal structure (cf. ''simli-
tude rule''[38]) and hence the excess entropy over and above
the ΔS_{pos} must result from deviation from random distribution

of ions due to the occurence of particular configurations
(e.g. ion-pairs, groupings, ''complexes'' etc.). In
addition, the value of $\triangle S_f$ may lead to valuable information
regarding the nature of packing[43] of the solid lattices,
changes in the internal configuration of molecules or ions
and the type of bonding that exists in the melt. A very
broad classification of liquids into different types or
classes (cf. Table A1, Appendix) can be given, on the basis
of the values of $\triangle S_f$.

Papoušek and Kucirek[44] examined the problem of
''structural contributions'' to the values of heat capacity,
volume expansion and compression of liquids on the basis of
simple thermodynamic relationships, which express these
contributions in the form of second derivatives of the
entropy, as functions of volume, pressure and temperature.
They considered the compressibility (β_T), coefficient of
volume expansion (α_T) and heat capacity (C_p or C_v) as being
made up of two additive terms, one being the geometrical
contribution and the other a structural contribution, viz.

$$\beta_T = \beta_s + \beta_g$$

$$\alpha_T = \alpha_s + \alpha_g$$

$$C_p = (C_p)_s + (C_p)_g$$

$$C_v = (C_v)_s + (C_v)_g$$

where the subscripts s and g stand for the structural and geometric contributions respectively. The geometric part of each of the properties discussed is taken to arise solely from changes in the intermolecular (or inter-ionic) distances due to changes in pressure volume and temperature. Fischmeister[45] concludes from his investigations on the thermal expansion of alkali halides, that fusion occurs at a ''corresponding temperature'' where the thermal lattice expansion of the valid halide, relative to the distance at absolute zero is the same for all alkali halides. This conclusion is similar to that of Papousěk and Kucirěk. The structural parts of the compressibility, heat capacity and coefficient of volume expansion occur as second derivatives of entropy (as functions of p, T and (p,T) respectively) and therefore represent the simultaneous increase or decrease in the molecular regularity of the liquid with changes in pressure, volume and temperature. In the case of unoriented liquids, Papousěk and Kucirěk found the structural contribution to be generally greater than the geometrical contribution. With an increase in the orientation (or orderliness) in the liquid, the value of the structural contribution is found to decrease and in the extreme case of an exceptionally dense packed, well ordered liquid (e.g. mercury) they found that the structural contribution is even lower than the geometric part. In the

case of mixtures of liquids, these considerations lead to
useful data on the structural changes taking place during
the process of mixing. Though Papousek and Kucirek applied
these ideas to ordinary liquids, an extension to ionic
melts is readily possible.

Thermodynamics of molten salt mixtures: Thermodynamic
data on molten salt mixtures provide an ideal testingground
for a critical evaluation of the applicability of
structural models to such systems. However, these data can
only tell in principle if a suggested structural model is
possible or not but may not be of help in deciding between
two or more possible structural models. Most of the work
in this field has been directed to an examination of the
excess properties, such as free energy, entropy and enthalpy.
The E.M.F. method has been successfully applied by many
workers[46] in determining the partial molar free energy and
the partial molar entropy of the measured component. The
excess free energy ($\bar{F}^E$) is given by the relation:

$$\bar{F}^E = \bar{H}^E - T \bar{S}^E$$

$$= R_T \ln a$$ where a is the activity of the

measured component and $\bar{H}^E$ and $\bar{S}^E$ are the excess enthalpy
(or heat of mixing) and excess entropy (or entropy of
mixing) respectively. Now, if the entropy of mixing has the
ideal value $\bar{S}^E = -R \ln N$, where N is the mole fraction of

the particular component, the heat of mixing is simply given by $\bar{H}^{-E}$ = RT ln γ. (γ = activity coefficient). The activity of a component in a molten salt mixture may also be calculated from phase diagram studies[47] of cryoscopic investigations. Murgelescu and Sternberg[48] give the following equation:

$$\ln a = \frac{\triangle H_f}{R} \left(\frac{1}{T} - \frac{1}{T_f}\right) + \frac{\triangle C_p}{R} \left(\ln \frac{T_f}{T} - \frac{T_f - T}{T}\right)$$

where   a = activity of the component.

$\triangle H_f$ = molar heat of fusion of the pure substance.

T_f = freezing point (^{O}K) of the pure substance.

T = freezing point (^{O}K) of the given mixture.

$\triangle C_p$ = difference between the molar heat capacities
      of the solid and liquid phases.

Direct measurement of heats of mixing of molten alkaline nitrates by Kleppa and Hersh[49] is the most notable of recent work in this field. Their results have been found to be in excellent agreement with the semi-empirical equation, developed by Forland[50], viz.,

$$\triangle H_{mix} = K \ U \ N_1 \ (1 - N_1) \ \delta^2 \text{ where}$$
$$\delta = (d_1 - d_2) \ / \ (d_1 + d_2)$$

d_1, d_2 are the sums of radii of the ions $(r_+ + r_-)$ present in the two pure salts; N_1 is the ionic fraction of the "solute"; U is the lattice energy of the salts and K

is a constant. This is in accord with the view that the principal source of the enthalpy of mixing arises from the reduction in the coulombic repulsion between second nearest neighbours in the mixture - as compared with the corresponding repulsion in the pure components. The fact that almost all of the cationic mixtures studied exhibit a negative enthalpy of mixing gives support for the Coulomb term in the above equation. In the case of anion mixtures, however, Kleppa and Meschel[51] observe a positive value for the enthalpy of mixing, in most cases. They explain this behaviour by introducing, in addition to the negative coulomb term, a van der waals interaction term and a short-range repulsive potential between ion cores (''packing effect''[52]), the latter two terms being positive.

Hildebrand and Salstrom[54] made use of the zeroth-order approximation of the regular solution theory[55], in their study of Silver bromide - alkali bromides mixtures by the EMF technique. They considered an anion lattice of fixed dimension and allowed mixing of the cations on the cation lattice only and put forward the simple relation,

$$\bar{F}_1^E = n_2^2 \omega$$

where $\bar{F}_1^E$ = excess free energy of the component 1. n_2 = ionic fraction of the component 2. ω = an interaction energy parameter defined as $\omega = \omega_{12} - \frac{1}{2}(\omega_{11} + \omega_{12})$, ω_{12}, ω_{11}, ω_{22} are the interaction

energies of 1-2, 1-1 and 2-2 ion-pairs. They found
excellent agreement between theory and experiment but made
no attempts to deduce the interaction energy from molecular
properties. Recent measurements on similar systems, by
Panish et al.[56], have indicated that ω does not remain
constant.

Utilising the ideas of Temkin[39], Flood, Forland,
Girjotheim[57] have calculated the activities in simple molten
salt solutions. A further modification[58] of the Temkin
theory is found to be applicable in the calculation of
activity in complex binary and ternary mixtures of molten
salts. A quasi-lattice model for reciprocal molten salt
systems has been proposed by Blander[59], who considers the
system A^+, B^+, C^-, D^- as an assembly of charges in vacuo
consisting of two interlocking sub-lattices, one a lattice
of cations (A^+ and B^+), the other of anions (C^- and D^-).
He further takes into account the Temkin model for reciprocal
ionic melts and some other restrictions. The agreement
between the calculated and observed values of the activity
coefficients and other derived data, is reasonable[60].

For the sake of continuity, the discussion of the
investigations on the partial molar volumes and thermal
data in fused salts and in their mixtures is given at the
appropriate chapters in this thesis.

Chapter II

NATURE AND SCOPE OF THE PRESENT INVESTIGATION

Low-melting Salts: Most of the literature pertaining to
molten salts deals with systems possessing a very high
degree of ionic character. Only recently, attention has
been focussed upon the relatively low melting salts, which
are predominantly covalent, e.g., alkali nitrates[61],
mercuric halides[62] and salts with complex anions[63]. The
abnormally low melting points of these salts seem to arise
from sources of entropy increase on fusion, other than the
increase of positional entropy. Since these additional
entropy terms do not require large increases in the energy
of the system, it is probable that the low melting points
of these salts result mainly from increases in the
denominator in the expression

$$T_f = \frac{\triangle H_f}{\triangle S_{pos.} + \triangle S_{other\ terms}}.$$

It has been observed[64] (see also page 16) that positional
entropy changes in low melting salts are much the same as
in predominantly ionic salts. Accordingly, the excess
contribution to the entropy of fusion, in low melting salts,
has been interpreted as being due to deviations from random
distribution of ions, occurrence of short-range low energy
configurations (or ''association complexes''), presence of
''clusters'' of molecular species etc.

Earlier work on lithium chlorate: The preparation of lithium chlorate in a state of very high purity by Campbell and Griffiths[65] of this laboratory, has made available an inorganic salt with an abnormally low melting point of 127.9°C. Earlier investigations[66] on this salt had been restricted to electrical conductance studies of its aqueous solutions. A comprehensive study of the properties of molten lithium chlorate has recently been undertaken in this laboratory. Campbell, Kartzmark and Williams[67] studied the electrical conductivity of pure molten lithium chorate and the effect of additions of non-electrolytes. They found that the equivalent conductance of molten lithium chlorate has a value in between those of predominantly ionic and strongly covalent melts. Phase diagrams of the systems: lithium chlorate - lithium nitrate and lithium chorate-sodium chlorate were obtained by the method of thermal analysis, by Campbell, Kartzmark and Nagarajan[68], and thus provided the basis for the present thermodynamic study of the system: lithium chlorate - lithium nitrate. The phase diagram of the system lithium chlorate-lithium nitrate is given in fig. (3). The system exhibits a simple eutectic at 100.8°C, the eutectic composition being 39.78 weight per cent lithium nitrate.

FIG·3·PHASE DIAGRAM FOR THE SYSTEM LiClO$_3$ - LiNO$_3$

FIG·3·PHASE DIAGRAM FOR THE SYSTEM LiClO$_3$ - LiNO$_3$
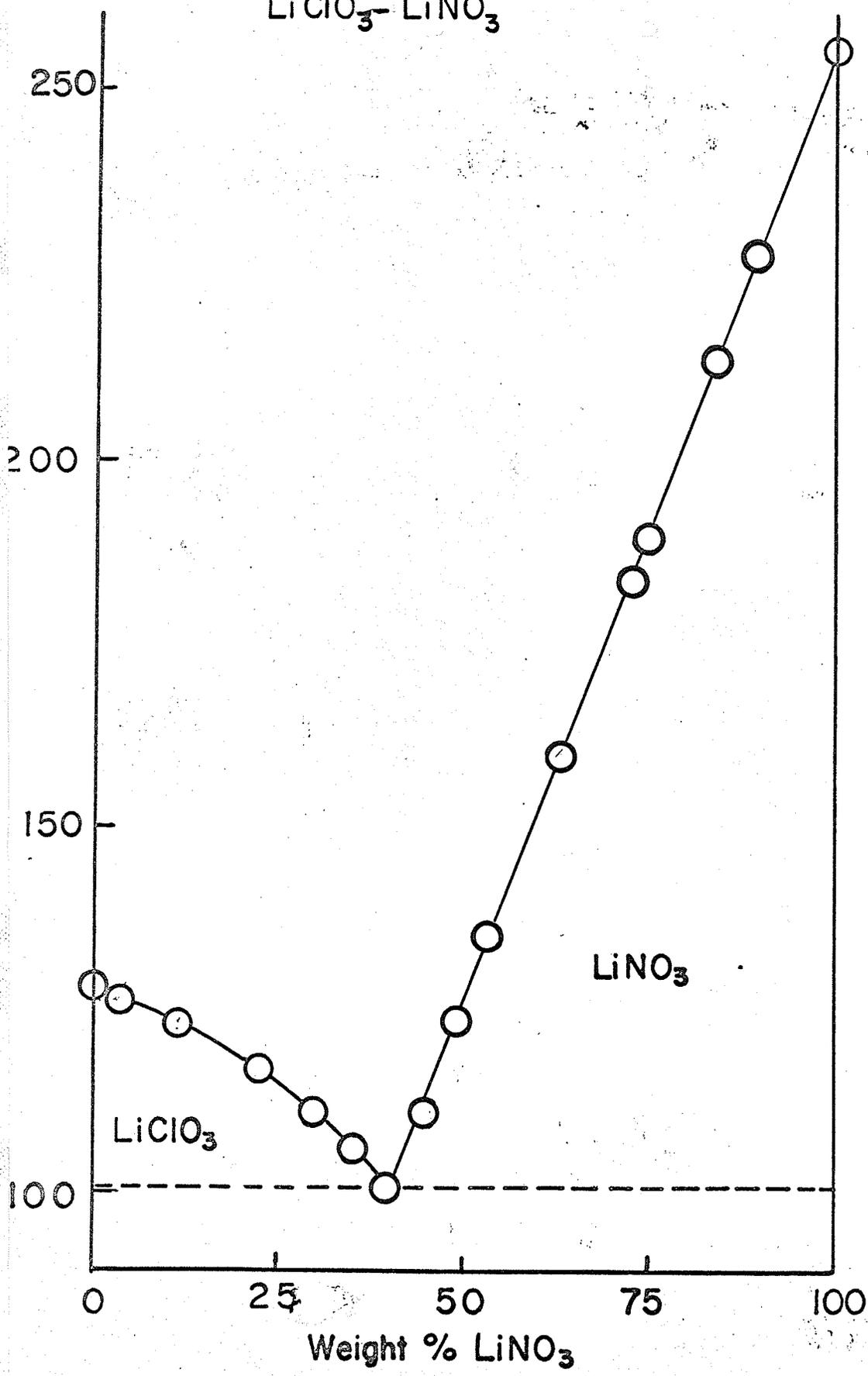
Present study: Densities and viscosities of pure molten

lithium chlorate and its mixtures with lithium nitrate

have been determined over the temperature range 130°- 170°C.

The low melting point of lithium chlorate permitted the

use of reliable classical techniques for the measurement of

these properties and a liquid thermostat for the temperature

control. Since slight decomposition is noticeable in

molten lithium chlorate above ca. 170°C, no measurements

were made beyond this temperature. Furthermore, lithium

chlorate-lithium nitrate mixtures containing more than ca.

30 weight percent lithium nitrate were found to be unstable

- as shown by the formation of bubbles in the bulk of the

liquid - even at lower temperatures (ca. 145°C). Therefore,

the present investigation is restricted to a concentration

range of 0 to 30 weight percent lithium nitrate in lithium

chlorate. The heats of fusion and the heat capacities, in

both solid and liquid state, of pure lithium chlorate and

of its mixtures with lithium nitrate have been determined by

the method of mixtures. The entropies of fusion and heats

of mixing were calculated from these primary data. Activities

of the constituents of the mixture and the excess free

energies were computed from the phase diagram[68] and

calorimetric data. The heat of the transition α LiCLO$_3$ $\rightleftharpoons$

β LiCLO$_3$, which occurs[69] at 99.1°C, was determined as the

difference between the measured heats of solution of the

two forms of lithium chlorate.

<u>Type of information sought:</u> The change in the molar
volume, viscosity, heat capacity and entropy of lithium
chlorate-lithium nitrate mixtures, with changes in the
temperature and composition of the melt, indicates the
structural changes associated with the process of fusion.
The deviations of the above-mentioned properties from the
''ideal'' behaviour is linked with the assumed structural
model and hence, such a study is bound to reveal the
suitability of a particular model of the liquid state. The
energetics of the interactions in the melt can be partly
understood from a consideration of the entropies of fusion
and heats of mixing. The entropy of the transition, which
occurs prior to the melting of lithium chlorate, must be
taken into account in any discussion on entropy changes
between the solid and the liquid state. The activity of
a particular species provides an indication of the nature
of that species in the melt. A knowledge of the extent of
ionic or molecular interactions in the melt (such as
formation of ion-pairs, groupings and ''complexes'') can be
gained from the excess free energy data.

Simultaneous with the present investigation,
Mr. D. F. Williams[70] of this laboratory has studied the
electrical conductance, surface tension and cryoscopy of
lithium chlorate-lithium nitrate mixtures. Combining the

my data with those of Mr. Williams, valuable
information on the nature of the melt, the type of species
present, the energy barriers of ion transport and the
change of order in the melt during the process of fusion
has been obtained. The application of current theories of
liquid state to the present system, though of a limited
nature, contributes considerably to our knowledge of the
constitution of covalent melts, such as lithium chlorate.

Chapter III

DENSITOMETRY

INTRODUCTION

From a knowledge of the density and thus the
molar volume changes with temperature information on the
change in the structure of the melt is gained. Some
approximate relations between the molar volume and the
ionic character of a melt have been given by Drossbach[3],
viz., (1) other factors being equal, molten covalent
compounds, owing to weak intermolecular forces, have
larger molar volumes than those of ionic melts which have,
in contrast, a strong coulomb field of force. (2) for the
same reason, the expansivity of covalent melts is greater
than that of ionic melts. (3) melts with different stages
of dissociation from the ionic to the covalent state are
possible.

Molar volume isotherms for ideal molten salt
mixtures, are linear when plotted against molar composition.
The ''ideal'' behaviour indicates that the free volume
varies uniformly with composition. Systems with both
positive and negative deviations from ideal behaviour are
known, wherein the free volume is greater or smaller than
that predicted by simple mixture theory. The changes of

partial molar volume with varying composition can tell
whether any pronounced interaction is taking place or
not. The information gained from molar volume data
assumes more importance in the case of covalent and highly
''associated'' melts. Quite apart from these considerations,
a knowledge of densities of melts is a prerequisite for the
computation of their relative viscosities.

The variations of density and molar volume with
temperature can be adequately represented, as a first
approximation by the following equations:

$$\rho = \rho_0 + A T$$

$$v = B + C T$$

$$= v_0(1 + \alpha T)$$

where v_0, ρ_0, A, B, C are constants.

The linear dependence of density or of molar
volume on temperature holds good only for the given range
of temperature.

PREVIOUS RELEVANT INVESTIGATIONS

Klotschko and Grigorew[71] have given a value for
the density of anhydrous lithium chlorate at its melting
point as 1.9715 gms ml^{-1}. However, they state that their
density determinations were only of minor importance in

their study of conductance and viscosity in lithium chlorate-water system. Moreover, they have not given their value for the melting point of anhydrous lithium chlorate but simply state that the density was determined at 128°C.

Archimedian techniques[72], which are undoubtedly the best methods, for the determination of densities are not suitable for very hygroscopic salts, such as the one used in the present investigation. Hence, dilatometric methods[73] have been extensively employed in the determination of the density of molten salt. The relatively low temperature region in which the present study was conducted, is especially suited for dilatometry, since at these low temperatures a well-controlled liquid thermostat - for effective thermal equilibration - can be employed. Therefore a dilatometric method, suitably modified to handle a very hygroscopic salt, was employed in the present study.

EXPERIMENTAL

Reagents: Lithium chlorate was prepared by a method originally suggested by Potilitzin[78] and by Kraus[74], and later modified by Campbell and Griffiths[65] of this laboratory. The method involved mixing of equimolecular quantities of Barium chlorate (British Drug Houses Co. Ltd.) and Lithium sulphate (Fisher analysed reagent grade). The precipitated barium

sulphate was filtered off and the resulting solution was titrated alternately with solutions of lithium nitrate and barium chlorate until tests revealed the presence of neither of the two and was concentrated by vacuum distillation at ca. 60°C. When the solution had attained a concentration of ca. 90% lithium chlorate, it was cooled in an ice-bath, when crystals of lithium chlorate separated out. The mother liquor was removed by filteration and the lithium chlorate crystals were stored over sulphuric acid for a period of 2-4 weeks. After the salt was sufficiently dry, it was pulverized to a fine powder inside a dry-box. The final drying was carried out by applying vacuum and trapping the escaped water vapour in barium oxide tubes. The melting point and specific electrical conductance were determined at various intervals during the drying process. These served as criteria for the purity of the lithium chlorate, since impurities other than water were negligible. The drying was continued until constant values for the melting point and specific conductance were obtained. The melting point of anhydrous lithium chlorate as determined in this work is 127.9°C. The specific electrical conductance, determined by Mr. D. F. Williams[67] of this laboratory is 0.1148 ± 0.0002 mho at 131.8°C. The lithium nitrate used in the present investigation was Fisher reagent grade material. It was used without any further purification

apart from powdering and drying at 110°C for several days.

Temperature Control and Measurement: Because of the
relatively low temperature region of study (130°C to 170°C)
it was possible to employ Dow-Corning silicone fluid 550
as the bath liquid. The thermostat consisted of a
rectangular Pyrex glass jar (ca. 1 gallon capacity)
surrounded by 1/4'' transite plates, a double-walled wooden
box and an outer metal casing. The space (3'') between the
double walls was filled with Vermiculite for effective
insulation. A solid steel lid with holes for the various
inserts covered the top of the thermostat. A glass window,
2-1/2'' x 5'', was installed in the front and was illumi-
nated directly from behind. The temperature was controlled
by means of a Thyratron relay and was always within ± 0.1°C
at ca. 130°C.

A copper-constantan thermocouple and a Vernier
Potentiometer capable of measuring to 1 microvolt, were
employed for the measurement of temperature. The thermo-
couple was calibrated with the boiling point of pure water
(with necessary pressure correction) and the melting point
of pure tin (231.9°C) as fixed points. The fluctuations in
the bath temperature were less than 5 microvolts, giving a
precision of better than ± 0.1°C for temperature measurements.

Dilatometer Construction: The dilatometers were made of
Pyrex glass and essentially consisted of bulbs of ca. 10 ml
capacity sealed to stems of 1 mm bore capillary. The latter,
ca. 8 cms in length, were precision drilled capillary tubes
with a manufacturer's (Corning Glass) reported precision of
$\pm$ 0.002 mm. Three fine circular marks ca. 20 mm apart, were
made on the stem to facilitate accurate measurement of the
liquid level inside the capillary. A slanted side arm
terminating in a bulb of ca. 3 ml capacity was attached very
near the top and served as an overflow for the excess melt
transfered into the dilatometer. Fig. 4 is an illustration
of the dilatometer employed in the present study.

Dilatometer Calibration: The dilatometers were calibrated
with Shawinigan redistilled reagent grade mercury at four
different temperatures. The dilatometers were cleaned with
hot chromic acid, thoroughly rinsed with distilled water,
dried and weighed. Mercury was then introduced by means of
a long drawn-out capillary tube extending to the bottom of
the bulb, taking care to avoid the entrapment of air bubbles.
The dilatometers were fixed in position inside the thermo-
stat with their tops protruding out of the liquid level.
The open ends were plugged with cotton wool. The meniscus
level of the mercury column inside the capillary was adjusted
to coincide with one of the three marks on the stem, by using

FIG· 4· DILATOMETER

to transfer tube

S

C

3ml

C—Imm capillary

S⌐ fritted glass disc·

10 ml
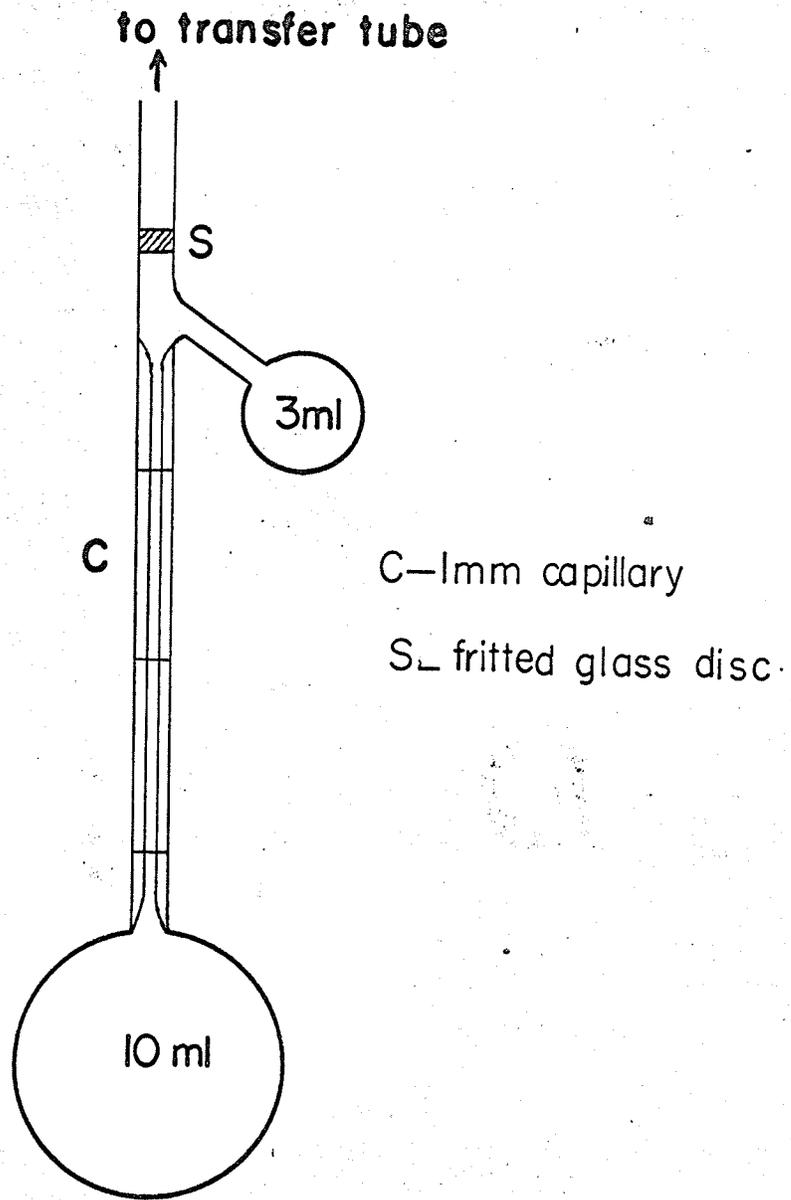
a long hypodermic needle and a syringe. This operation
was aided by a micro-cathetometer placed on a rigid plat-
form made of heavy concrete blocks. The micro-cathetometer
was capable of measuring lengths correct to 0.002 mm. The
dilatometer was removed from the thermostat, its outside
cleaned thoroughly, dried and weighed. Using the density
of mercury[75] at the given temperature, the volume corres-
ponding to one of the three marks on the stem was calculated.
This procedure was repeated for each of the three marks and
at three other temperatures. Fig. 5 gives an example of
the calibration graph for a dilatometer. The plots of
volume vs. temperature are essentially linear. In this
method of calibration it is not necessary to apply arbitrary
correction for the expansion of the glass. The non-
uniformity of the bore, if any, is also taken into account.

Filling Technique: Due to the extremely hygroscopic nature
of anhydrous lithium chlorate, the transfer of material to
the dilatometer had to be conducted in a moisture-free
atmosphere. A specially designed transferring apparatus
(Fig. 6) was employed for this purpose. It consisted of an
18 mm Pyrex glass tube separated into two compartments by a
fritted glass disc of medium porosity. A side arm, carrying
a stop-cock was attached to the tapering end of the tube to
facilitate evacuation of the assembly. The transfer tube
was sealed to the top of the dilatometer as indicated in

FIG·5· CALIBRATION PLOTS FOR DILATOMETER

FIG·6· TRANSFER TUBE

15cms

←—24mm—→

S

S— fritted glass disc

to dilatometer
or
viscometer
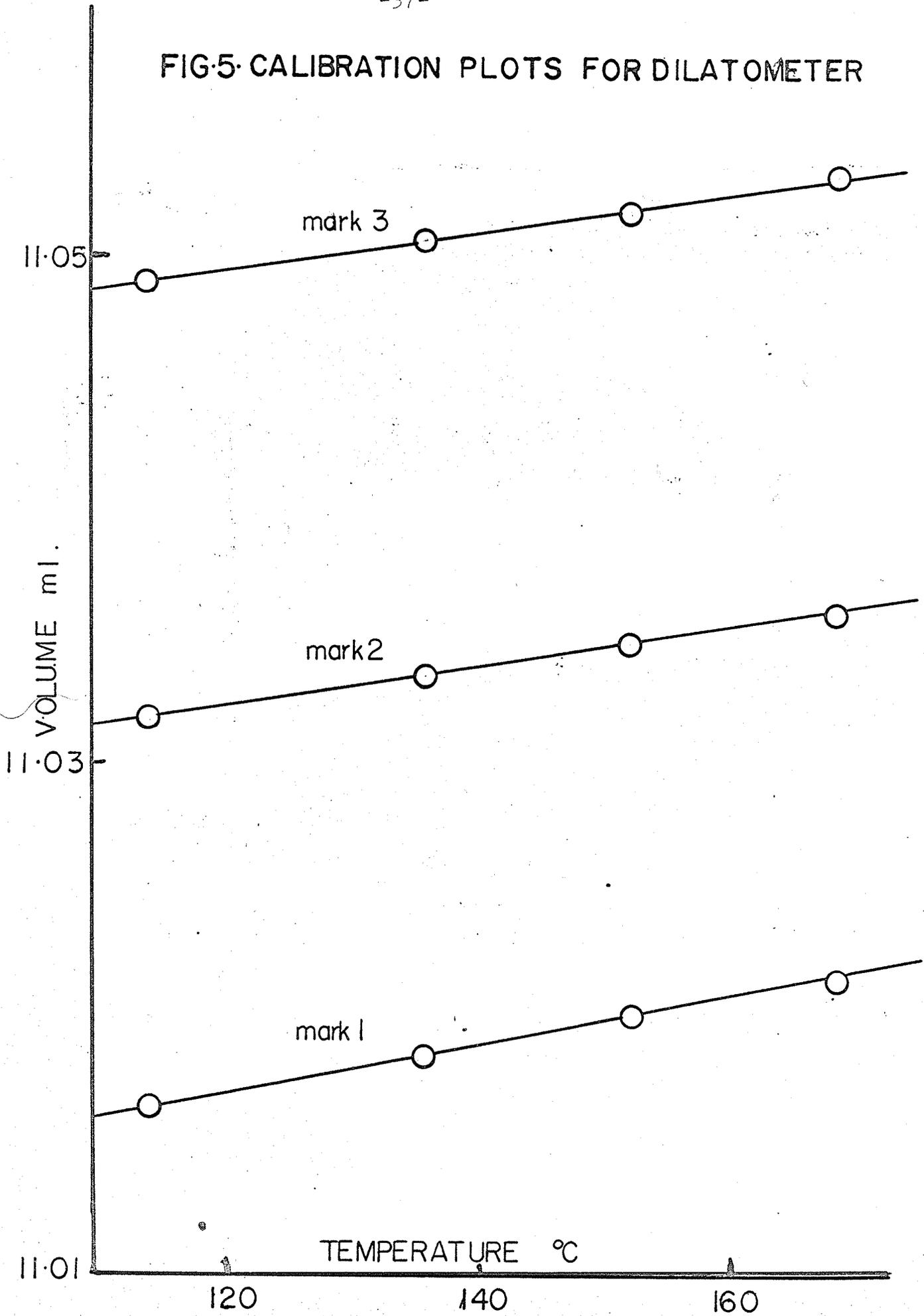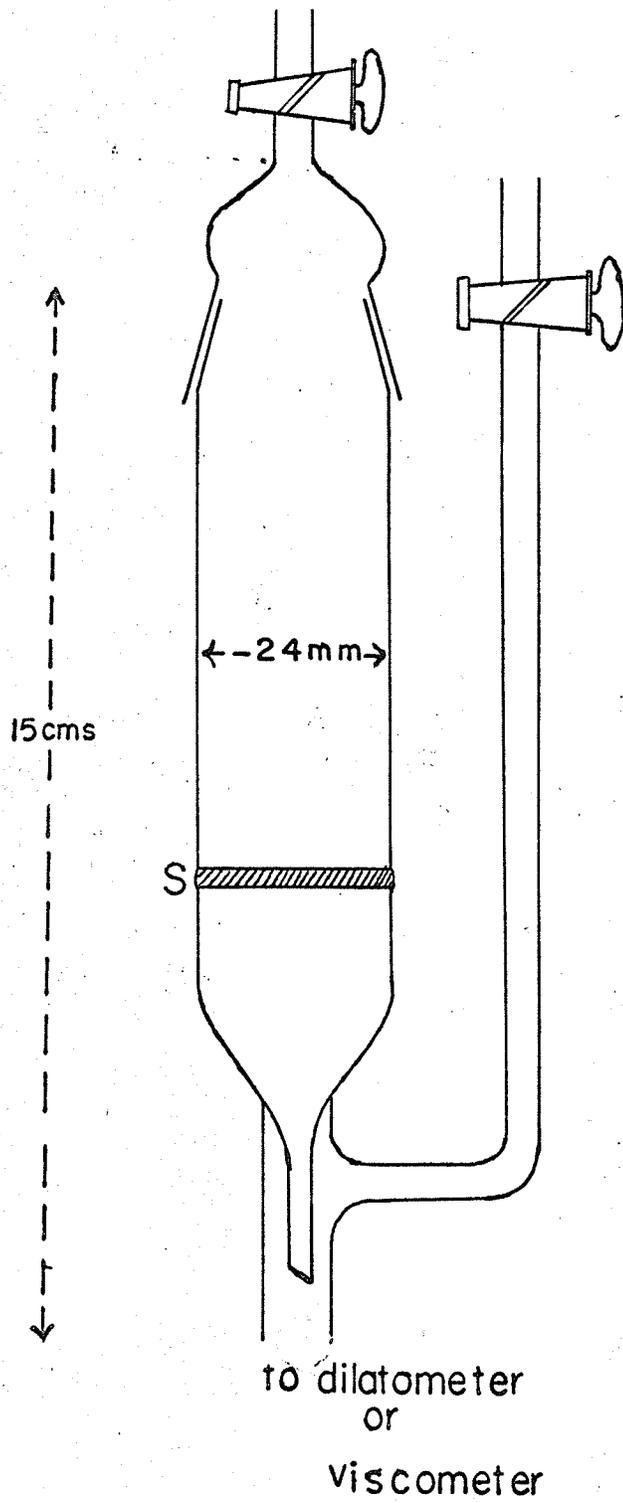
Fig. 5. The top compartment of the transfer tube was loaded with a sufficient amount of anhydrous lithium chlorate, the loading operation being carried out inside a nitrogen filled dry-box. The entire assembly was evacuated and placed in a thermostat kept at ca. 165°C. The molten lithium chlorate collected gradually in the bulb, filling it without air-bubbles. When the bulb and the stem were full (care being taken to avoid any air-bubbles) the excess lithium chlorate overflowed into the side bulb. In this way, it was possible to fill the dilatometer to the desired level without having to add or remove material. The dilatometer was removed from the thermostat and vacuum sealed at the constriction just above the small fritted glass disc (see Fig. 5). The purpose of the small fritted glass disc was to prevent any silt (arising out of the decomposition of the thin layer of lithium chlorate during sealing) from getting into the capillary bore. This disc proved very effective and indispensable. When dealing with mixtures of lithium chlorate and lithium nitrate, it was necessary to prepare the desired mixtures in advance and transfer only the homogeneous melt to the transfer apparatus. The preparation of the mixture and transfer of the homogeneous melt were carried out inside the dry-box.

Density Measurement: The dilatometer filled with either
pure lithium chlorate or a mixture was immersed completely
in the thermostat and held in a vertical position. After
thermal equilibration, the height of the liquid meniscus
level with reference to one of three marks on the stem was
measured accurately using the micro-cathetometer. The
distances between the marks were also measured at this
temperature. Using the calibration graph, the distance
between two marks and the height of the meniscus level
above a certain mark on the stem, the volume of the liquid
was calculated by an interpolation technique. This pro-
cedure was repeated at intervals of ca. $2^\circ C$ in the temperature
range $130^\circ C$ to $170^\circ C$. The heights were reproducible at a
given temperature within $\pm$ 0.01 mm. The weight of the
specimen alone was obtained by carefully breaking the
dilatometer and weighing the cleaned broken pieces. Density
measurements were made for pure lithium chlorate and four
mixtures with 0.108, 0.171, 0.227 and 0.292 molefraction
lithium nitrate.

Over-all precision of the Method: It was mentioned earlier
that the heights could be measured correct to $\pm$ 0.01 mm.
The capillary had a volume to length ratio of ca. 0.0008 ml/mm.
The total volume was ca. 10 ml. Hence the possible error in
the volume is approximately $\pm$ 0.0002. The temperature

coefficient of density is ca. $\pm$ 0.0001 gm ml^{-1} deg^{-1}.
Since the temperature fluctuations were within 0.1%,
this introduces negligible deviation in the density
(ca. $\pm$ 0.00001 gm ml^{-1} deg^{-1}). All weighings were made
on a precision balance and were correct to better than
$\pm$ 0.0001 gm. The over-all precision in the density values
is therefore $\pm$ 0.0002 gm ml^{-1} or $\pm$ 0.01%.

RESULTS

Tables I to V give the densities of pure lithium
chlorate and four mixtures of lithium chlorate and lithium
nitrate, at different temperatures. These values are
plotted in Fig. 7. Tables I to V also contain calculated
molar volumes. In the case of pure lithium chlorate
(molecular weight 90.397), molar volumes were calculated
using the simple relationship $V = \dfrac{M}{\rho}$. An additive
relation was employed for the calculation of molar volumes
of mixtures, viz.,

$$V = \frac{(n_1 M_1 + n_2 M_2)}{\rho}$$

where n_1, n_2 are mole fractions and M_1, M_2, molecular
weights of lithium chlorate and lithium nitrate respectively.
($M_2 = 68.948$). Fig. 8 illustrates diagrammatically the
dependence of molar volume on temperature. Least square

analysis of these data, according to the equation
$V = B + cT$, was carried out by means of Bendix G-15
computer. The programme used in the computer was also
capable of yielding standard deviations. The equation
for the 'best' line, along with standard deviation, is
given at the bottom of each table.

Isothermal cuts from the basic molar volume
data were obtained in order that the dependence of molar
volume on composition might be interpreted. The inter-
polations at arbitrarily chosen temperatures ($390^{\circ}K$ to
$450^{\circ}K$ at 10° intervals) were carried out on the computer,
employing the equations for the 'best' straight lines.
The values so obtained are given in Table VI and illustrated
graphically in Fig. 9. The dependence of molar volume on
the mole fraction of lithium nitrate (n_2) at constant
temperature, was found to satisfy the quadratic equation:

$$V = A_0 + A_1 n_2 + A_2 n_2^2$$

where A_0, A_1 and A_2 are constants. The data were fitted
to a 'best' curve by the method of least squares. The
values of the constants, A_0, A_1 and A_2, at different
temperatures are shown collectively in Table VII.

The values of coefficients of thermal expansion (α) were calculated, by suitably transforming the equation $V = B + cT$ into the more common form $V = V_o(1 + \alpha t)$, where 't' is in Centigrade scale. These values are given in Table VIII, at different mole fractions of lithium nitrate.

TABLE I

Densities and Molar Volumes of Pure Lithium Chlorate

Freezing Point: 401.0°K

t°C	T°K	d(gms ml^{-1})	V(ml mole^{-1})
135.0	408.1	2.0854	43.3476
138.5	411.6	2.0825	43.4079
139.9	413.0	2.0812	43.4350
141.8	414.9	2.0798	43.4643
143.8	416.9	2.0783	43.4957
145.3	418.4	2.0770	43.5229
147.9	420.2	2.0750	43.5648
148.3	421.4	2.0741	43.5837
149.7	422.8	2.0728	43.6111
151.2	424.3	2.0713	43.6426
152.7	425.8	2.0699	43.6722
154.3	427.4	2.0685	43.7017
155.5	428.6	2.0673	43.7271
157.6	430.7	2.0657	43.7610

'Best' line: $V = 35.503 + 0.0192T$

Standard deviation $= \pm 0.0063$ ml

TABLE II

Densities and Molar Volumes of Lithium Chlorate-Lithium Nitrate Mixture

Freezing Point: 397.6°K

n_2 = Mole fraction Lithium nitrate = 0.108

t°C	T°K	d(gms ml^{-1})	V(ml mole^{-1})
141.2	414.3	2.0743	42.8244
144.1	417.2	2.0721	42.8698
147.3	420.4	2.0698	42.9175
148.5	421.6	2.0688	42.9382
150.1	423.2	2.0674	42.9673
152.3	425.4	2.0659	42.9985
153.8	426.9	2.0646	43.0256
155.8	428.9	2.0632	43.0548
157.9	431.0	2.0614	43.0924
159.3	432.4	2.0604	43.1133
161.0	434.1	2.0591	43.1405
162.7	435.8	2.0579	43.1657

'Best' line: $V = 36.130 + 0.016_2 \, T$

Standard deviation = $\pm$ 0.0021 ml

TABLE III

Densities and Molar Volumes of Lithium
Chlorate-Lithium Nitrate Mixture

Freezing Point: $395.5^{\circ}K$

n_2 = mole fraction Lithium nitrate = 0.171

$t^{\circ}C$	$T^{\circ}K$	$d(gms\ ml^{-1})$	$V(ml\ mole^{-1})$
138.7	411.8	2.0689	42.3016
141.3	414.4	2.0666	42.3486
143.1	416.2	2.0649	42.3835
145.0	418.1	2.0634	42.4143
147.0	420.1	2.0622	42.4390
148.8	421.9	2.0609	42.4658
150.2	423.3	2.0598	42.4885
151.7	424.8	2.0587	42.5112
153.4	426.5	2.0569	42.5484
155.2	428.3	2.0558	42.5711
157.3	430.4	2.0537	42.6147
158.8	431.9	2.0526	42.6375
160.2	433.3	2.0514	42.6624
161.1	434.4	2.0506	42.6791

'Best'line: $V = 35.156 + 0.017_3\ T$

Standard deviation = $\pm\ 0.0074$ ml

TABLE IV

Densities and Molar Volumes of Lithium
Chlorate-Lithium Nitrate Mixture

Freezing Point: 392.9°K

n_2 = mole fraction Lithium nitrate = 0.227

$t°C$	$T°K$	$d(gms\ ml^{-1})$	$V(ml\ mole^{-1})$
139.6	412.7	2.0585	41.8759
141.7	414.8	2.0567	41.9126
144.2	417.3	2.0551	41.9452
145.7	418.8	2.0534	41.9799
148.2	421.3	2.0519	42.0106
150.0	423.1	2.0505	42.0393
151.4	424.5	2.0494	42.0619
153.5	426.6	2.0479	42.0927
154.8	427.9	2.0467	42.1174
156.2	429.3	2.0457	42.1380
157.8	430.9	2.0445	42.1627
160.3	433.4	2.0424	42.2060
161.5	434.6	2.0417	42.2205

'Best' line: $V = 35.733 + 0.014_9\ T$

Standard deviation $= \pm\ 0.0066ml$

TABLE V

Densities and Molar Volumes of Lithium Chlorate-Lithium Nitrate Mixture

Freezing Point: $389.2^\circ K$

n_2 = mole fraction Lithium nitrate = 0.292

$t^\circ C$	$T^\circ K$	$d(gms\ ml^{-1})$	$V(ml\ mole^{-1})$
138.4	411.5	2.0514	41.1415
139.7	412.8	2.0505	41.1595
141.0	414.1	2.0496	41.1776
142.8	415.9	2.0484	41.2017
144.0	417.1	2.0475	41.2198
146.2	419.3	2.0459	41.2521
147.9	421.0	2.0447	41.2763
149.4	422.5	2.0435	41.3005
150.8	423.9	2.0424	41.3228
152.4	425.5	2.0412	41.3471
154.1	427.2	2.0399	41.3734
156.0	429.1	2.0386	41.3998
158.3	431.4	2.0368	41.4364
160.0	433.1	2.0356	41.4608

'Best' line: $V = 35.031 + 0.0148\ T$

Standard deviation: ± 0.0020 ml

TABLE VI

Isothermal Molar Volume as a Function of Mole
Fraction of Lithium Nitrate

T $n_2 \rightarrow$	0.000	0.108	0.171	0.227	0.292
390.0	(42.985)	(42.428)	(41.916)	(41.548)	40.819
400.0	(43.177)	42.590	42.089	41.697	40.968
410.0	43.369	42.751	42.262	41.846	41.116
420.0	43.561	42.913	42.436	41.995	41.264
430.0	43.753	43.074	42.609	42.144	41.413
440.0	43.945	43.236	42.782	42.293	41.561
450.0	44.737	43.397	42.956	42.442	41.710

Note: Values in parenthesis refer to the molar
volumes in the supercooled liquid state.

TABLE VII

Values of Constants in the Equation for the 'Best' Curve by the Method of Least Squares

$$V = A_o + A_1 \, n_2 + A_2 \, n_2^2$$

Temperature ($^\circ$K)	A_o	A_1	A_2
390.0	42.983	-3.961	-11.573
400.0	43.172	-4.158	-11.386
410.0	43.363	-4.386	-11.101
420.0	43.553	-4.578	-10.942
430.0	43.744	-4.800	-10.672
440.0	43.934	-5.000	-10.488
450.0	44.124	-5.200	-10.284

TABLE VIII

Coefficient of Thermal Expansion for Mixtures of Lithium Chlorate and Lithium Nitrate

$$V = V_o (1 + \alpha t)$$

n_2	V_o (ml)	$\alpha \times 10^4$
0.000	40.747	4.71
0.108	40.554	4.00
0.171	39.881	4.34
0.227	39.802	3.74
0.292	39.073	3.79
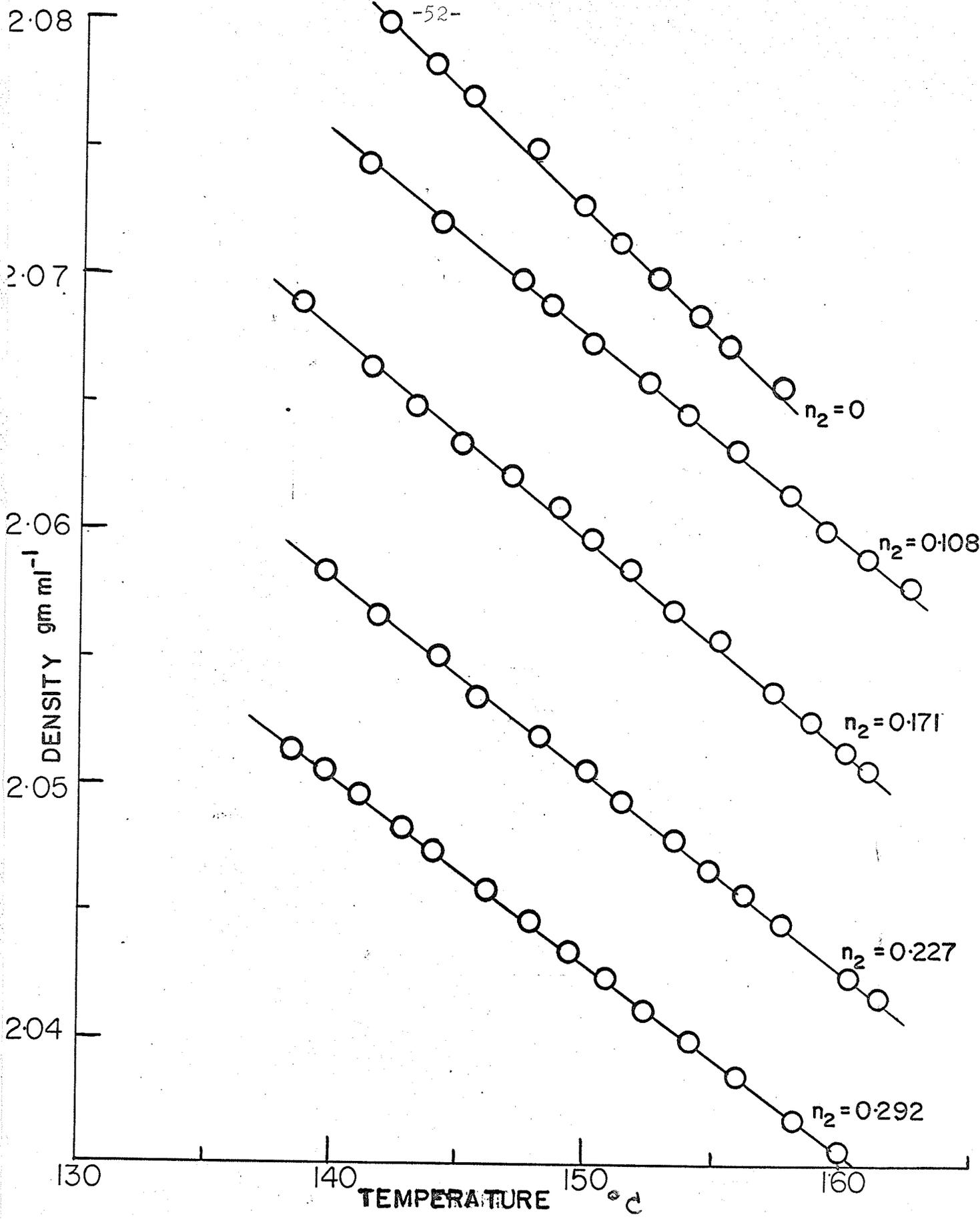
FIG·7 DENSITY vs TEMPERATURE

FIG·8 MOLAR VOLUME vs TEMPERATURE

FIG·8 MOLAR VOLUME vs TEMPERATURE
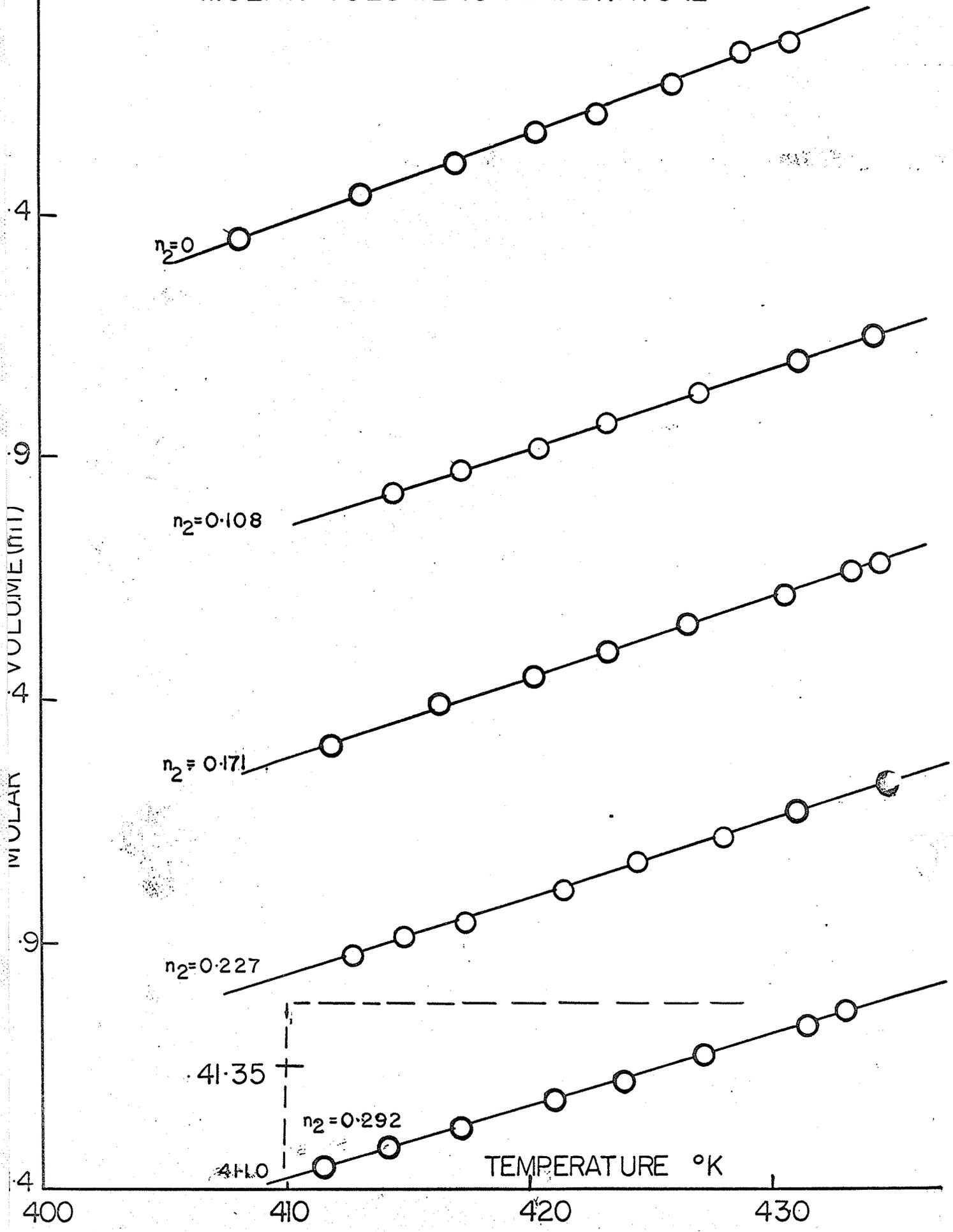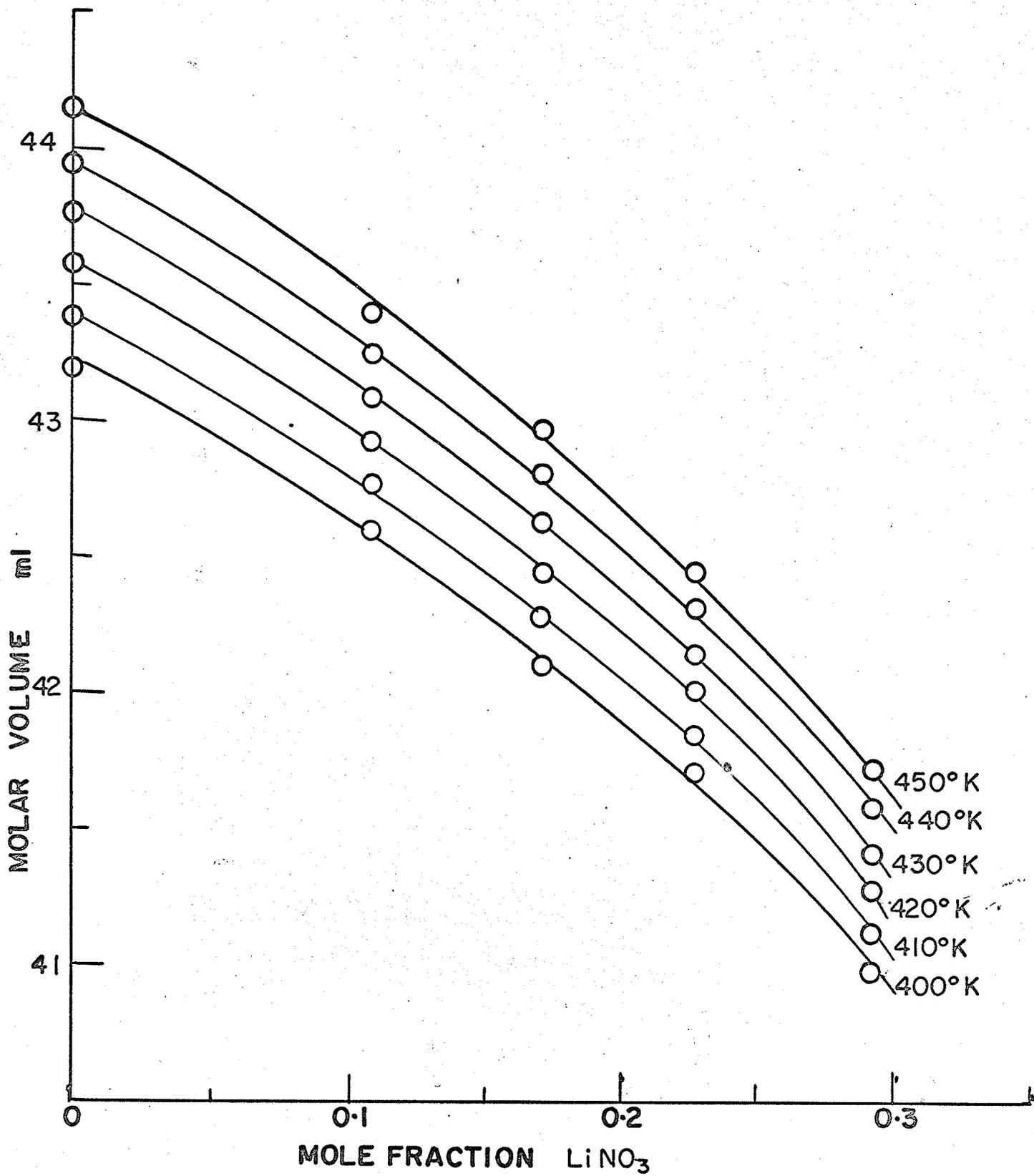
FIG·9   MOLAR   VOLUME   ISOTHERMS

DISCUSSION

I have found that the dependance of the molar volume of molten lithium chlorate on temperature is given by the linear relation:

$V = (35.503 + 0.0192\ T)$ mls with an observed standard deviation of $\pm$ 0.006 ml. It is generally agreed[76] that salts with non-spherical polyatomic anions, such as nitrates and chlorates, possess a more covalent character than salts with spherical anions (e.g. chlorides, bromides, iodides). Attention has been drawn to Klemm's rule[3] (see page 29) which states that in general covalent melts possess higher molar volumes than ionic melts, owing to the weaker intermolecular forces prevalent among salts of the former type. For the same reason the value of the coefficient of expansion (α) is also, generally, higher in covalent melts than in ionic melts. A comparison of some molar volumes (at their melting points) and coefficients of volume expansion of different types of liquid is given in the Appendix. The values of molar volume and α of molten lithium chlorate suggest that the melt is probably more covalent than ionic in character, but such a comparison is only approximate and should be made only when other corroborative evidences are available - as in the present case.

In the study of mixtures of molten salts, it is common practice to discuss changes in partial molar volume with varying composition (at a constant temperature), in order to derive information on the interactions, if any, in the melt. Furthermore, the variation in the excess volume, $V^E = V_{obs} - (n_1 V_1 + n_2 V_2)$, with composition is also relevent in such a discussion. Such a procedure however has not been adopted in this thesis for the following two reasons: 1) Because of experimental difficulties mentioned in Chapter II (page 26), molar volume data have only been obtained in a restricted range of composition. 2) The conventional equations for partial molar volume necessarily involve the assumption, either explicit or implicit, that the higher melting, second component exists in the super cooled state at the temperature of the mixture (which is much below the melting temperature of the pure second component).   In the absence of definite theories as to the real nature of the mixing process in molten salts, it is superfluous to include the above mentioned assumption in a discussion on the nature of molten salts mixtures.   In the light of these comments it was thought desirable to discuss the molar volume data on lithium chlorate-lithium nitrate. mixtures, according to an argument closely related to that developed by Papousek and Kucirek[44], which has already been commented upon in the Introduction.

All changes in molar volume of lithium chlorate-
lithium nitrate mixtures are discussed relative to an
assumed standard or reference state, in this case, one
mole of pure, molten lithium chlorate at its melting point
(401.0°K). This assumption necessarily implies that the
basic lattice of the reference state predominates over the
entire region of tempe ature and composition involved. In
other words no major change or breakdown of the basic
reference state lattice occurs in the region of investigation.
The molar volume is considered to be a function of only two
variables viz., temperature (T) and composition, i.e.
$V = f(T, n_2)$ where n_2 is the mole fraction of lithium nitrate.
The change in molar volume (dv) from the reference state
volume is then defined by the equation:

$$dv = \left(\frac{\partial v}{\partial T}\right)_{n_2} dT + \left(\frac{\partial v}{\partial n_2}\right)_T dn_2$$

where $\left(\dfrac{\partial v}{\partial T}\right)_{n_2}$ is the rate of change in molar volume with
temperature at a fixed composition; $\left(\dfrac{\partial v}{\partial n_2}\right)_T$ is, likewise,
the rate of change in molar volume with composition, at a
constant temperature and dT, dn_2 are increments of temperature
and composition over and above that of the reference state.
In the above equation the term $\left(\dfrac{\partial v}{\partial T}\right)_{n_2}$ accounts for the
change in the interparticle distances with temperature and
therefore can be considered to be a ''geometrical''

contribution to the total change in molar volume. The
term $\left(\frac{\partial v}{\partial n_2}\right)_T$, however, denotes on the effect of inter-
actions of added lithium nitrate with the reference lattice
(viz. lithium chlorate) on molar volume and therefore can
be designated, the ''structural'' contribution to the total
change in molar volume. For the sake of convenience the
notations, defined as follows, are used:

$$V_g \equiv \left(\frac{\partial v}{\partial T}\right)_{n_2}$$

$$V_s \equiv \left(\frac{\partial v}{\partial n_2}\right)_T$$

The above suposition that the change in molar volume is
composed of two separate parts, one due to geometrical and
the other due to structural contributions, may not describe
the real state of affairs. It is quite probable that such a
sharp cleavage of the total change in volume may not be
justifiable on theoretical grounds. However, the above
equations do present a convenient and elegant way of dis-
cussing the molar volume data, without any accompanying
assumptions as to the mechanism of interactions in the melt.

The values of V_g at different compositions were
obtained by differentiation of the equations of 'best'
lines given in Tables I to V and are tabulated in Table IX.

TABLE IX

Values of V_g (Interpolated) at Different Compositions
for $LiClO_3$ - $LiNO_3$ mixtures

n_2 = mole fraction lithium nitrate

n_2	V_g
0.000	0.0192
0.100	0.0168
0.200	0.0155
0.300	0.0145

The coefficients of volume expansion are also included in the above table for comparison purposes. The geometrical contribution decreases with the addition of lithium nitrate. Since a larger change in the interparticle distances can be expected for covalent melts than for ionic melts, the decreasing trend shown by V_g indicates that the melt becomes progressively more ionic with increasing concentration of lithium nitrate. The same conclusion is reached by considering the change in values of α. The equivalent conductances of lithium chlorate-lithium nitrate mixtures have been shown[67] to exhibit a slight increasing trend with increase in the concentration of lithium nitrate. This observation is in agreement with the conclusion reached from the molar volume data.

The isothermal molar volumes have been found to satisfy the equation:

$$V_T = A_o - A_1 n_2 - A_2 n_2^2$$

where n_2 is the mole fraction of lithium nitrate. Partial differentiation of the above equation gives,

$$\left(\frac{\partial v}{\partial n_2}\right)_T = V_s = - A_1 - 2A_2 n_2$$

From the values of A_1 and A_2 in Table VII the values of V_s have been calculated at randomly selected fixed temperatures and are shown as function of composition in Table X and are graphically illustrated in Fig. 10. It is seen from the

TABLE X

Values of V_S at Different Temperatures for $LiClO_3$ - $LiNO_3$ mixtures
n_2 = mole fraction of lithium nitrate

$T^{\circ}K$	$n_2=0.000$	$n_2=0.100$	$n_2=0.200$	$n_2=0.300$
390.0	- 3.961	- 6.276	- 8.590	- 10.905
410.0	- 4.386	- 6.606	- 8.826	- 11.047
430.0	- 4.800	- 6.934	- 9.069	- 11.203
450.0	- 5.200	- 7.257	- 9.314	- 11.370
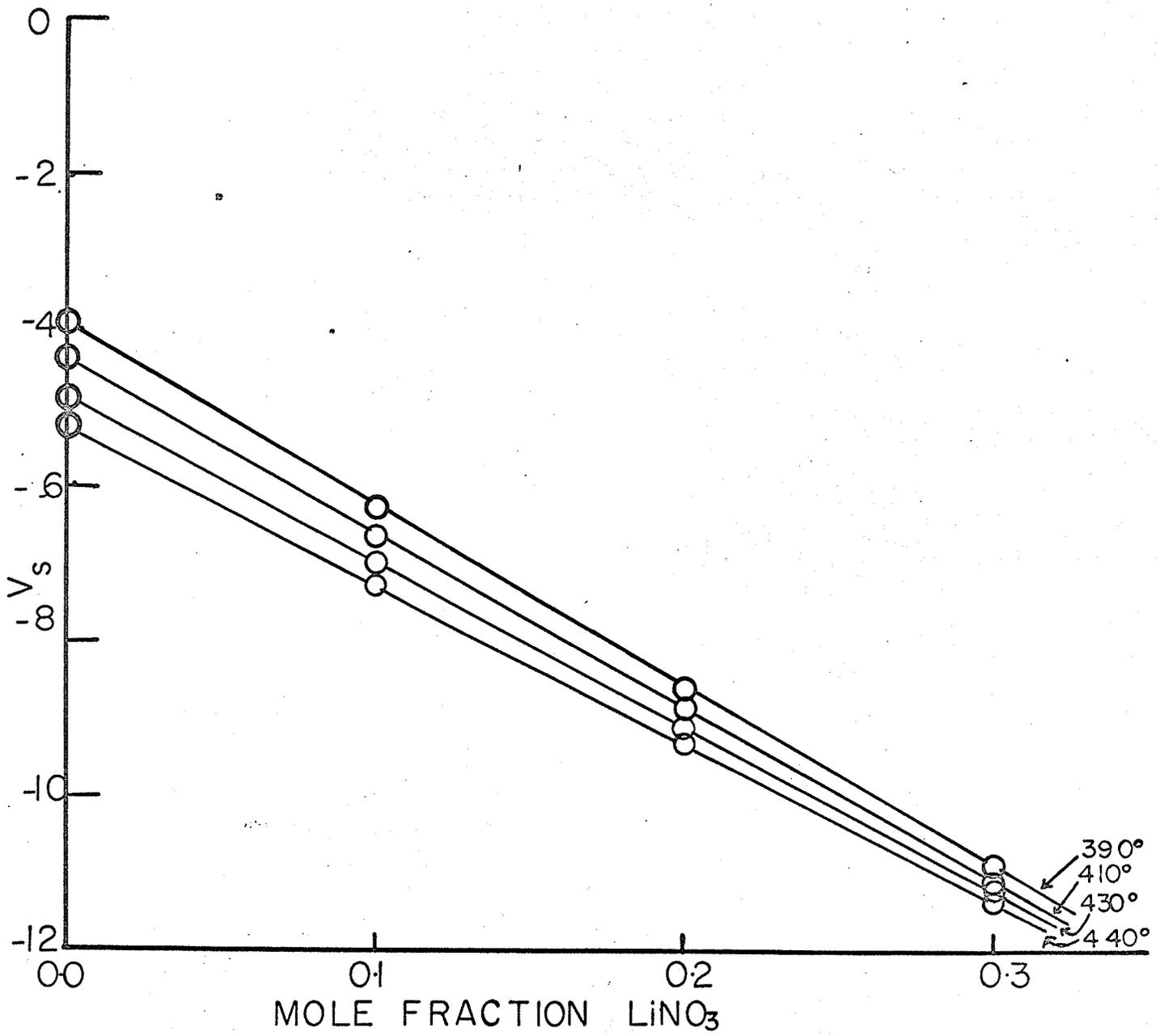
FIG·10·PLOT OF V_S AGAINST COMPOSITION

values of V_s tabulated, that the isothermal structural
contribution to the total change in molar volume, is
negative and becomes progressively more negative on further
additions of lithium nitrate. Therefore, it is probable
that the interaction of nitrate ion with the chlorate
lattice of the reference state, results in a more compact
configuration. Mr. D. F. Williams[70] has shown that the
degree of dissociation is very small and that there is no
substantial increase in this value on adding lithium nitrate.
In view of this, the reference lattice of lithium chlorate
can be considered to be predominantly molecular in nature.
Therefore, the introduction of a dissimilar anion, viz.
nitrate, may somehow strengthen the covalent character of
the reference lattice, perhaps by drawing togehter some
number of lithium chlorate molecules. A similar explanation
has been put forward by Kleppa and Meschel[51] in their
attempt to account for the thermal data on silver nitrate-
halide mixtures. The value of V_s takes on more negative
values at increased concentrations of lithium nitrate and
this indicates an increase in the compactness of the con-
figuration of the entities present in the melt. The viscosity
and thermal data obtained by me also support the above
conclusions (cf. page 105, 149).

The individual parts of the equation,
$dv = V_g dT + V_s dn_2$, viz., the geometrical part ($V_g dT$) and the

structural part $(V_s dn_2)$ of the total change (dv) in molar

volume from that at the reference state, have also been

calculated. In the case of structural part, since V_s is a

function of n_2, it was necessary to find the value of the

integral, $\int_{T_{sr}}^{T} V_s dT$, where $T_{sr} = 401.0^{\circ}K$. The values of the

above integrals were obtained by a graphical integration of

Fig. 10, using appropriate limits. The geometrical and

structural parts of the total change in volume are shown

collectively in Table XI. These values are plotted in

Fig. 11, as functions of composition of the melt. The

structural part of the change in volume predominates at low

temperatures and high concentrations of lithium nitrate.

Thus, though the geometrical part is always positive above the

reference temperature, the interactions taking place in the

melt somehow contribute a large negative value, thus making

the total change negative (with respect to the volume at

the reference state). The fact that the structural part of the

change in volume is significant in the entire region of

temperature and composition studied, suggests that whatever

interation that is taking place in the melt is of much

importance. The fact that the geometric part of the change

in volume considerably increases with increase of temperature

probably reflects the process of break down of the compact

configurations. The agreement between the calculated and

observed values of dv is satisfactory. The values of dv in

Table XI and Fig. 11 refer to the change in volume from that
at the reference state and <u>not</u> to the conventional excess
volume.

TABLE XI

Geometrical and Structural Parts of the Change in Molar Volume

n_2 = mole fraction of lithium nitrate

$T^{O}K$	$n_2=0.000$			$n_2=0.100$			$n_2=0.200$			$n_2=0.300$		
	$V_g dT$	$V_s dn_2$	dV	$V_g dT$	$V_s dn_2$	dV	$V_g dT$	$V_s dn_2$	dV	$V_g dT$	$V_s dn_2$	dV
390.0	-0.211	0.000	-0.211	-0.185	-0.512	-0.697	-0.171	-1.255	-1.426	-0.160	-2.230	-2.390
410.0	+0.173	0.000	+0.173	+0.151	=0.550	-0.399	+0.140	-1.322	-1.182	+0.131	-2.316	-2.185
430.0	+0.557	0.000	+0.557	+0.487	-0.587	-0.100	+0.450	-1.388	-0.938	+0.421	-2.403	-1.982
450.0	+0.941	0.000	+0.941	+0.823	-0.623	+0.200	+0.760	-1.452	-0.692	+0.711	-2.487	-1.776

FIG·II STRUCTURAL AND GEOMETRICAL PARTS OF CHANGE IN VOLUME
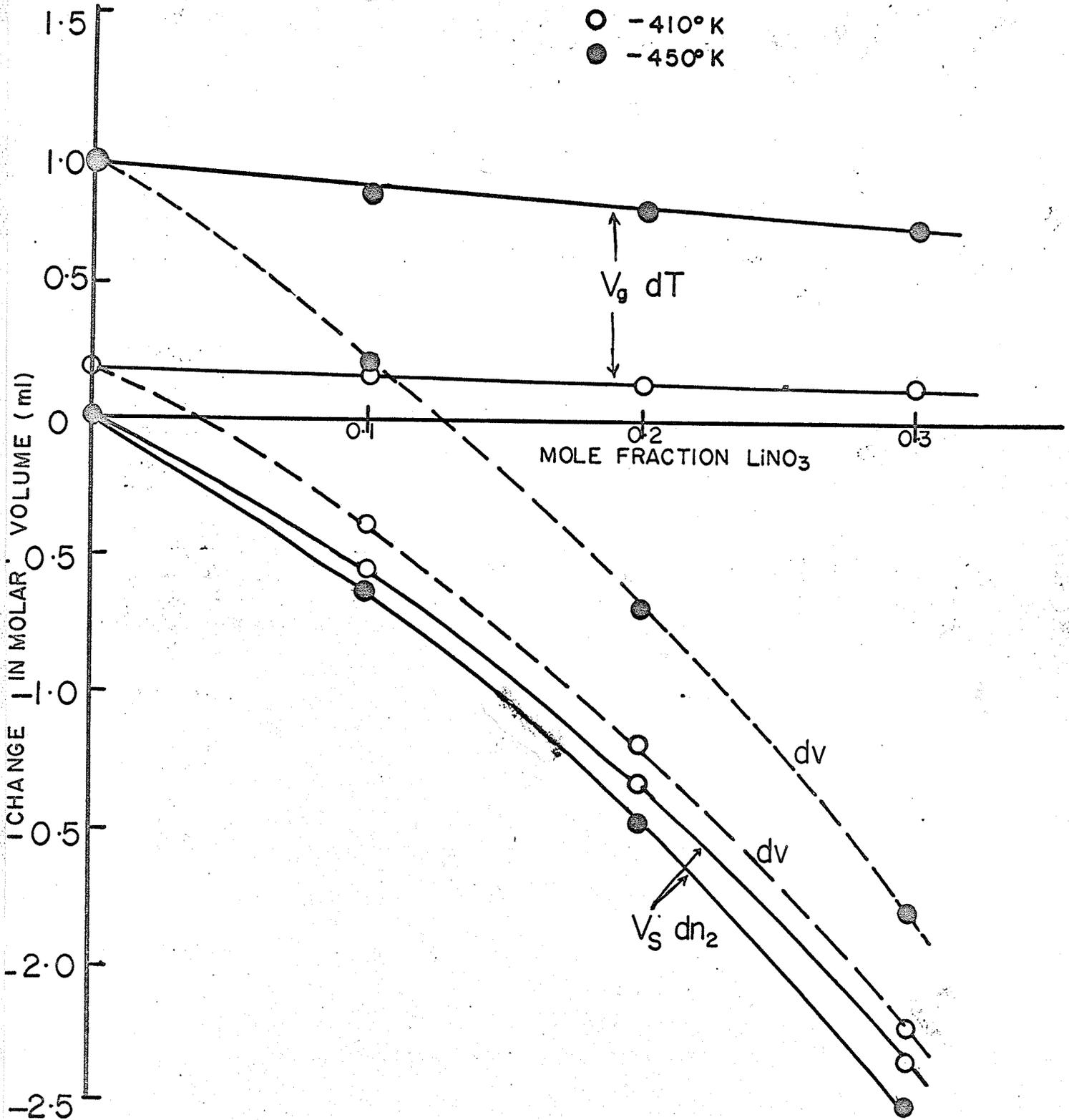
Chapter IV

VISCOMETRY

INTRODUCTION

The motion of a particle in a fluid depends to
a large extent on the internal structure of that fluid. In
molten salts, where interionic effects are considerable
even in dilute solutions, one can expect strong fields of
force and potential barriers to affect the migration of an
ion. Measurements of diffusion, conductance, transport
number and viscosity, therefore yield important information
on the transport properties of molten salts. The relation
between viscosity of a fluid and thermodynamic properties
like entropy of fusion and specific volume have also been
pointed out by several workers. For instance, Batchinski[77]
considered that viscosity is inversely proportional to free
volume and showed that the plot of viscosity against
inverse of specific volume is linear, for a number of systems.
According to this a plot of viscosity against specific
volume must give a straight line. A linear relationship
between the entropies of fusion and the ratio of bulk
viscosity (η_B) and shear viscosity (η_S) has been put forward
by Higgs and Litovitz[78]. They found that the equation

$$\ln \eta_B / \eta_S = A - B \triangle sf / R$$

satisfied the experimental data for a series of nitrates.
According to Marchessault and Litovitz[79], there may exist
a series of such relationships, each satisfying a particular
family of molten salts.

The temperature dependence of viscosity of fluids
in general, has been the subject of much discussion, ever
since Guzman[80] proposed the exponential relationship for
room temperature liquids, viz.,

$$\eta = B \ e^{E_{vis}/RT} \quad \text{where}$$

E_{vis} is the activation energy of viscous flow and B is a
constant, independent of temperature. Andrade[81] gave a
similar relation based on the concept of momentum transfer
in liquids. The constant B has been found to be temperature
dependent, particularly by Frenkel[82] and this has given rise
to speculations as to the nature of the pre-exponential term.
A number of equations[83] involving quantities such as pressure,
volume, surface tension, density, velocity of sound,
refractive index, latent heat of fusion and evaporation and
molecular weight, have been given to describe viscosity
data. Eyring and coworkers[84] applied Eyring's reaction rate
theory to obtain the following equation for the viscosity of
a fluid:

$$\eta = 1.09 \times 10^{-3} \ \frac{M^{1/2} \ T^{3/2}}{V^{2/3} \ \Delta H_{vap}} \ e^{E_{vis}/RT}$$

where   M = molecular weight

V = molar volume

ΔH_{vap} = latent heat of vapourization

E_{vis} = activation energy of viscous flow

This equation has been shown[85] to describe satisfactorily the temperature dependence of viscosity for a number of liquids. This relation has further given rise to many attempts[86] to relate E_{vis} with ΔH_{fusion} and ΔH_{vap}.

Irrespective of the detailed mechanism of viscous flow, the experimental data for a large number of liquids yield a linear relationship between $\log \eta$ and $\frac{1}{T}$, thus providing experimental support for the exponential relationship of Guzman[80] and Andrade[81].

The activation energy of viscous flow, E_{vis}, provides a satisfactory temperature-independent quantity for comparison purposes. A high value of E_{vis} suggests that much of the three dimensional lattice of solid state is retained in the liquid (e.g. liquid silicates), since more energy is required to break up the bonds in such a lattice. It has been suggested by Bloom and Heymann[87] that the units of flow in electrical conductance and viscosity may be different. The ratio E_{vis}/E_Λ (where E_Λ is the activation energy of equivalent conductance) has been found to have a value greater than unity, in most of melts studies. This indicates a much larger configurational change in the melt for viscous flow than for ionic migration. The ratio E_{vis}/E_Λ presents a convenient test of the ionic (or covalent) nature of molten salt, viz., a high value of E_{vis}/E_Λ denotes a predominantly

ionic melt; whereas, a low value indicates strong covalent character in the melt.

There is no simple theory which describes quantitatively the relationship between viscosity and composition for molten salt mixtures. Bloom and Heymann[88] determined the viscosity in a number of molten salt mixtures and found, in each case, the viscosity isotherm to be either ''ideal'' or to exhibit negative deviation from ideality, with respect to the composition of the mixture. In some cases their results suggested the formation of a complex between the two constituents of the mixture.

PREVIOUS RELEVANT INVESTIGATIONS

The only reported study of viscosity of molten lithium chlorate is by Klotschko and Grigorew[71]. As already pointed out in the densitometry chapter (page 30), their determination of viscosity was only of minor importance in the work reported. Their value for the viscosity of molten anhydrous lithium chlorate (66.2 cp at 128°C), is almost twice that found in the present work. A possible explanation for this disparity is given in the discussion part of this chapter. There is no work in the literature, on the viscosity of mixtures of molten salts containing lithium chlorate as one of their constituents.

The viscosity of molten lithium nitrate has been shown to satisfy[89] the equation

$$\eta = 11.9 \times 10^4 \, e^{\frac{4230}{RT}}$$

Experimental techniques that have been employed for the determination of viscosity of molten salts, range from conventional Ostwald flow viscometers[90] to the more recent techniques such as determination[91] of the logarithmic decrement of an oscillating pendulum whose bulk contains the fluid and maximum bubble pressure method[92]. Since the temperature range in which the present investigation was carried out was sufficiently low, the conventional Ostwald type viscometer as modified by Campbell and Debus[93] was employed by me.

EXPERIMENTAL

Viscometer construction: The viscometers were made of Pyrex glass and had the shape shown in Fig. 12. The tip of the capillary had a trumpet-shape, so as to minimise the kinetic energy correction. A small fritted glass disc (E) attached to the side arm prevented any silt or suspended impurities from getting into the viscometer.

FIG·12 VISCOMETER
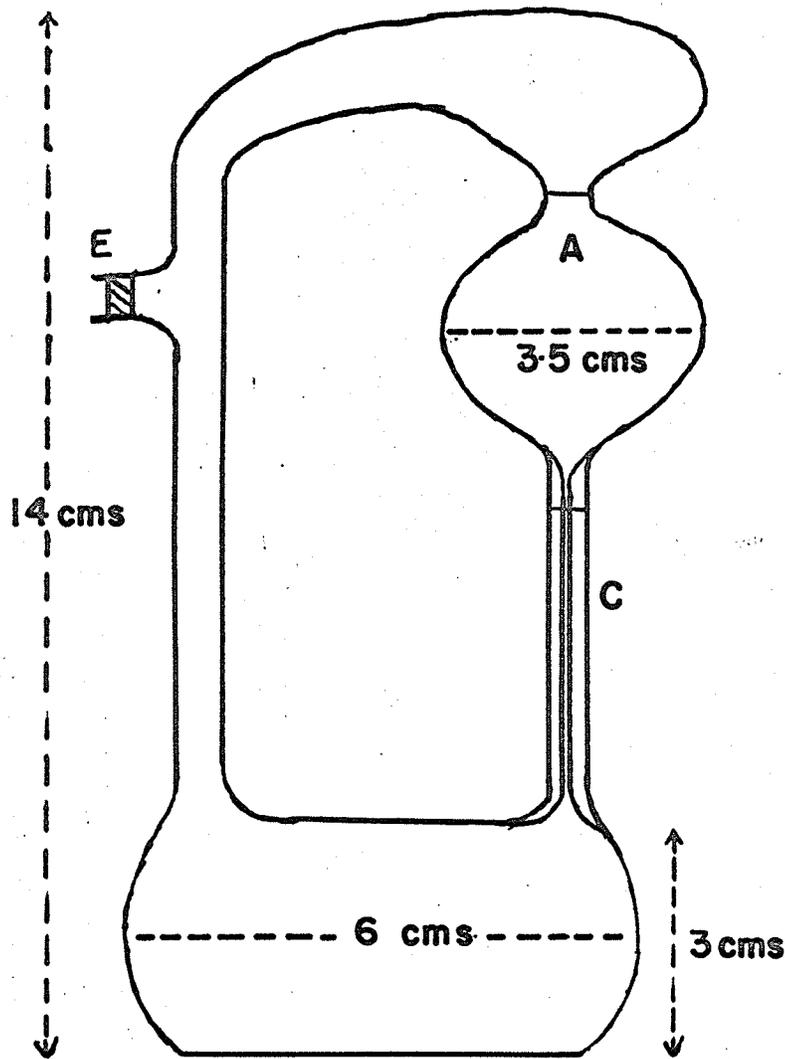
E fritted glass disc

C 1 mm i·d· capillary

<u>Viscometer calibration</u>: The viscometers were calibrated with distilled water at different temperatures, in the region 110°C - 160°C. Sufficient distilled water was placed in the bulb B. The bulb B was immersed in a bath of liquid nitrogen and a vacuum pump was attached to the side tube E. When the water in the bulb B had frozen, the viscometer was evacuated. The bulb B was then allowed to stand in the air till all the ice was transformed into liquid. This process of freezing, evacuating, and re-melting was repeated at least four times, in order to remove all the dissolved gases (particularly oxygen) from the water. Finally the side tube E was vacuum sealed.

The sealed viscometer was then held in position by means of clamps (E) in a rotating device, Fig. 13. This rotating device was helpful in filling the pear-shaped bulb A without removing the viscometer from the thermostat. It consisted of a thick brass rod (R) driving a suitably positioned set of toothed-wheels (C). A turn on the knob (B) attached to the top of the rod (R), rotated the disc (D)(to which the viscometer was clamped) through 180°. In this way it was possible to tilt the viscometer through any desired angle and fill the pear-shaped bulb (A).

The bulb (A) having been filled, the viscometer was kept in a vertical position. The temperature of the

FIG·13 ROTATING DEVICE FOR VISCOMETER
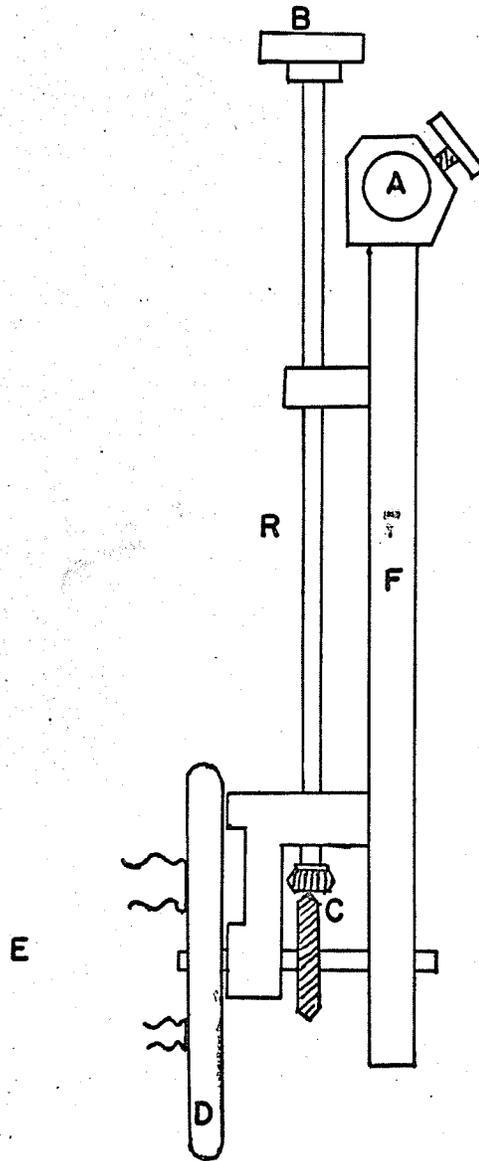
(see text for description of parts.)

thermostat was controlled and measured as described on page 33. The time was measured to $\pm$ 0.1 sec by means of an electrical clock. The flow times were measured at various temperatures in the range $100^{\circ}C$ to $160^{\circ}C$. A plot of flow time vs temperature for one of the viscometers employed in the present study is given in Fig. 14. Using the literature values for the viscosity[94] and density[95] of water, a factor $C = \frac{\eta}{\rho t}$ was calculated, where η = viscosity of water in millipoise; ρ = density of water in gm ml^{-1} and t = time of flow in seconds. This calibration factor was plotted against temperature and is given in Fig. 15.

Filling technique: The technique of filling the viscometer with lithium chlorate or its mixtures was indentical with that described for filling dilatometers (p.36). After filling the viscometer with the desired quantity of the experimental substance, it was vacuum sealed at a point immediately in front of the small fritted glass disc. The fritted glass disc effectively prevented any suspended impurities from getting into the viscometer.

Viscosity determinations: The measurement of flow time for molten lithium chlorate and its mixtures was carried out in an identical manner to that of water. The rotating device was extremely helpful in ref lling the pear-shaped bulb.

FIG.14 FLOW TIME vs TEMPERATURE (water)
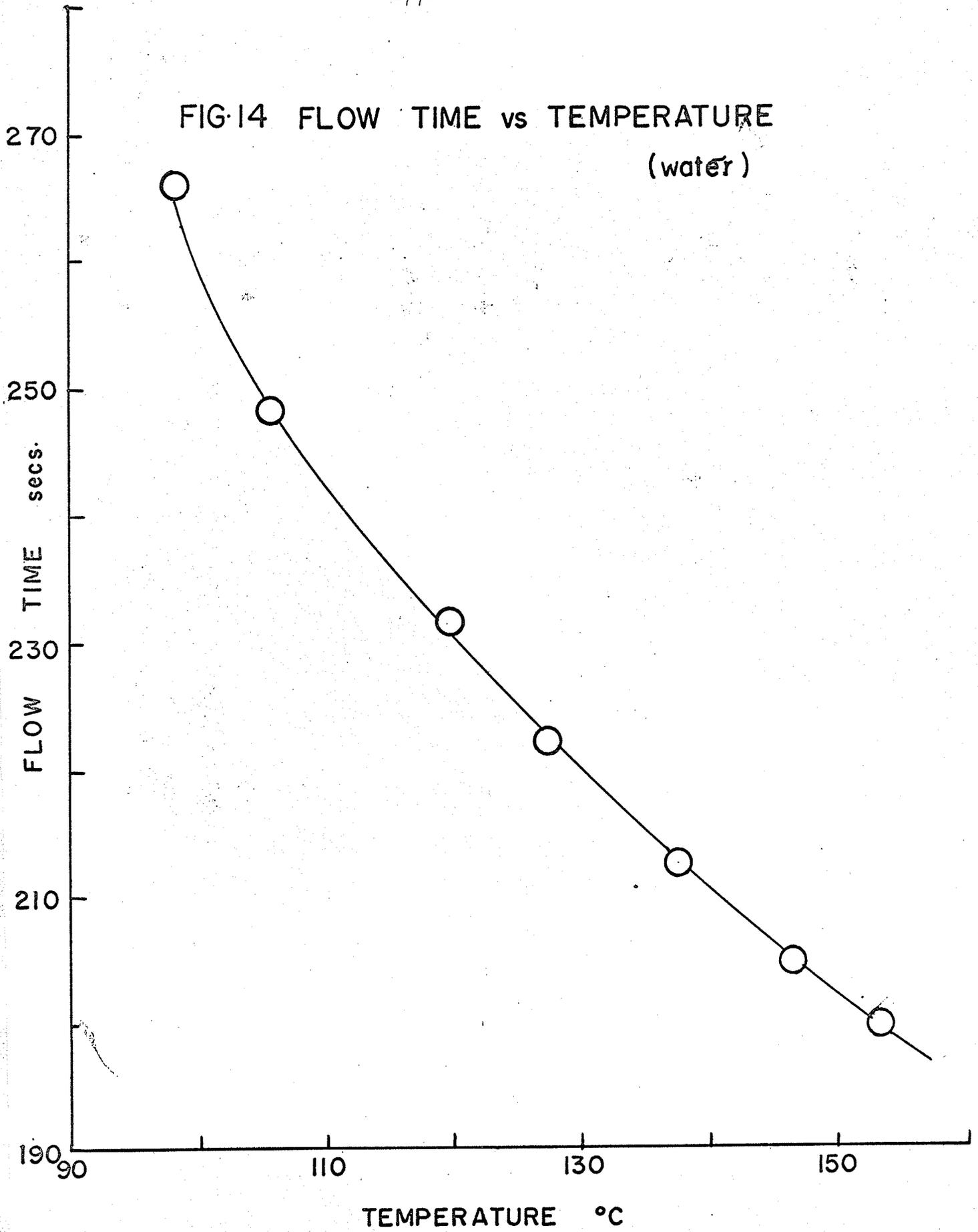
FIG·15   CALIBRATION PLOT FOR VISCOMETER
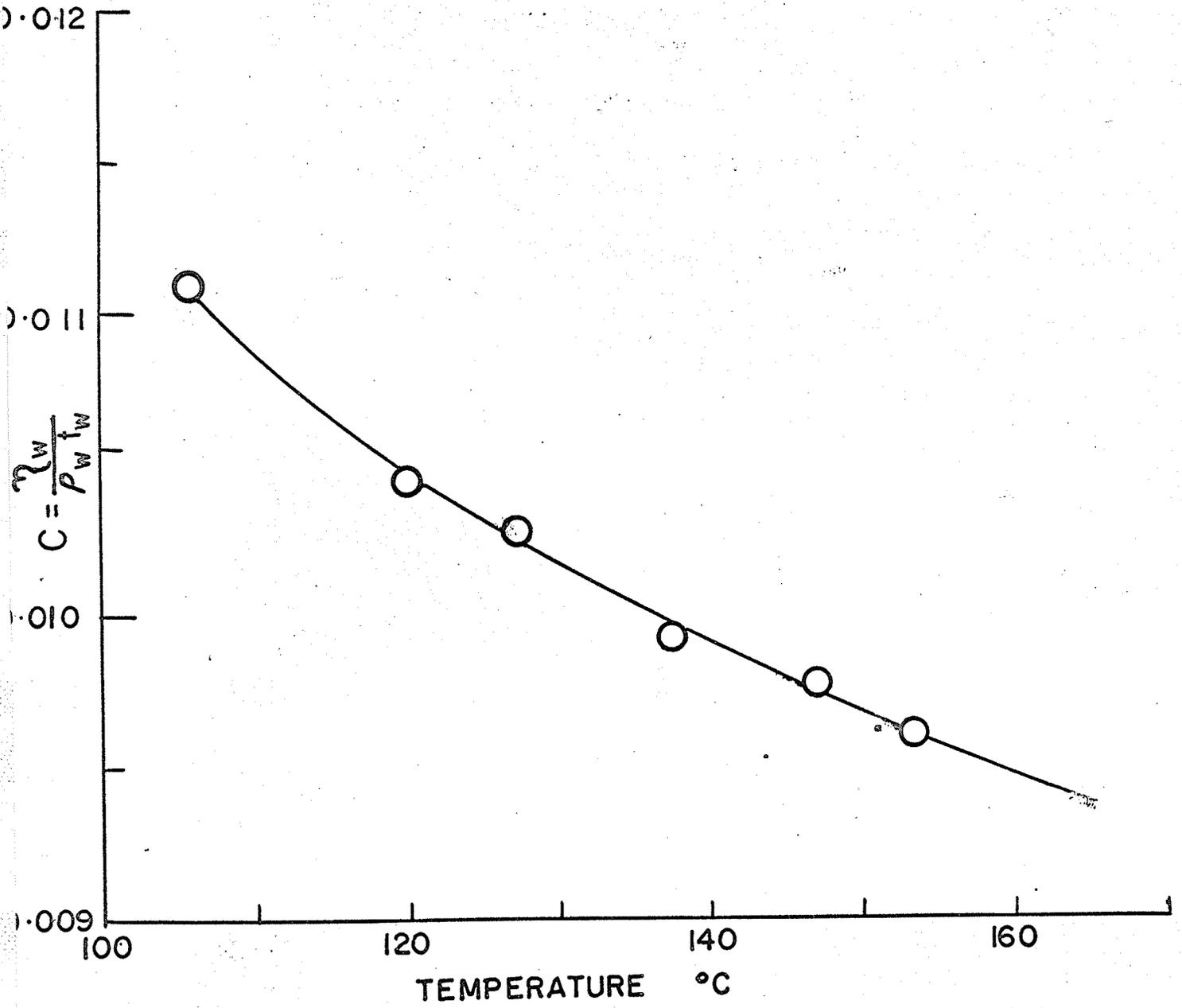
The time of flow was measured, as before, to $\pm$ 0.1 sec. The reproducibility of this time of flow was $\pm$ 5 secs in a total flow time of ca. 10,000 secs. The flow times were measured at different temperatures and for mixtures with 0.000, 0.030, 0.082, 0.131, 0.206 and 0.260 mole fraction of lithium nitrate in lithium chlorate. The viscosity is simply given by the relation, η = Cρt where t is the flow time for the melt and ρ its density. The appropriate density values were obtained by standard interpolation techniques from the density data on page   .

Over-all precision of the method: The flow times were measured to $\pm$ 5 secs in ca. 10,000 secs. This gives a deviation of $\pm$ 0.05%. Densities (see page 40) were measured correct to $\pm$ 0.01%. This points to an over-all precision of at least $\pm$ 0.1% in the viscosity values, but the viscosities of water (used as the standard) are only correct to $\pm$ 1%. Therefore, the reproducibility of the data is $\pm$ 0.1%; but the accuracy is only ca. $\pm$ 1%. It should be pointed out that at lower temperatures, the temperature fluctuations (though only $\pm$ 0.1%) cause an observable error in the viscosity values, since the temperature coefficient of viscosity, at low temperatures is large. But the deviation due to this effect is well within the accuracy of the experiment.

RESULTS

The viscosities, in units of poise, of pure lithium chlorate and its mixtures with lithium nitrate containing 0.030, 0.082, 0.131, 0.206 and 0.260 mole fraction lithium nitrate are given in Tables XII to XVII. The plots of η vs T are given in Fig. 16. The viscosity temperature data have been fitted to the equation

$$\eta = \eta_o \, e^{\frac{E_{vis}}{RT}}$$, by the method of least squares on a computor. The last column in each of the above tables gives values of $\log \eta$ which are plotted against $\frac{1}{T}$ in Fig. 17. Table XVIII lists the values of η_o and E_{vis} for the different mixtures as obtained from the 'best' equation.

The variation of viscosity with changes in composition at constant temperature is shown in Table XIX and Fig. 18. The interpolations at arbitrarily chosen temperatures were carried out by means of the computor, employing the equations of 'best' fit. The data so obtained were analysed by the method of least squares and were found to fit the equation $\eta = B_o + B_1 n_2 + B_2 n_2^2$ satisfactorily. The values of B_o, B_1 and B_2 corresponding to each mixture are tabulated in Table XX.

TABLE XII

Viscosities of Pure Lithium Chlorate

$t^\circ C$	$T^\circ K$	$\frac{1}{T} \times 10^3 (deg^{-1})$	η (poise)	$\log \eta$
131.8	404.9	2.4698	0.334	-0.4763
133.3	406.4	2.4606	0.320	-0.4949
135.0	408.1	2.4504	0.305	-0.5157
137.5	410.6	2.4355	0.296	-0.5287
138.7	411.8	2.4284	0.277	-0.5575
142.7	415.8	2.4050	0.249	-0.6038
144.7	417.8	2.3935	0.235	-0.6289
148.4	421.5	2.3725	0.218	-0.6615
152.4	425.5	2.3502	0.199	-0.7011
156.3	429.4	2.3288	0.194	-0.7122
158.6	431.7	2.3164	0.177	-0.7520
162.1	435.2	2.2978	0.168	-0.7747
166.9	440.0	2.2727	0.155	-0.8097

Equation for 'best' fit: $\eta = 1.979 \times 10^{-5} e^{\frac{7813}{RT}}$

Standard deviation: $\pm$ 0.005 poise

TABLE XIII

<u>Viscosities of Lithium Chlorate-Lithium Nitrate Mixture</u>

n_2 = mole fraction lithium nitrate = 0.030

$t^{\circ}C$	$T^{\circ}K$	$\frac{1}{T}$ x10^3(deg^{-1})	η (poise)	log η
134.0	407.1	2.4564	0.364	-0.4389
136.7	409.8	2.4402	0.341	-0.4672
139.4	412.5	2.4242	0.315	-0.5017
142.6	415.7	2.4056	0.290	-0.5376
147.4	420.5	2.3781	0.258	-0.5884
150.4	423.5	2.3613	0.243	-0.6144
155.7	428.8	2.3321	0.212	-0.6737
157.3	430.4	2.3234	0.209	-0.6799
161.7	434.8	2.2999	0.191	-0.7190
167.8	440.9	2.2681	0.170	0.7696
171.7	444.8	2.2482	0.158	-0.8013

Equation for the 'best' fit: $\eta = 1.814 \times 10^{-5} e^{\frac{8002}{RT}}$

Standard deviation: $\pm$ 0.003 poise

TABLE XIV

Viscosities of Lithium Chlorate-Lithium Nitrate Mixture

n_2 = mole fraction Lithium nitrate = 0.082

$t°C$	$T°K$	$\frac{1}{T}$ x10^3(deg^{-1})	η (poise)	log η
133.2	406.3	2.4612	0.436	-0.3605
136.9	409.0	2.4450	0.408	-0.3893
138.4	411.5	2.4301	0.386	-0.4134
140.8	413.9	2.4160	0.365	-0.4377
145.4	418.5	2.3895	0.322	-0.4921
149.8	422.9	2.3646	0.289	-0.5391
157.2	430.3	2.3240	0.244	-0.6126
161.2	434.3	2.3026	0.223	-0.6517
167.7	440.8	2.2686	0.194	-0.7122

Equation for the 'best' fit: $\eta = 1.202 \times 10^{-5} \; e^{\frac{8481}{RT}}$

Standard deviation: $\pm$ 0.002 poise

TABLE XV

Viscosities of Lithium Chlorate-Lithium Nitrate Mixture

n_2 = mole fraction Lithium nitrate = 0.131

$t^{\circ}C$	$T^{\circ}K$	$\frac{1}{T} \times 10^3 (deg^{-1})$	η (poise)	$\log \eta$
136.4	409.5	2.4420	0.444	-0.3526
138.7	411.8	2.4284	0.420	-0.3768
143.9	416.0	2.4039	0.375	-0.4260
146.5	419.6	2.3832	0.338	-0.4711
153.1	426.2	2.3463	0.290	-0.5376
158.6	431.7	2.3164	0.259	-0.5867
165.9	439.0	2.2779	0.221	-0.6556
172.6	445.7	2.2437	0.192	-0.7167

Equation for the 'best' fit: $\eta = 1.446 \times 10^{-5} \ e^{\frac{8401}{RT}}$

Standard deviation: $\pm$ 0.003 poise

TABLE XVI

Viscosities of Lithium Chlorate-Lithium Nitrate Mixture

n_2 = mole fraction Lithium nitrate = 0.206

$t^{o}C$	$T^{o}K$	$\frac{1}{T}$ x10^3(deg^{-1})	η (poise)	$\log \eta$
135.4	408.5	2.4480	0.502	-0.2993
140.6	413.7	2.4172	0.417	-0.3799
144.9	417.0	2.3981	0.385	-0.4145
147.9	421.0	2.3753	0.349	-0.4572
152.3	425.4	2.3507	0.320	-0.4949
160.3	433.4	2.3073	0.272	-0.5654
162.7	435.8	2.2946	0.255	-0.5935
167.8	440.9	2.2681	0.232	-0.6345
170.9	444.0	2.2523	0.213	-0.6716

Equation for the 'best' fit: $\eta = 1.848 \times 10^{-5} \, e^{\frac{8254}{RT}}$

Standard deviation: $\pm$ 0.008 poise

TABLE XVII

Viscosities of Lithium Chlorate-Lithium Nitrate Mixture

n_2 = mole fraction Lithium nitrate = 0.260

$t^{\circ}C$	$T^{\circ}K$	$\frac{1}{T} \times 10^3 (deg^{-1})$	η (poise)	$\log \eta$
136.9	410.0	2.4390	0.495	-0.3054
137.7	410.8	2.4343	0.490	-0.3098
139.6	412.7	2.4231	0.457	-0.3401
142.6	415.7	2.4056	0.420	-0.3768
146.7	419.8	2.3821	0.372	-0.4295
152.5	425.6	2.3496	0.328	-0.4841
157.3	430.4	2.3234	0.294	-0.5317
158.2	431.3	2.3186	0.289	-0.5391
165.8	438.9	2.2784	0.249	-0.6038
169.4	442.5	2.2599	0.231	-0.6364
171.8	444.9	2.2477	0.221	-0.6556
172.5	445.6	2.2442	0.213	-0.6716

Equation for the 'best' fit: $\eta = 1.621 \times 10^{-5} e^{\frac{8399}{RT}}$

Standard deviation: $\pm$ 0.006 poise

TABLE XVIII

Activation Energies for Viscous Flow

$$\eta = \eta_o \; e^{E_{vis}/RT}$$

n_2	$\eta_o \times 10^5$	$E_{vis(cals)}$
0.000	1.979	7813
0.030	1.814	8002
0.082	1.202	8481
0.131	1.446	8401
0.206	1.848	8254
0.260	1.621	8399

TABLE XIX

Isothermal Viscosities of Lithium
Chlorate-Lithium Nitrate Mixtures

n_2 = mole fraction lithium nitrate

$T^{O}K$	n_2=0.000 (poise)	n_2=0.030 (poise)	n_2=0.082 (poise)	n_2=0.131 (poise)	n_2=0.206 (poise)	n_2=0.260 (poise)
390.0	(0.473)	(0.553)	(0.680)	0.738	0.781	0.826
400.0	(0.367)	0.428	0.518	0.563	0.599	0.630
410.0	0.289	0.334	0.399	0.435	0.465	0.487
420.0	0.230	0.265	0.312	0.340	0.365	0.381
430.0	0.185	0.212	0.246	0.269	0.290	0.302
440.0	0.150	0.171	0.196	0.215	0.233	0.241
450.0	0.123	0.140	0.158	0.174	0.189	0.195

NOTE: Values in paranthesis correspond to those of supercooled liquid.

TABLE XX

Values of B_0, B_1 and B_2 in the Equation

$$\eta = B_0 + B_1 n_2 + B_2 n_2^2$$

$T^{\circ}K$	B_0	B_1	B_2	Standard deviation (poise)
390.0	0.479	2.676	-5.341	$\pm$0.014
400.0	0.372	1.958	-3.828	$\pm$0.009
410.0	0.292	1.451	-2.775	$\pm$0.006
420.0	0.233	1.088	-2.033	$\pm$0.003
430.0	0.187	0.825	-1.503	$\pm$0.002
440.0	0.152	0.632	-1.119	$\pm$0.001
450.0	0.124	0.489	-0.840	$\pm$0.001

FIG·16 VISCOSITY vs TEMPERATURE
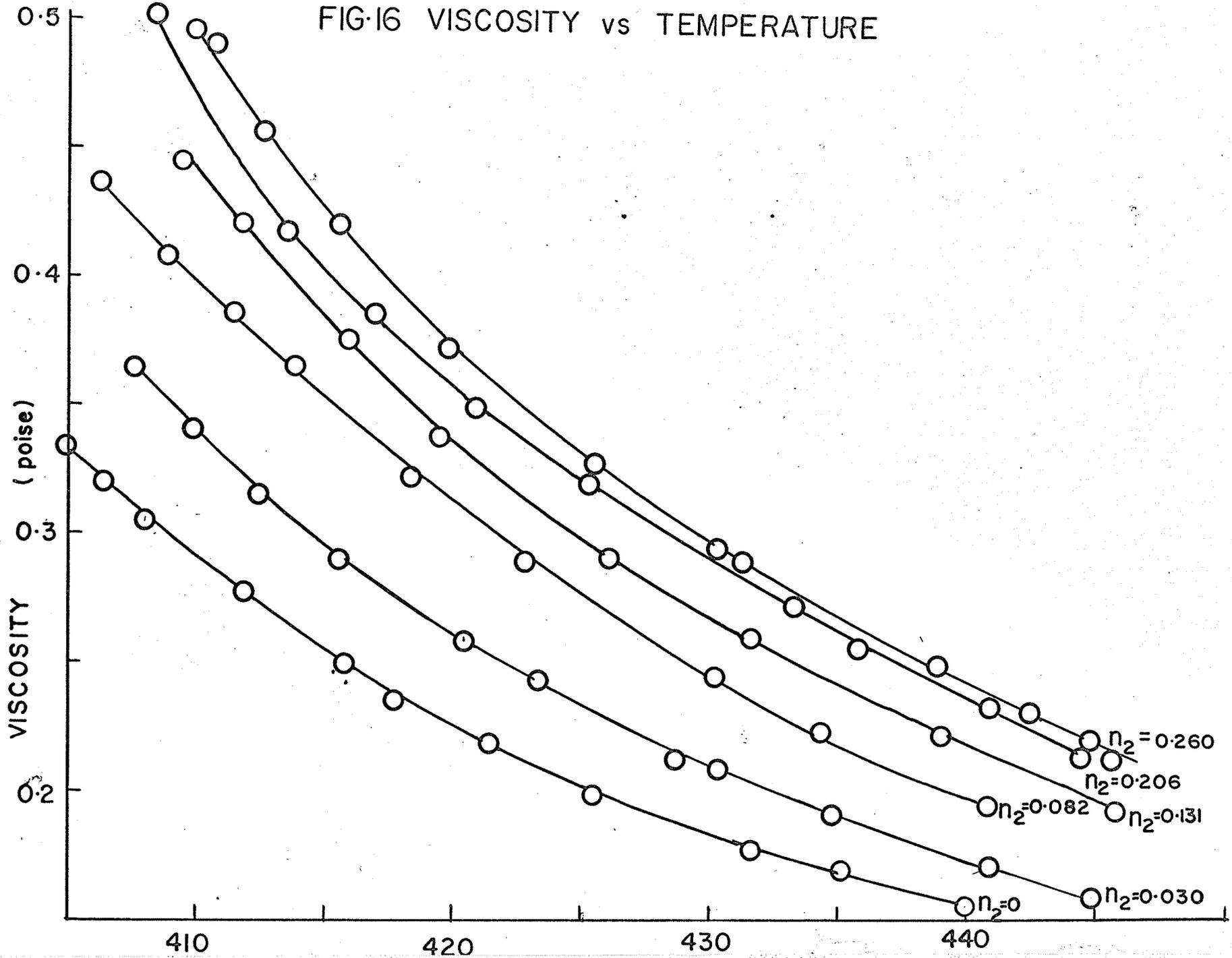
FIG·17 ACTIVATION ENERGY FOR VISCOUS FLOW:
$\log \eta$ vs $\frac{1}{T}$ plots
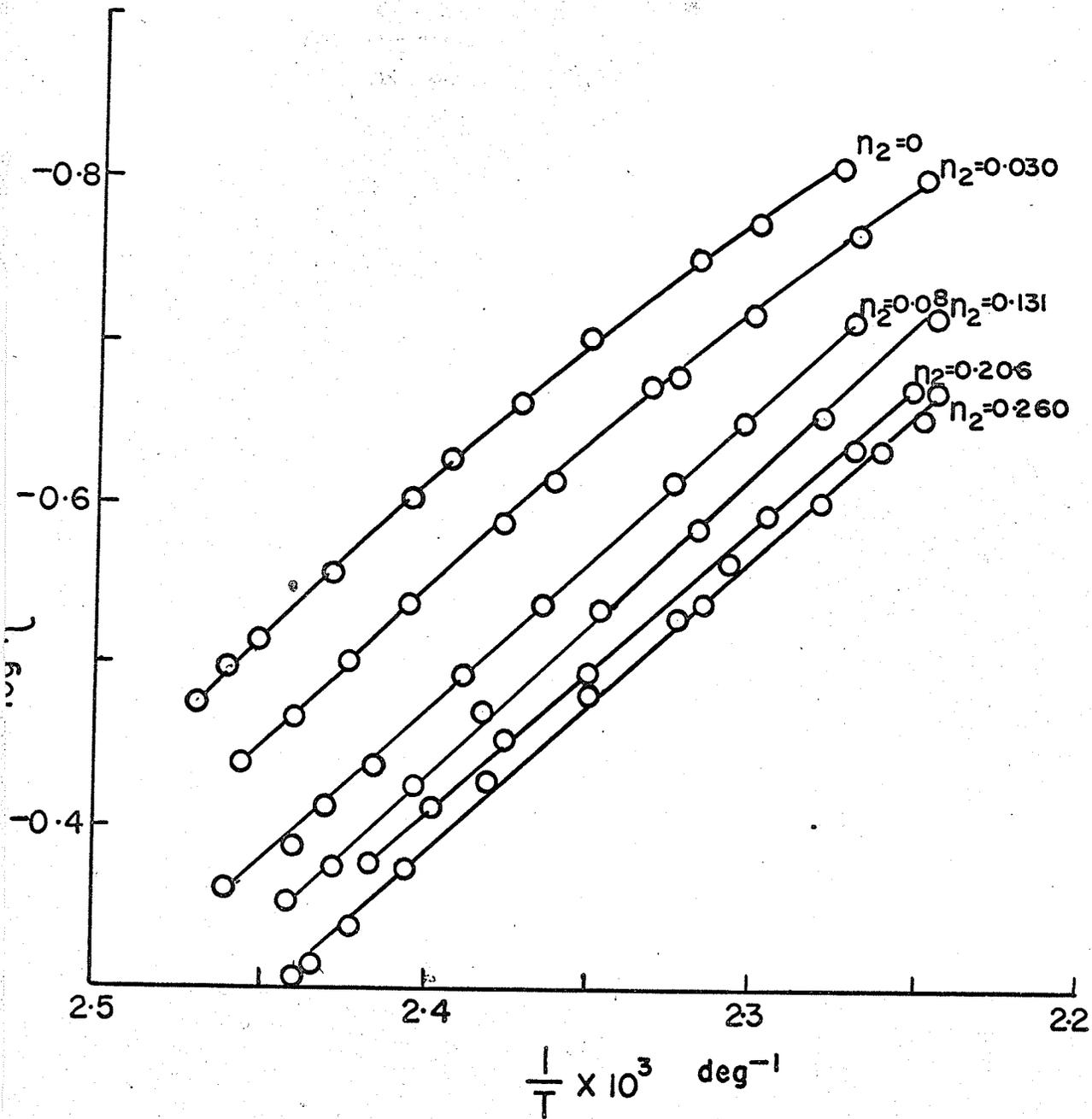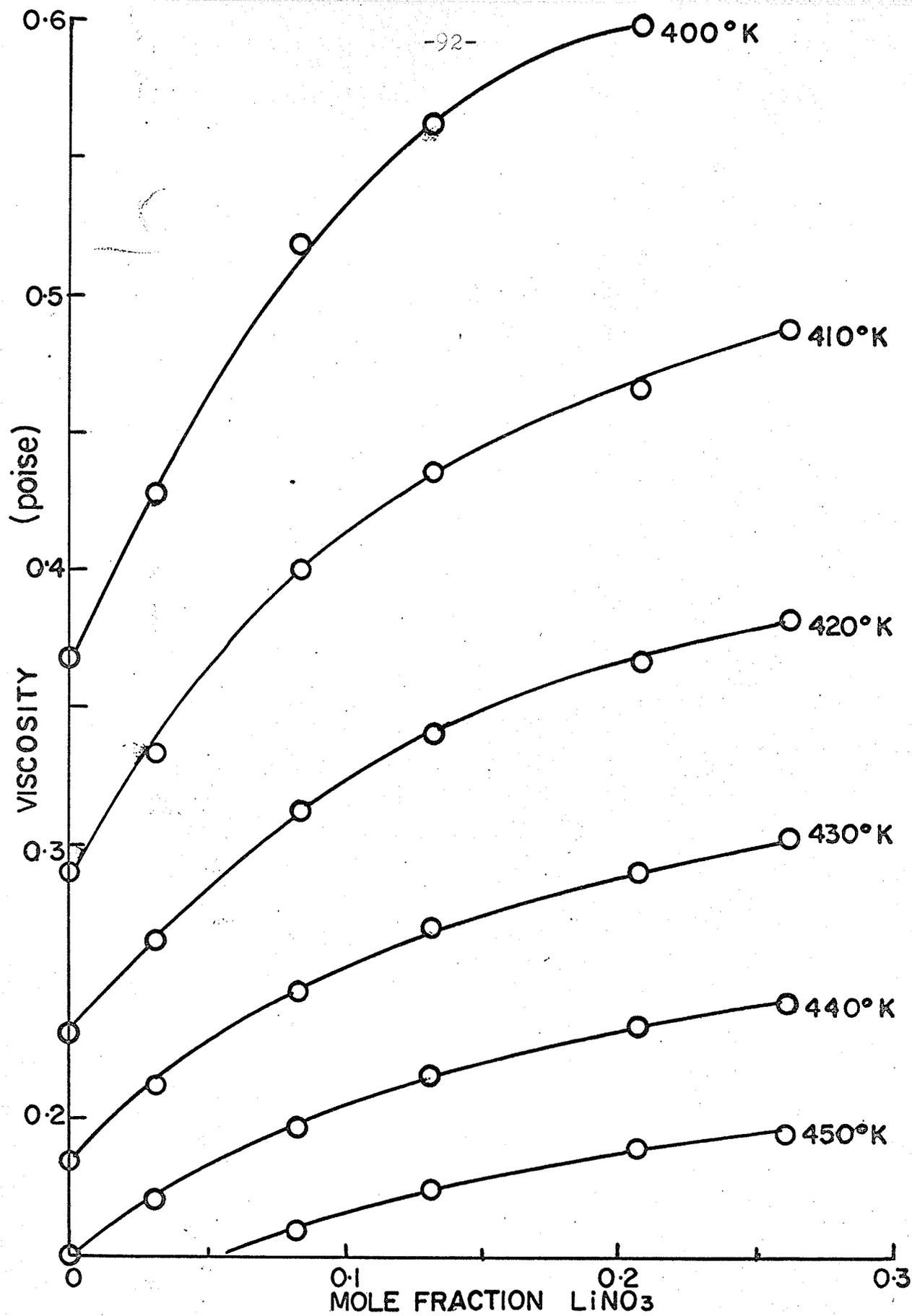
FIG·18 VISCOSITY ISOTHERMS

DISCUSSION

I have found that the viscosity of molten lithium chlorate in the temperature range 128° - 170°C is represented by the relation:

$$\eta = 1.98 \times 10^{-4} \ e^{\ 7860/RT}$$

Klotschko and Grigorew[71] reported the values of viscosity of molten lithium chlorate as 66.2 cp and 52.2 cp at 128° and 136°C respectively. The values consistently obtained by me at these temperatures are 38.3 cp and 29.8 cp respectively. The abnormally high value of Klotschko and Grigorew may have resulted from 1) failure to calibrate their flow-type viscosmeter for the appropriate temperature region and 2) clogging of the capillary due to the silt normally present in the absence of filtration. From the calibration of the viscometer used in the present work, it can be said that the value of viscosity obtained by utilising the calibration data at 35°C is approximately one and a half times that obtained from the calibration data at 128°C. Since, Klotschko and Grigorew neither describe their experimental technique nor make any mention of their precautions to prevent clogging of the capillary, it is not possible to point out the exact cause for their high value. In the present work the calibration was carried out over the entire region of temperature

studied and special precautions were taken to prevent any suspended impurity from entering the viscometer (cf. page **72**).

A viscosity of 38.3 cp at the melting point for lithium chlorate is very large compared to any known values for simple salts. Generally molten salts possess viscosity values of between 1 to 4 centipoises. The viscosity of molten lithium chlorate is, in fact, comparable to those of molten oxides, silicates and especially to those of complex salts like $K_2Cr_2O_7$. Such a high value of viscosity for lithium chlorate not only indicates a very strong covalent character of its melt, but also suggests the presence of much more ordered lattice than is normally present in covalent melts. By analogy with molten oxides and silicates (whose viscosities are, however, much higher i.e. of the order of a few poises), the lithium chlorate melt probably contains ''clusters'' of molecules held together by some kind of a network structure. Elaboration of this idea is deferred until Chapter VI of this thesis, where all the available data on molten lithium chlorate have been coordinated in the general discussion of the nature of the melt.

The activation energy for viscous flow has been found to be 7.86 k cal. This value compares favourably with those reported in the literature for a number of salts. (cf. Appendix). It is of interest to note that E_{vis} of lithium chlorate is closer to those of ionic melts

(viz., NaCl, KCl, etc.) than to those of covalent melts, such as alkali nitrates. It is probable that a much greater configurational change is involved in viscous flow in molten lithium chlorate than in other covalent melts. The activation energy for electrical conductance has been found to be 6.13 k cal, by Mr. D. F. Williams. The ratio E_{vis}/E_Λ has a value of 1.27, which is in very good agreement with those reported for covalent melts (cf. Appendix).

Yaffe and Van Artsdalen[96] postulated that the activation energy for viscous flow in lithium and sodium salts must increase with temperature for the following reason: As the melt expands with temperature, coulombic forces between ions decrease and therefore E_{vis} decreases with increase of temperature. On the other hand, expansion of the melt results in a net decrease in the coordination number in the melt (due to an increasing number of holes) and hence the attractive force per nearest neighbour increases. This, according to Yaffe and Van Artsdalen, results in an increase of E_{vis} with increase in temperature. Yaffe and Van Artsdalen consider that the latter effect is much greater if the difference between size of cation and anion is larger. Fig. 17 indicates that E_{vis} actually decreases slightly with temperature for the lithium chlorate melt. This is in direct contradiction to the views expressed above by Yaffe and Van Artsdalen. However, it is probable that because of the existence of clusters of molecules in molten lithium

chlorate, the expansion of the melt does not result in a
decrease in coordination number but in a breaking down of
the clusters. The decrease in E_{vis} with increasing
temperature is then quite natural, since there is a lesser
number of bonds to be broken at higher temperatures.

The viscosity data on molten lithium chlorate-
lithium nitrate mixtures have been interpreted in a manner
identical with that described on page 57. The conventional
approach in discussing the deviation from ''ideal''
behaviour (a positive deviation in the present case) has not
been adopted for reasons much the same as those given under
densitometry (cf. page 56). Viscosity is considered as a
function of temperature and composition and all changes in
viscosity are referred to a common standard, i.e. reference
state. As before the reference state has been assumed to
be the viscosity of molten lithium chlorate at its own
melting point (401.0°K). Therefore, the following equation
defines the change in viscosity ($d\eta$):

$$d\eta = \left(\frac{\partial \eta}{\partial T}\right)_{n_2} dT + \left(\frac{\partial \eta}{\partial n_2}\right)_T dn_2.$$

Although the above equation is not based on any theoretical
model of transport in liquids, the interpretation of the data
is made more elegant by adopting such a technique. The following

notations are used:

$$\left(\frac{\partial \eta}{\partial T}\right)_{n_2} \equiv \eta_g$$

$$\left(\frac{\partial \eta}{\partial n_2}\right)_T \equiv \eta_s$$

As in the case of molar volume, η_g refers to the geometrical contribution and η_s to the structural contribution to the total change in viscosity from that of the reference state.

Values of η_g and η_s were calculated by differentiation of the following equations:

$$\eta_{n_2=const.} = \eta_o \, e^{E_{vis}/RT}$$

$$\eta_{T=const.} = B_o + B_1 n_2 + B_2 n_2^2$$

Thus we have,

$$\eta_g = -\frac{\eta_o E_{vis}}{RT^2} \, e^{E_{vis}/RT}$$

$$\eta_s = B_1 + 2B_2 n_2$$

Tables XXI and XXII, give the values of η_g and η_s so calculated and these are graphically illustrated in Fig. 19 and Fig. 20. The geometrical and structural parts of the

FIG·19 PLOT OF η_g AGAINST TEMPERATURE
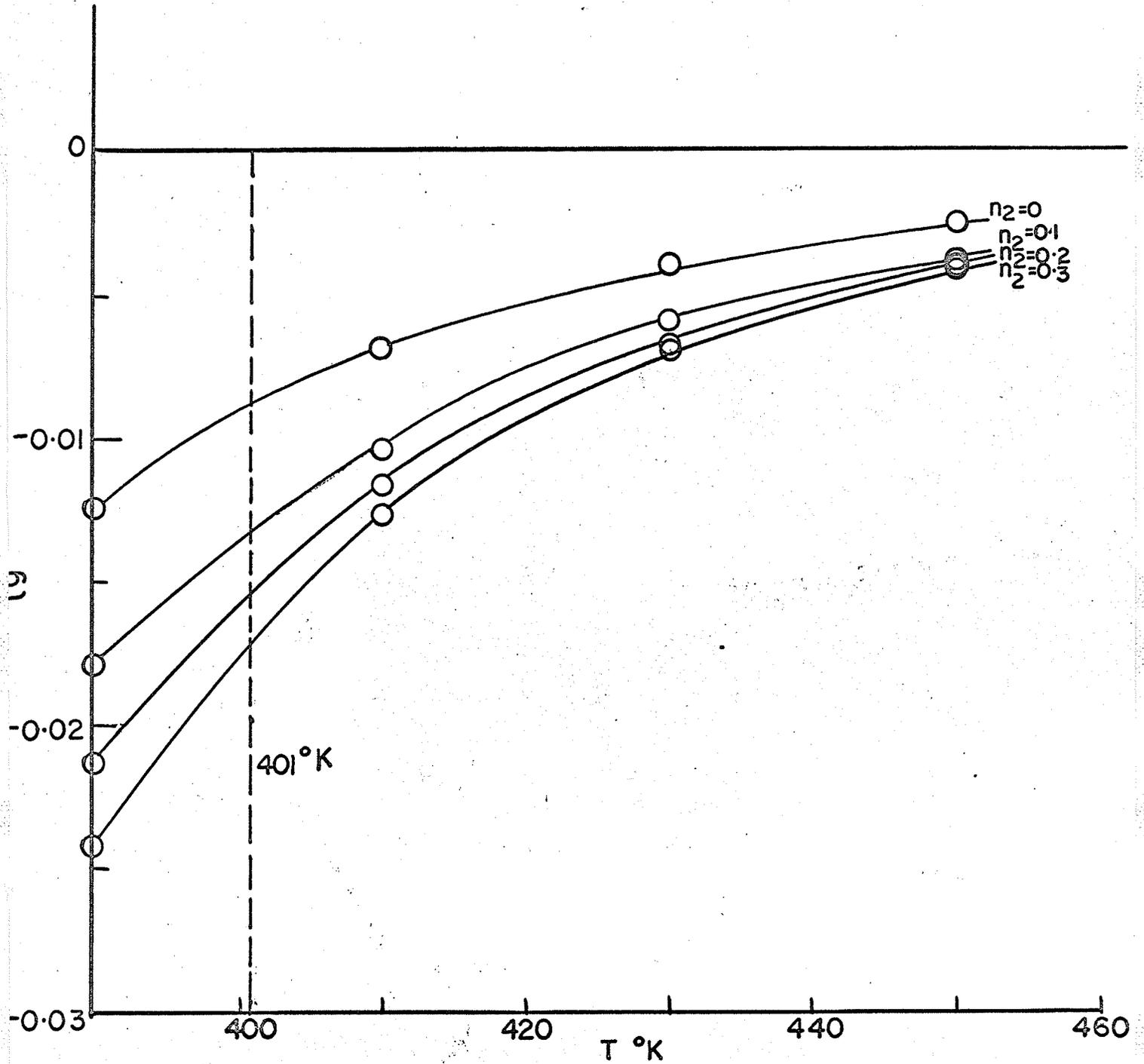
FIG·20 PLOT OF η_s AGAINST COMPOSITION
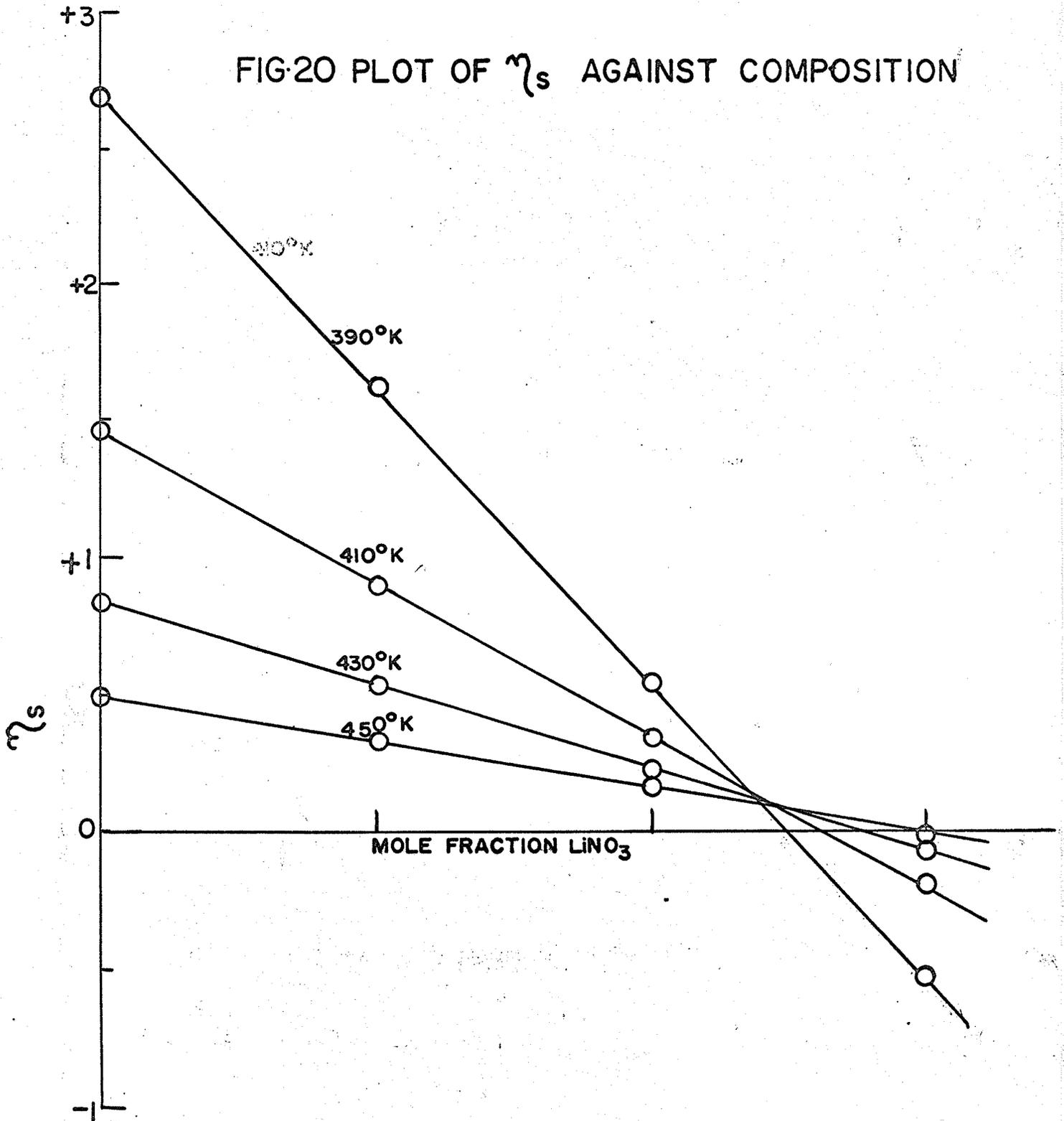
change in viscosity at the reference state are $\eta_g dT$ and

$\eta_s dn_2$ respectively. Since η_g and η_s were not constants

but varied with temperature and n_2 respectively, a

graphical integration procedure was employed to calculate

the values of $\eta_g dT$ and $\eta_s dn_2$. The two parts of the total

change in viscosity $(d\eta)$ are given by,

$$\text{Geometrical part} = \int_{T_{ref}}^{T} \eta_g \, dT$$

$$\text{Structural part} = \int_{n_2=0}^{n_2} \eta_s \, dn_2$$

where T_{ref} = temperature of the reference state

$$= 401.0^{\circ}K$$

The values of the above two integrals were obtained by

measuring the area bounded by the appropriate limits already

defined. Table XXIII lists the values of $\eta_g \, dT$, $\eta_s dn_2$,

and $d\eta$ $(d\eta = \eta_g dT + \eta_s dn_2)$ at different temperatures and

compositions of the melt. These are plotted in Fig. 21 as

functions of composition at the four selected temperatures.

An evaluation of Tables XXI - XXIII and Figs.

19 -21, shows that, at relatively low temperatures and large

concentrations of lithium nitrate, the geometrical contri-

bution is markedly more negative. Considerable sensitivity

to temperature of the geometrical part of $d\eta$ (i.e. $\eta_g dT$)

TABLE XXI

Values of ηg (interpolated) at Selected Compositions

n_2 = mole fraction lithium nitrate

n_2	390.0°K	410.0°K	430.0°K	450.0°K
0.000	-0.0122	-0.00675	-0.00392	-0.00240
0.100	-0.0178	-0.0103	-0.00585	-0.00371
0.200	-0.0212	-0.0115	-0.00642	-0.00385
0.300	-0.0243	-0.0125	-0.00670	-0.00420

TABLE XXII

Values of ηs at Selected Temperatures

n_2 = mole fraction lithium nitrate

n_2	390.0°K	410.0°K	430.0°K	440.0°K
0.000	2.676	1.451	0.825	0.489
0.100	1.608	0.896	0.524	0.321
0.200	0.540	0.341	0.223	0.153
0.300	-0.528	-0.214	-0.078	-0.015

TABLE XXIII

Geometrical and Structural Parts of Total Change in Viscosity

n_2 = mole fraction lithium nitrate

$T \, °K$	$n_2 = 0.000$			$n_2 = 0.100$			$n_2 = 0.200$			$n_2 = 0.300$		
	$\eta_g dT$	$\eta_s dn_2$	$d\eta$	$\eta_{dg} dT$	$\eta_s dn_2$	$d\eta$	$\eta_g dT$	$\eta_s dn_2$	$d\eta$	$\eta_g dT$	$\eta_s dn_2$	$d\eta$
390	+0.118	0	+0.118	+0.177	+0.213	+0.390	+0.208	+0.320	+0.528	+0.231	+0.321	+0.552
410	-0.074	0	-0.074	-0.110	+0.116	+0.006	-0.127	+0.176	+0.049	-0.138	+0.181	+0.043
430	-0.177	0	-0.177	-0.269	+0.068	-0.201	-0.303	+9.104	-0.199	-0.326	+0.111	-0.215
450	-0.235	0	-0.235	-0.360	+0.040	-0.320	-0.412	+0.063	-0.349	-0.444	+0.071	-0.373

FIG.21 GEOMETRICAL & STRUCTURAL CONTRIBUTIONS TO CHANGE IN VISCOSITY
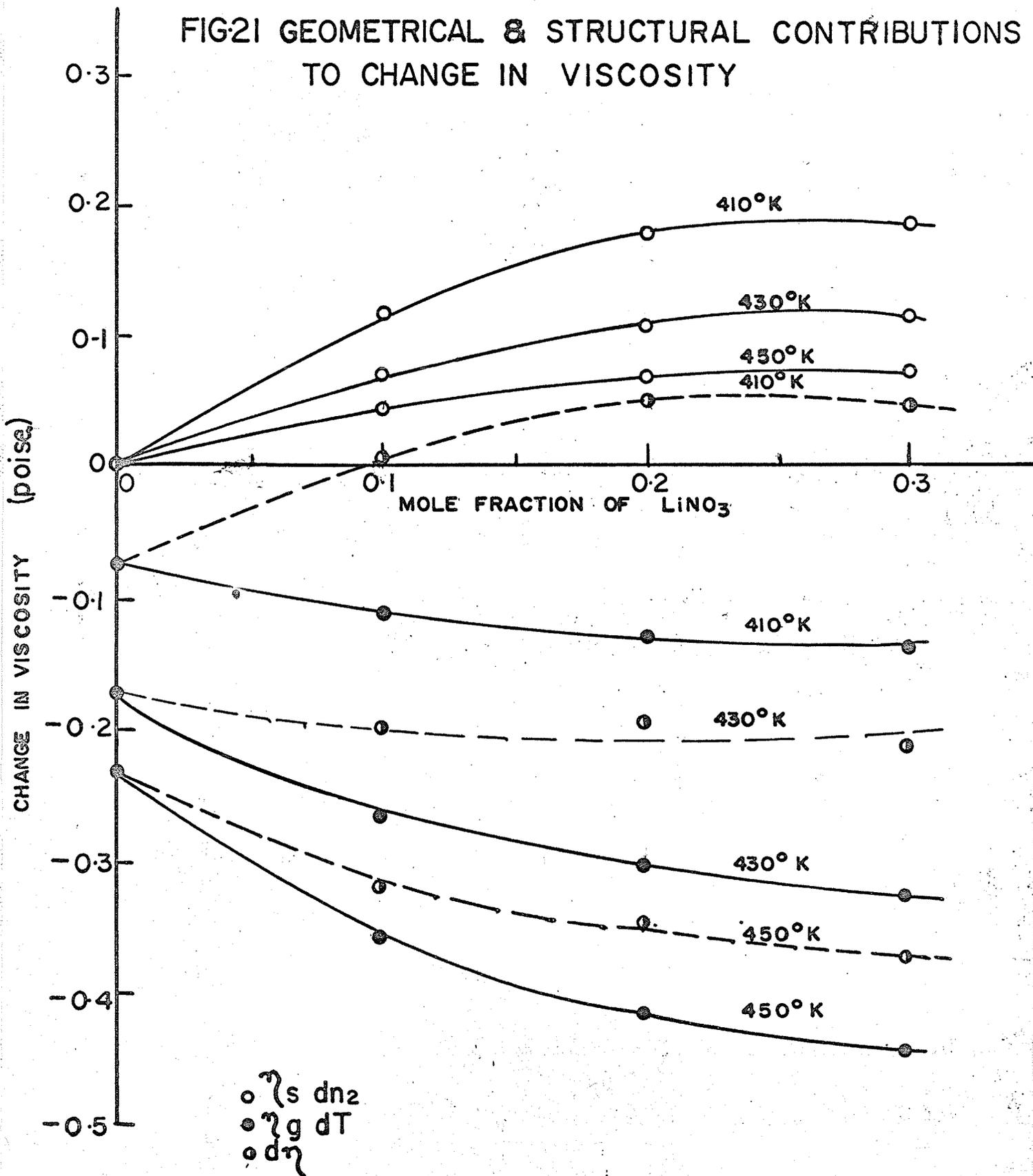
is noticeable in Fig. 21. The sharp fall in viscosity values, in the lower temperature region, with increasing temperature is more marked for molten lithium chlorate systems than for most other molten salt systems. The structural contribution on the other hand, is generally positive and has a higher value at lower temperatures and lower concentrations of lithium nitrate. η_s is very sensitive to both temperature and composition. The presence of nitrate ion in the rather compact lithium chlorate lattice, leads to an increase in viscosity and thus suggests possible formation of bigger and more unsymmetrical ''clusters''. It must be pointed out that in all systems of molten salt mixtures studied so far, only a decrease in viscosity (negative deviation from ''ideality'') is noticed[97]. In this connection the positive deviation exhibited by lithium chlorate-lithium nitrate is very interesting. An examination of Fig. 21 shows why such a positive deviation occurs. Though the effect of temperature (of which $\eta_g dT$ is a measure) is to decrease the viscosity of the reference state, the presence of nitrate ion gives rise to a positive structural contribution, thus neutralising at least a part of the temperature effect. Therefore the net change in viscosity (e.g. in the case of T = 410) is some-times positive. Even at higher temperatures, the observed viscosity is higher than the ideal value,

i.e. $\eta_{obs.} > (n_1 \eta_1 + n_2 \eta_2)$ where η_1 and η_2

are the viscosities of pure lithium chlorate and lithium

nitrate at the temperature of experiment, e.g. at $440^{\circ}K$ $\eta_{obs.}$ is 0.237 poise, whereas $n_1\eta_1 + n_2\eta_2$ is 0.154 poise for a mixture containing 0.2 mole fraction of lithium nitrate.

As to the nature of the interaction between nitrate ion and chlorate lattice, no direct evidence is available. A possible mechanism of the interaction is as follows: Molten lithium chlorate probably consists of ions, free molecules and clusters of molecules of varying sizes. A positive structural contribution indicates either 1) the activation energy for viscous flow has increased or 2) the unit of viscous flow has become more complex or 3) the number of vacant sites or holes available for the migration of the particle has decreased. While there is no direct evidence either to support or contradict the third possibility (see also p.158), there is some evidence for the first two statements. The activation energy for viscous flow has actually increased (cf. Table XVIII) by a small amount. The structural contributions to molar volume (V_S) are negative (cf. p. 61) and therefore it is probable that some kind of a rearragement takes place on the addition of nitrate ion to the chlorate lattice, in such a way as to reduce the volume. This reduction in volume might be the result of formation of more compact structures, arising out of the presence of nitrate ion in the chlorate lattice. Furthermore, the abnormally high viscosity of molten lithium

chlorate might be due to the existence of ''clusters'' and the increase in its value on addition of lithium nitrate might result from the formation of bulkier clusters. The increase in the size of the clusters possibly results from a ''bridging'' of two or more clusters (or of clusters and molecules) by the nitrate ion. The fact that temperature has a more pronounced effect on the viscosity of mixtures with higher concentrations of lithium nitrate (see Figs. 16 and 20), also points towards a more complex structure in molten mixtures than in the pure state. It will be seen later (p. 149) that the thermal data on lithium chlorate-lithium nitrate also support the above mechanism.

The agreement between the observed and calculated values of $d\eta$ is good at lower temperatures and lower concentrations of lithium nitrate, but at higher concentrations of lithium nitrate in the higher temperature regions the calculated values differ by as much as 15% from the observed value. This might result from a break down of the reference state lattice under these conditions. Also, the basic assumption that viscosity in lithium chlorate-lithium nitrate system, is only a function of temperature and composition may not represent adequately the actual case. Other factors, such as free volume, isothermal compressibility, volume and number of holes etc. may also influence viscosity, but in the absence of such data on lithium chlorate, it is very difficult to describe the viscosity changes in mixtures of molten salts, more exactly.

Chapter V

CALORIMETRY

INTRODUCTION

Although calorimetric measurements are among the earliest investigations on molten salts, the real potential of this field remained practically unexplored, until very recently. The importance of heats of fusion and derived quantities such as free energies and entropies of fusion, has already been emphasised in the Introduction. The need for an accurate value of heat of fusion in the interpretation of the results of cryoscopic measurements has been pointed out by Janz and coworkers[98]. For a comparison of entropies of fusion of a large number of salts, some of which exhibit one or more transitions prior to melting and others do not, a knowledge of the heat(s) of transition(s) (in cases where they do occur) is essential. The structural changes taking place, after fusion, in the immediate neighbourhood of the meling point, can be better understood if reliable data on changes in heat capacity of the melt are available. The entropy change in the melt, from a suitably chosen standard state (e.g. the melting point), can easily be evaluated according to the equation:

$$\triangle s = \int_{T_s}^{T} cp \, \frac{dT}{T} \quad , \text{ where } T_s \text{ is the temperature}$$

of the standard state. This entropy change will be considerable in the case of a covalent or highly associated melt - such as lithium chlorate. If other auxilliary data on the salt are available, the value of ΔS can be computed on the basis of an assumed structural model for the melt and hence a correlation with the experimental value provides a satisfactory test for the model.

In the study of mixtures of molten salts, calorimetric data provide a means of understanding the interactions taking place in the melt. The heats of mixing (ΔH^M) of a large number of anion mixtures of molten salts have been shown[99] to satisfy the equation:

$$\frac{\Delta H^M}{n_2} = \Delta H^f (t) + a\, n_1$$

where n_1, n_2 are the mole fractions of the two components, $\Delta H^f(t)$ is the hypothetical heat of fusion of the higher melting component at the temperature of the mixture and 'a' is a constant, designated as an ''interaction parameter''. Kleppa and Meschel[99] suggest that it may be possible to explain their results for the alkali halide-nitrate systems by taking into account, in addition to the electrostatic and van der Waals forces, the short range, repulsive potential between the ion cores. They consider that the anion-anion (i.e. second nearest neighbour) core repulsion may be significant, but they do not give any explicit

equations involing the interaction parameter a.

The method of calculation of activities in molten salt mixtures has already been indicated in Chapter 1 (see page 20). The free energy of mixing can then be obtained according to the equation:

$$\triangle F^M = \overline{\triangle F} - \overline{\triangle F^O} = \overline{\triangle H_1} - \overline{\triangle H^O} - T(\overline{\triangle S_1} - \overline{\triangle S^O})$$

$$= RT \ln a$$

where $\overline{\triangle F_1}$, $\overline{\triangle H_1}$, and $\overline{\triangle S_1}$ refer to the mixture and $\overline{\triangle F^O}$, $\overline{\triangle H^O}$ and $\overline{\triangle S^O}$ to one of its components in its pure state. The deviation of $\triangle F^M$ or $\triangle H^M$ from ideal behaviour is generally related to some type of interionic interaction process, which in the extreme case can lead to the formation of finite complexes. However, unless corroborative evidence is obtainable from other type of measurements, it is very difficult to decide about complex formation in molten salt mixtures from activity data alone.

PREVIOUS RELEVANT INVESTIGATIONS

No calorimetric work of any kind has been reported in the literature, for either anhydrous lithium chlorate or its mixtures. The transition in the solid state between α and β lithium chlorate was first reported by Kraus and

Burgess[100] and was later confirmed by Campbell and Griffiths[65]. The work of Campbell and Nagarajan[68] yielded a value of 99.1°C for the temperature of transition, in close agreement with the values reported by the other workers. No estimate of the heat of this transition is available.

Thermal data on the melting process of lithium nitrate have been obtained by various workers[101]. The heat of fusion of lithium nitrate[101] has been reported as 6060 cals mole^{-1}. The molar heat capacity of solid lithium nitrate is 26.68 cal mole^{-1} deg^{-1} at 210°C and that of liquid lithium nitrate 26.89 cal mole^{-1} deg^{-1} at 280°C. There are no direct experimental data on the temperature dependence of heat capacity of lithium nitrate.

Heats of fusion of molten salt are generally measured by the conventional method of mixtures. Elaborate designs[102] for calorimeters, capable of yielding results of great accuracy, are available in the literature. The calorimetric assembly designed by Goodkin, Solomons and Janz[103] for the determination of heats of fusion of inorganic compounds has a reported accuracy of $\pm$ 2%. Though the arragement described in this thesis is quite similar to that of Goodkin et al[103], a number of modifications have been made to increase the accuracy of results obtained. The molar heat capacity can also be determined by the same method.

The heat of mixing in molten salt mixtures was directly measured in a specially designed high temperature calorimeter by Kleppa and coworkers[104] . Until their direct measurement, the heat of mixing was usually obtained from either EMF data or from phase diagrams. The method described in this thesis for the determination of heats of mixing is less indirect. A recent paper[104a] describes a technique for the determination of heats of mixing almost identical with that described in this thesis.

The techniques for measurement of heats of solution are very well known and need not be reviewed. The design of the calorimetric assembly described in this thesis is very similar to that described by Campbell and coworkers[105] in their determination of heats of mixing of organic liquids.

EXPERIMENTAL

A. Heat of fusion and molar heat capacity

Furnace design: Fig. 22 illustrates the essential components of the furnace employed in the present investigation. It consisted of a large heat sink for maintaining uniform temperature, heating coils, thermal insulation and a device for suspending the sample tube. A 2 cms thick brass cylinder (A), open at both ends, with an internal diameter of 5 cms and a total length of 50 cms served as the inner core. The

FIG·22   FURNACE   DESIGN
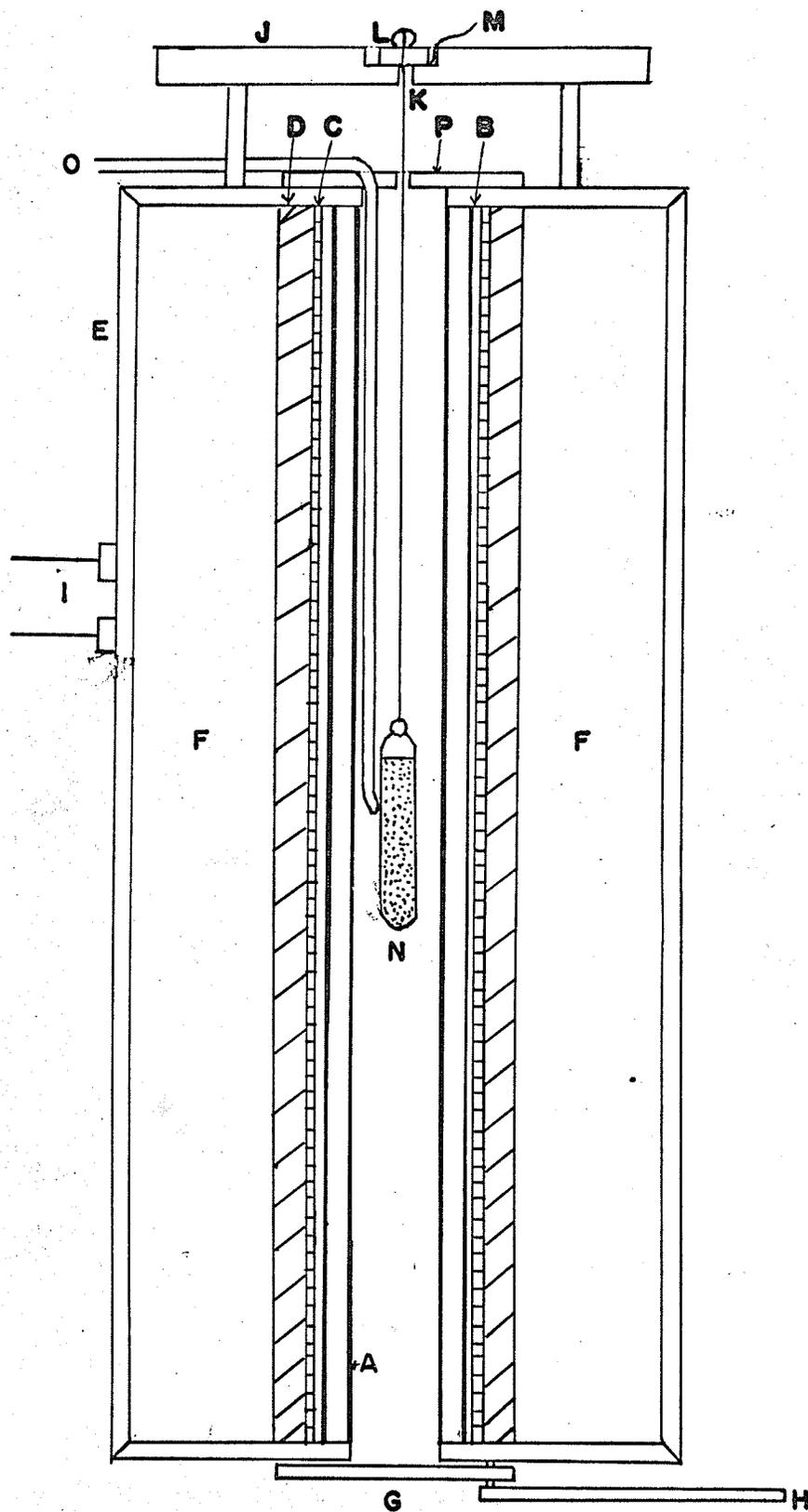
large bulk of brass provided an efficient heat sink and made
possible a uniform temperature region of at least 12 cms in
length, situated centrally inside the furnace. The inner
core of brass was covered with an adhesive teflon coated
glass fibre tape (B), which provided sufficient electrical
insulation for the coil windings (C). A length of 22 gauge
nichrome wire was wound around the insulated core, closer
together near the open ends than at the centre. The leads
(I) of this coil protruded out of the outer casing of the
furnace. The coil was covered with 1 cm thick layer of
asbestos (D). The asbestos covered cylinder was placed
centrally inside a double-walled box (1 cm thick transite
plates)(E). The space between the walls of the box was filled
with vermiculite. Transite discs (1 cm thick) with 5 cms
diameter holes, covered the top and bottom part of the box.
A circular transite platform (I) was mounted on top of the
box, its centre coinciding with the centre of the brass tube.
A fine hole (K) was drilled in the centre of this platform,
through which a fine cottom thread (M) could be introduced.
The sample tube (N) was suspended in the centre of the
furnace by means of this thread, which was held in position by
a movable lock (L) on the platform. A thermocouple well(O)
was placed in such a way that its tip was in the centre of
the furnace, just touching the sample tube. A sliding door
(G), operated by a handle (H), fitted snugly to the bottom

of the brass cylinder. A removable transite lid (P), with
a fine hole for allowing the thread to pass through,
covered the top of the furnace when the experiment was in
progress. The furnace was mounted by means of dexion frames
about 3 feet above the table level.

Temperature control and measurement: The technique of con-
trolling the temperature of the furnace was that of Lutz
and Wood[106], as modified by Campbell and Kartzmark[107] of
this laboratory. A copper-constantan thermocuple, which had
been calibrated using boiling point of water (with
appropriate pressure correction) and melting point of tin
(231.9°C) as fixed points, was used to measure the temperature
of the furnace in conjunction with a potentiameter capable of
reading to one microvolt.

The method of temperature control consisted of the
calibrated thermocouple, inserted well into the thermocouple
tube (O) of Fig. 22, connected in series with a sensitive
galvanometer and opposed by an EMF equal to that produced by
the thermocouple at the experimental temperature. A beam of
light reflected from the mirror on the galvanometer suspendion,
operated a photo-electric relay, which regulated the heating
current in the furnace, in such a way as to maintain the
desired temperature. A circuit diagram of the apparatus used
is shown in the upper part of Fig. 23. The thermocouple
leads (TC) from the furnace were connected to a DPST switch,

FIG·23 CIRCUIT DIAGRAM FOR CALORIMETRY
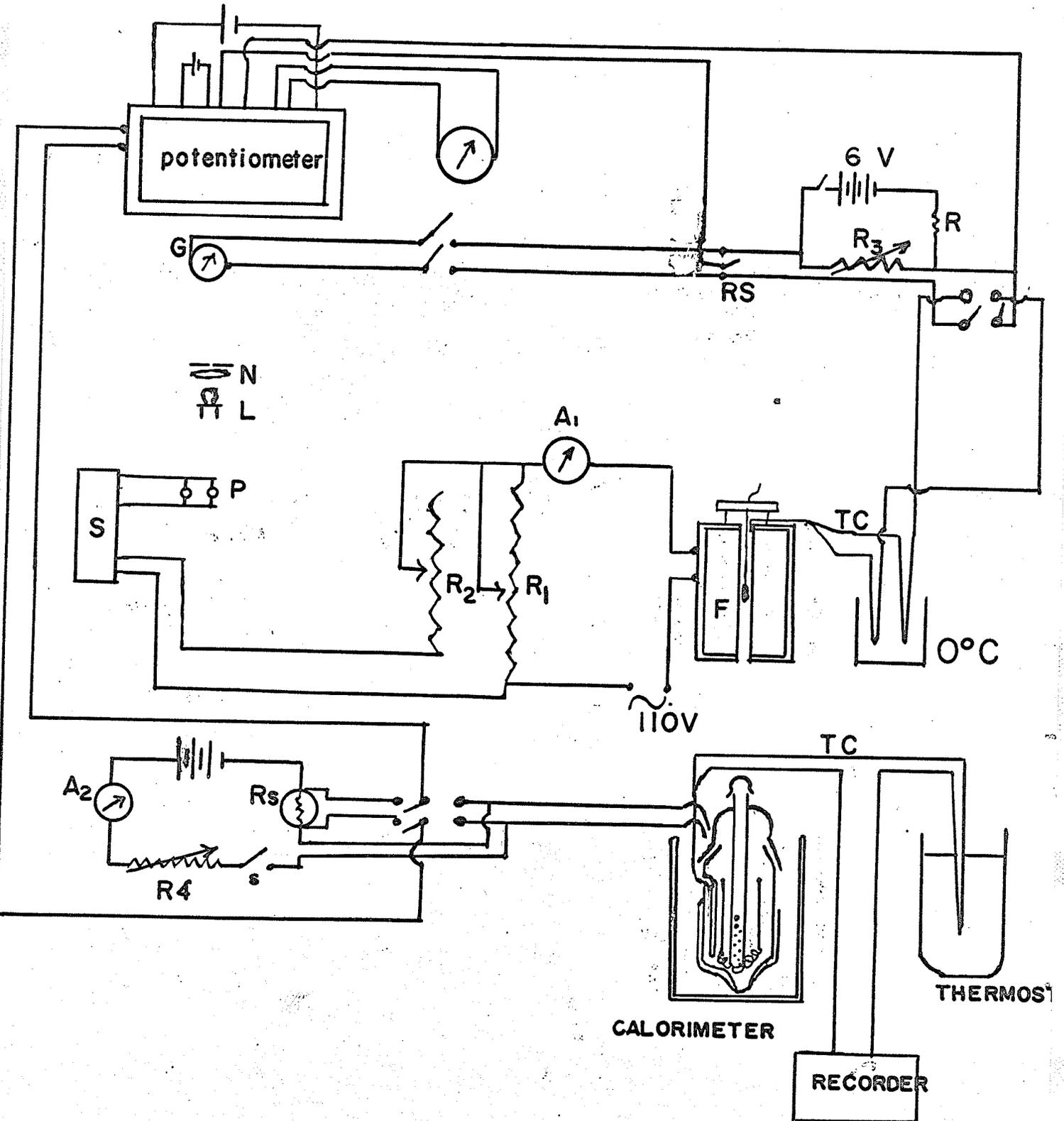
the other two terminals of which were connected to the potentiometer. Another switch (RS) made it possible to connect the thermocouple leads either to the potentiometer or to the galvanometer (G) and the opposing EMF which controlled the temperature of the furnace. The opposing EMF was that across a variable resistance (R_3), which was connected in series with a 6 volt storage battery and a 240,000 ohms fixed resistance (R).

The temperature controlling mechanism was the same as that used by Campbell and Kartzmark[10]. It contained a light source (L), a sensitive galvanometer (G) and a photo cell assembly (P) which activated the electronic realy (S) that controlled the furnace temperature. The heating circuit of the furnace consisted of an ammeter (A_1), and a water-cooled resistance R_1 (max. 100 ohms) connected in series with the heating coil of the furnace. A second resistance (R_2) (max. 20 ohms) was connected in parallel with R_1 through a mercury make and break relay, which was operated by the electronic relay S. The purpose of the resistance R_2 was to provide the additional current needed to maintain the furnace at the desired temperature. The method of control of temperature was as follows: The resistance R_1 and R_2 were adjusted to give cooling and heating currents required to maintain the furnace at a few degrees below and above the desired temperature. The EMF corresponding to the temperature

required was selected by setting R_3 and was opposed to the EMF arising from the thermocouple. The galvanometer (G) was then included in the control circuit. If the temperature of the furnace was below that of the desired temperature, the excess EMF flowing through the galvanometer caused the reflected light to fall away from the photo cells. The electronic relay was de-energized and the mercury switch relay brought the resistance R_2 into the circuit. Since $R_2 << R_1$, this gave rise to a heating current. As the furnace approached the required temperature, the reflected light slowly moved towards the photo-sensitized surface. At the EMF corresponding to the desired temperature, there was no current passing through the galvanometer (i.e. null position) and hence the electronic relay was energized and this cut off the resistance R_2 from the circuit. This caused the furnace to cool. The temperature of the furnace decreased and the cycle was repeated.

In this way it was possible to obtain a band of uniform temperature region at least five inches long, at the centre of the furnace. A check for uniformity of temperature was done by means of a thermocouple probe and was found to be satisfactory. In the region $90^{\circ}C$ to $180^{\circ}C$, temperature could be controlled to within $\pm 0.2^{\circ}C$.

<u>Calorimeter construction</u>: The calorimeter shown in Fig. 24 was made of Pyrex glass and consisted of a 9 cms internal diameter tube (A) sealed at the bottom, with a ground glass cover (S). The lower portion of the tube had a double walled vacuum jacket (B). A 30 mm bore glass tube (C) was sealed to the top and extended almost to the bottom of the calorimeter vessel. A number of holes (P) in the lower part of tube C provided easy flow of liquid between the smaller tube and the main calorimeter vessel. A thermocouple well (TC) and lead tubes (H) for the heating element (E) were also provided. The heating element was made of platinum wire with mercury-well connections. The calorimeter assembly was placed inside a double-walled wooden box filled with Vermiculite. The space between the calorimeter and the box was stuffed with rock-wool. A piece of sponge (D) at the bottom of the inner tube C cushioned the fall of the sample tube. The wooden box, with the magnetic stirrer, was mounted on wheels, which moved on rails running directly below the centre of the furnace. The calorimeter assembly could be placed so that the centre of tube C coincided with the centre of the mounting platform of the furnace (K of Fig. 22). Furthermore the calorimeter assembly can be quickly moved away from the furnace.

FIG·24 CALORIMETER FOR METHOD OF MIXTURES
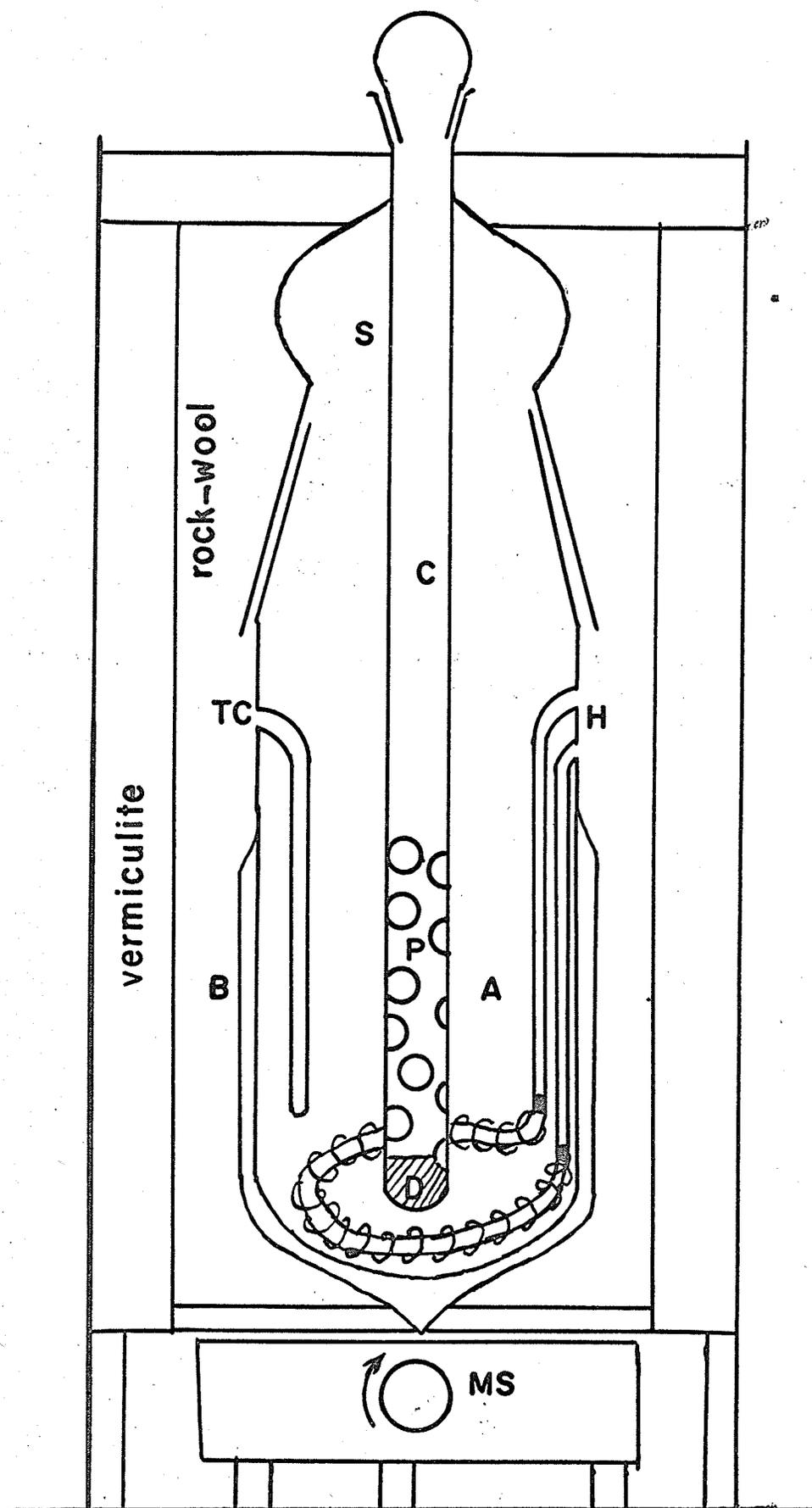
<u>Measurement of water equivalent of calorimeter</u>: During the present investigation heat given out by the hot sample tube was measured indirectly, by heating the water and contents in the calorimeter electrically and measuring the input electrical energy. The platinum heating coil in the calorimeter was connected (see Fig. 23) in series with a 6 V storage battery, an ammeter (A2), a variable resistance (R_4), a knife switch (S) and a standard resistance (R_S). The resistance R_S consisted of five 5 ohms, 20 watt insulated resistors connected in parallel, giving rise to an effective resistance of about 1 ohm. Its resistance was measured accurately with a Mueller bridge and was found to be 0.97440 ohm. The potential across the heating coil (E_1) and that (E_2) across the standard resistance R_S were measured on the potentiometer. The current flowing through the heating coil is given by $\dfrac{E_2}{R_S}$ and the potential across its terminals is E_1. When the current was passed for a period of t seconds, the total heat liberated by the heating coil was given by $\dfrac{E_1 E_2 t}{4.186 R_S}$. Since E_1, E_2 and R_S were measured accurately, the heat given out was known very precisely. The heat was measured to at least $\pm$ 0.1 cal. The time of passage of current was measured by an electrical clock (correct to $\pm$ 0.1 sec). The error in the measurement of heat was due mainly to the error in the time measurement.

Specific heat of copper: An evaluation of the reliability of the apparatus was done by carrying out an experiment to determine the specific heat of very pure copper. A copper cylinder (15 mm diameter) weighing ca 60 gms was suspended in position in the centre of the furnace by means of a thread. The temperature of the furnace was maintained at ca. 160°C. About 200 ml of distilled water were placed in the calorimeter. A ten-junction copper-constantan thermopile was inserted into the thermocouple-well of the calorimeter. The other junction of the thermopile was maintained at 28.0°C ± 0.01°C by means of a water thermostat. The temperature of the water in the calorimeter was adjusted slightly above 28°C. The thermopile leads were connected to a Varian G-10 recorder which had a total span of ca 3 mV. The recorder chart paper was calibrated and found to have a sensitivity of 0.073°C per division. It was possible to estimate the length on the chart paper to within ± 0.1 division. This gave a precision in temperature measurement of ± 0.007°C comparable to a Beckmann thermometer. Stirring was accomplished by means of a magnetic stirrer.

At the time of experiment, the calorimeter was pushed into a position in line with the centre of the furnace. The lid on the inner tube of the calorimeter was removed, the sliding door of the furnace was opened and the string holding the copper cylinder was cut by setting a match to it. The

hot copper cylinder fell into the inner tube of the calorimeter (cushioned by the water and sponge), the lid was replaced and the calorimeter assembly quickly moved away from the furnace. The temperature increase of the calorimeter contents was recorded on the chart paper of the Varian recorder. Fig. 25 is a reproduction of such a heating curve. After a constant temperature in the calorimeter was reached, the electrical heating was started. The current was passed for a sufficient time so as to give approximately the same increase in the temperature of the calorimeter contents as that produced by the hot copper cylinder. The heat produced electrically (He) was measured as described before. The temperature increments due to the hot copper cylinder (ΔT_{cu}) and electrical heating (ΔT_e) were measured in units of divisions on chart paper. The heat given out by the hot copper cylinder (H_{cu}) is simply given by

$$H_{cu} = H_e \times \frac{\Delta T_{cu}}{\Delta T_e}$$

The specific heat of copper is given by,

$$s = \frac{H_{cu}}{m_{cu}(t_2 - t_1 - \delta t)} \qquad \text{where,}$$

s = specific heat of copper at t_2

m_{cu} = mass of copper in gms

t_1 = temperature of calorimeter and contents before the experiment (28.0°C).

FIG.25 TYPICAL CURVE FOR CALORIMETRY
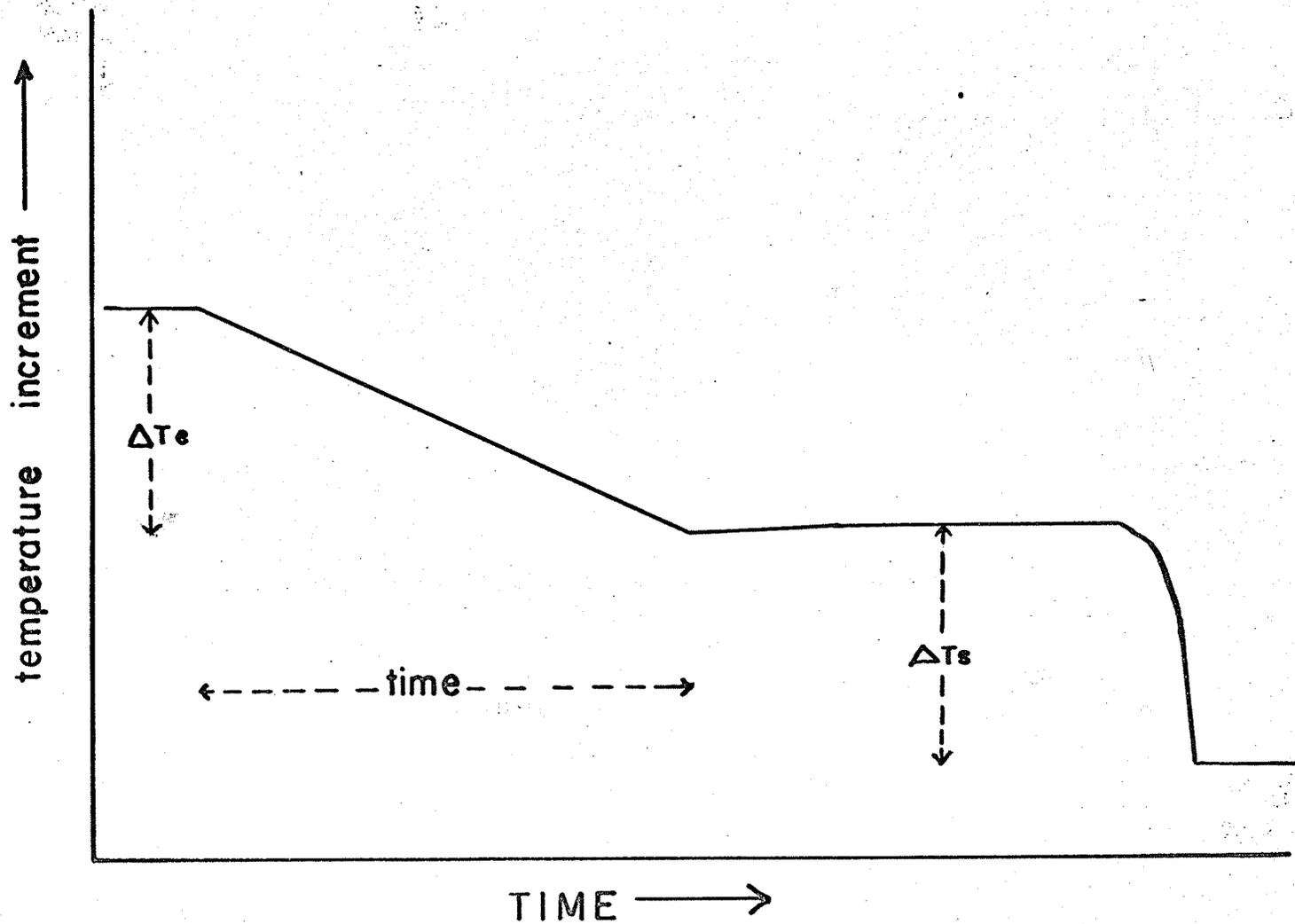
t_2 = temperature of the furnace

δt = increase in temperature of the calorimeter and contents due to the hot copper cylinder.

The specific heats of copper were determined at two temperatures, 160.0°C and 198.8°C. The values obtained in the present study are 0.0959 cal gm^{-1} and 0.0967 cal gm^{-1} respectively. The literature values[108] are 0.0953 cal gm^{-1} and 0.0962 cal gm^{-1} respectively.

Specific heat of Pyrex glass No. 7740: Since in the present study the experimental substances were sealed in glass tubes, it was necessary to apply corrections for the specific heat of glass. The Pyrex catalogue[109] gives a value of 0.20 cal gm^{-1} as the specific heat of glass No. 7740. But the temperature range in which this value is applicable is not given. It was therefore considered desirable to determine the specific heat of glass under the present experimental conditions. Solid Pyrex glass rods were employed for this purpose and measurements were made at four different temperatures. The technique of measurement of specific heat was the same as that described on page 121. Table XXIV gives the results obtained and these are plotted in Fig. 26. Since the graph is linear, interpolations at other temperatures can easily be made without much error.

TABLE XXIV

Specific Heat of Glass (Pyrex No. 7740)

Temperature °C	Specific heat cal deg^{-1} gm^{-1}
97.5	0.1626
126.4	0.1661
153.0	0.1692
173.1	0.1714

FIG26 SPECIFIC HEAT OF GLASS
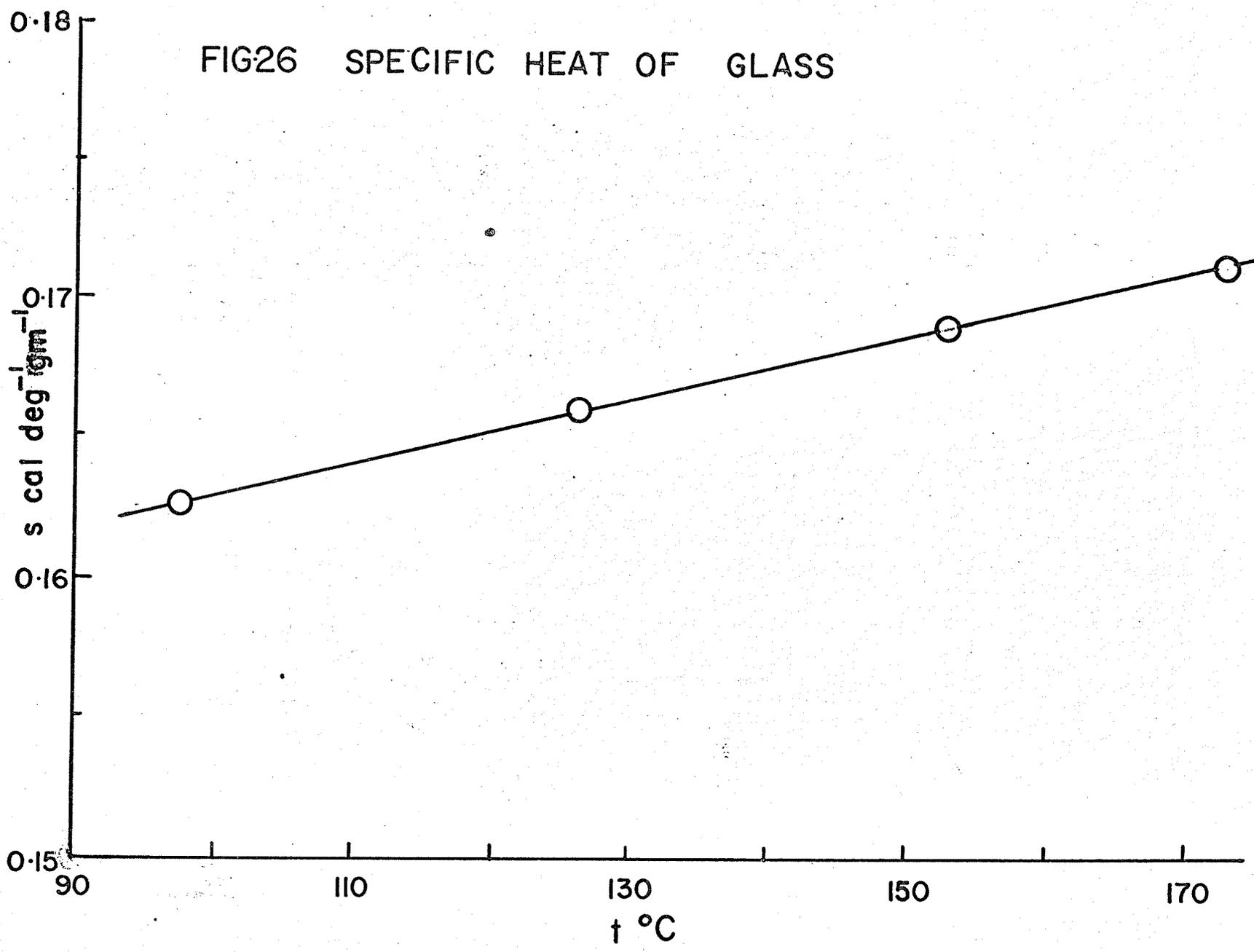
Preparation of samples: Anhydrous lithium chlorate and lithium chlorate-lithium nitrate mixtures were loaded into glass tubes, 20 mm in diameter and 5 cms in length. The transferring of the substance was done in much the same way as that described under densitometry, (page 36) and viscometry (page 76). The filled tubes were sealed under vacuum and provided with hooks for suspending them in the furnace.

Measurement of heat evolved by samples: The sample tube containing the experimental substance was weighed and suspended in position inside the furnace. The heats given out by the tube plus substance at various temperatures in the range 90°C to 170°C were determined in a manner identical to that described already. It was found that the same tube could be employed at various temperatures though some cracking of the tube occurred towards the end of the series. At the end of a series of measurements at different temperatures, the specimen tube was carefully cracked open, its contents washed away and the clean, dry broken pieces were weighed. The calculation procedures are described on page 133.

Over-all precision of the method: In an experiment, such as this one, where a number of different measurements go to make up the final result, it is very difficult to estimate the

probable error in the final value. In arriving at an over-all precision of the heat measured, the following have been taken into account: (i) Fluctuations in the temperature of the furnace $\pm$ 0.2°C, (ii) The probable error in the estimation of relative heights on chart paper: $\pm$ 0.1 div. in 20-80 divs. (iii) Error due to loss of heat of the specimen tube during fall cannot be estimated. In the absence of reliable estimates of various errors, the observed deviation of the results from linearity of molar heat content vs. temperature, is the only guide. The probable error in the value of molar heat capacity is $\pm$ 1% at higher temperatures and close to $\pm$ 2% at lower temperatures. Since larger values of heat content are involved when measuring the heat capacity of liquid salts, one can expect better values for the liquid region.

B. Heat of solution

Calorimeter construction: Fig. 27 shows the essential parts of the calorimeter used in the present investigation. It was made of Pyrex glass and consisted of a 3 inches internal diameter tube (A) sealed at the bottom, with a ground glass top (B) carrying all the connections. The powedered sample was contained in the bulb (C) which was connected, by means of a ground glass joint, to a tube (D) sealed to the ground glass top B. The bulb C had a very thin bottom so that it

could be broken by pushing the rod (E) running along the entire length of the tube D. Ground glass cap (S) sealed to the top of the rod E fitted snguly once the bulb C was broken. Platinum heating coils with mercury-well connections (H) and a thermocouple well (T) were also sealed on to the ground glass top B. A stirrer (F) introduced through an open tube sealed to the ground glass top B, was operated manually. The entire assembly was placed in a large Dewar flask and the interspaces were filled with cotton wool.

Preparation of samples: The low temperature α-form of lithium chlorate was prepared according to the method described on page 31 , and pulverized to a fine powder inside a dry box. The sample tubes were filled with this fine powder, the operation being carried out in a dry box, and the sample weight noted. The transition $\alpha \rightleftharpoons \beta$ occurs at 99.1°C . To prepare the high temperature β form of lithium chlorate, a Vycor tube was filled with anhydrous lithium chlorate (by methods already described in this thesis, page 36), sealed under vacuum and suspended in the centre of the furnace as described on page 121. The temperature of the furnace was maintained at ca. 10°C above the transition temperature for a period of two weeks. At the end of two weeks, the Vycor tube containing the β form was suddenly dropped into a container of liquid nitrogen, thereby freezing the metastable phase. The β form

FIG·27 CALORIMETER FOR HEATS OF SOLUTION
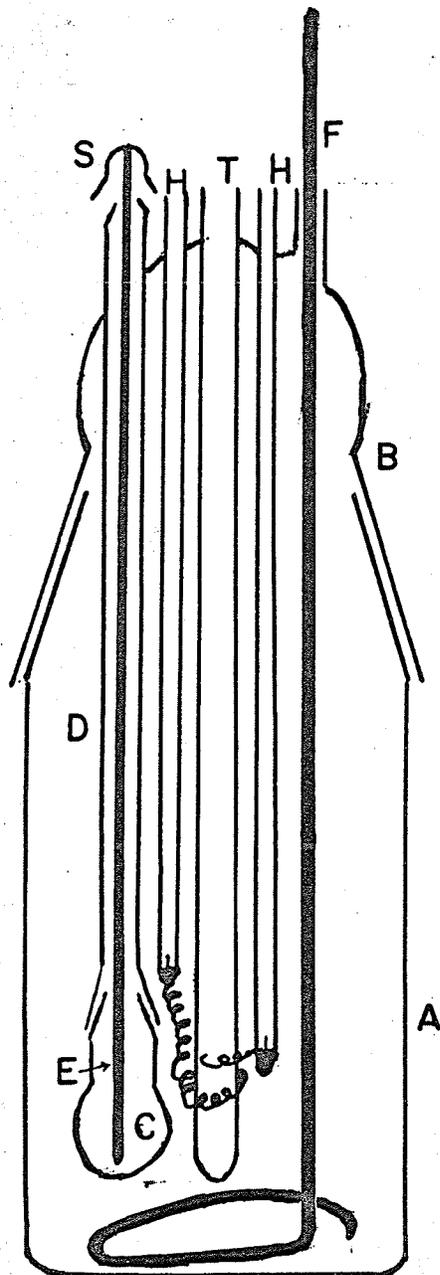
was converted into a fine powder and transferred to sample
tubes in a manner with that used for α form. The sample
tubes had independent ground glass tops which were removed
just before attaching the sample tubes to the calorimetric
assembly.

Measurement of heat evolved by the sample: The sample tube
was attached to the tube D of Fig. 27 , by means of a wire
wound around the hooks provided therefore. A known amount of
(ca. 150 ml) distilled water was placed in the calorimeter.
The sample tube was surrounded by water in the calorimeter
and therefore was at the same temperature as the water. The
measurement of heat evolved was the same as that described
for the method of mixtures (page 120). Stirring was maintained
throughout the measurement. The sample tube was broken by
jamming the rod and the temperature of the water rose. The
temperature was recorded on the G-10 Varian recorder. The heat
evolved was measured indirectly by means of the electrical set
up described on page 120. The method of calculation is given
on page 133. Three samples were used for each of the two
forms of lithium chlorate and each time the sample weight
was ca. 3 gms.

Over-all precision of the method: The main source of error
came from the time measurement in the electrical heat calcu-
lation. This error varied according to the total time of

passage of current, but was never more than $\pm$ 0.2%. The error involved in measuring the relative heights of temperature-time curves on the recorder chart paper was $\pm$ 0.1 div. in ea. 10 divs. This contributes the major share to the over-all precision. The precision obtained in this method is $\pm$ 5 cals in ca 400 cals or ea. $\pm$ 1.5%.

CALCULATIONS AND RESULTS

Molar heat capacities and heats of fusion: The heat given

out by sample is given by

$$h_m = \frac{E_1 E_2 t}{4.186 \, R_s} \times \frac{\Delta T_s}{\Delta T_e}$$

where ΔT_s and ΔT_e are the heights of the temperature-time

graph for the sample and electrical heating respectively.

All the other terms have been defined earlier (cf. Tables

of Symbols).   A correction was applied for the heat given

out by glass alone.   The heat given by one mole of the

sample is,

$$\Delta H_{obs} = h_m \times \frac{M}{m}$$

where M is the molecular weight of the sample.   For mixtures,

$M = n_1 M_1 + n_2 M_2$, where n_1, n_2 are the mole fractions of the

two components and M_1 and M_2 are their molecular weights.   To

provide a basis for comparison, all heats evolved by specimens

were computed to the same final temperature using the

equation,

$$\Delta H_{corr} = \Delta H_{obs} + C_p (t_{sr} - t_2)$$

where ΔH_{corr} and ΔH_{obs} are the molar heat changes corrected

to the arbitrary final temperature t_{sr} and the observed value

of molar heat change; and C_p is the molar heat capacity of the

sample at constant pressure over the temperature range

$(t_{sr} - t_{obs})$.   Since the molar heat capacity of lithium

chlorate is not known at low temperatures ($t_{sr} = 25.0^{\circ}C$), an

approximation given by Goodkin, Solomons and Janz[103] was used, viz.

$$\Delta H_{corr} = \Delta H_{obs} \frac{(t_1 - t_{sr})}{(t_1 - t_2)} .$$

In using the above equation it is assumed that molar heat capacity is essentially constant over the range of temperature $t_1 - t_2$ or $t_1 - t_{sr}$. Any errors arising out of this approximation are quite small.

Table XXV gives the results obtained for pure lithium chlorate and Fig. 28 illustrates these results graphically. The molar heat of fusion (ΔH_f) was determined as the difference between the molar heat changes for the liquid and solid at the melting point, T_f, (see Fig. 28). The entropy of fusion was calculated using the equation $\Delta S_f = \frac{\Delta H_f}{T_f}$ and is also included in Table XXV. Molar heat capacities of solid and liquid mixtures were obtained by fitting the 'best' line (according to a least squares technique) to the thermal data given in Table XXV. The slope of the straight line so obtained is the molar heat capacity. These values are also given in Table XXV. Similar calculations were done for the thermal data obtained for mixtures of lithium chlorate and lithium nitrate. The values of molar heat capacity, heat and entropy of fusion are tabulated in Table XXVI.

TABLE XXV

Calorimetric Data on Pure Anhydrous Lithium Chlorate

Total no. of moles in sample: 0.2088

$T_f = 401.0°K$

Initial (hot) temperature of sample $t_1°k$	Corrected heat evolved per mole of sample $\Delta H_T - \Delta H_{298.1}$ cal mole^{-1}
361.7	1135
367.5	1249
371.1	1376
382.4	1642
394.3	1951
404.3	4651
406.7	4694
413.7	4918
417.3	5009
424.3	5178
429.7	5351

C_p (solid) = 24.51 $\pm$ 0.21 cal deg^{-1} mole^{-1}

C_p (liquid) = 29.20 $\pm$ 0.13 cal deg^{-1} mole^{-1}

ΔH_f = 2470 $\pm$ 12 cal mole^{-1}

ΔS_f = 6.16 cal deg^{-1} mole^{-1}

FIG·28 HEAT CONTENT DATA FOR PURE LITHIUM CHLORATE
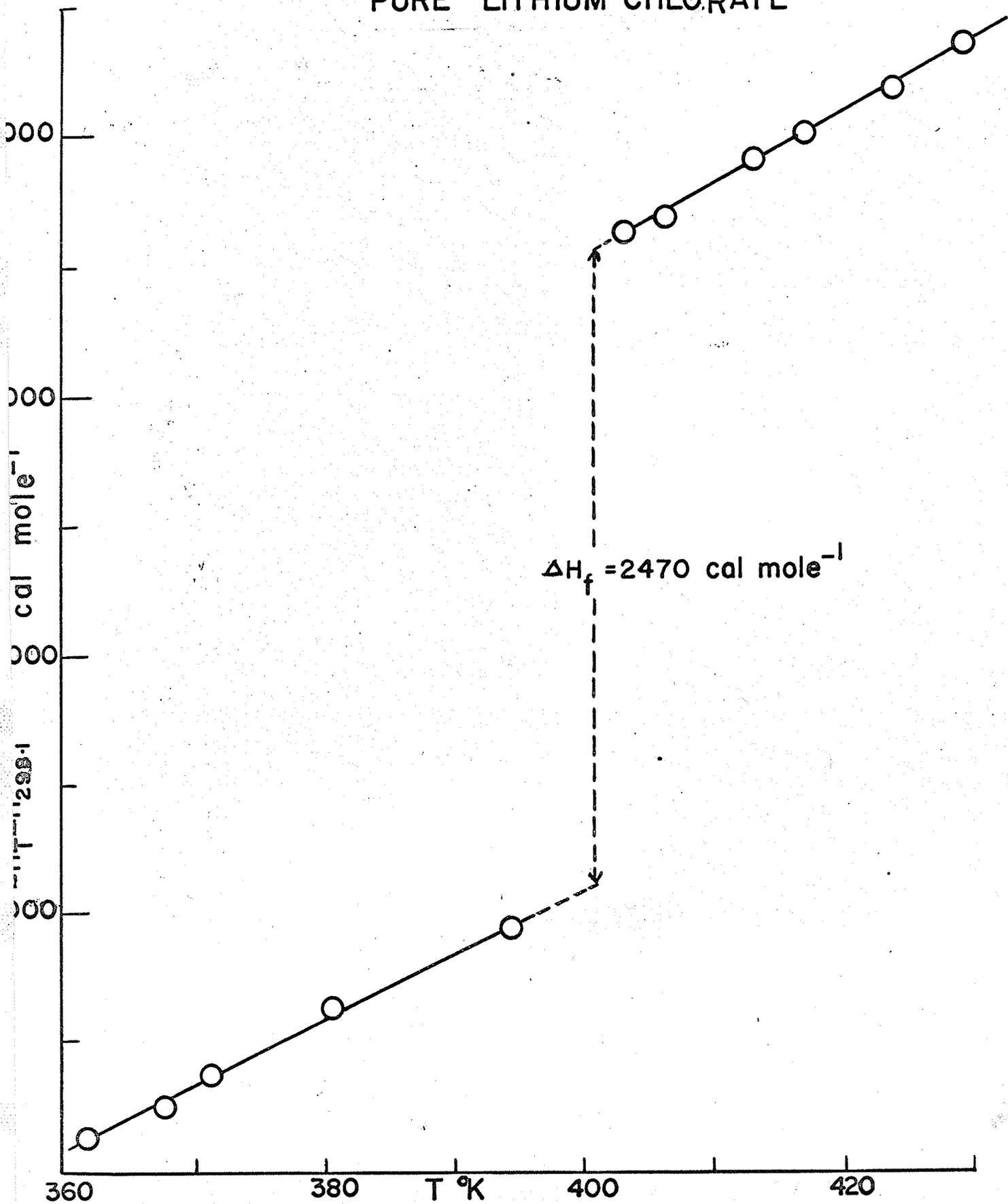
TABLE XXVI

Calorimetric Data on Lithium Chlorate-Lithium Nitrate System

n_2 = mole fraction of lithium nitrate

n_2	Molar heat capacity (C_p) (cal deg^{-1} mole^{-1})		Freezing Point T_f(°K)	$\triangle H_f$ cal mole^{-1}	$\triangle S_f$ cal deg^{-1} mole^{-1}
	Solid	Liquid			
0.000	24.51 $\pm$ 0.21	29.20 $\pm$ 0.13	401.0	2470 $\pm$ 12	6.16
0.050	24.66 $\pm$ 0.22	29.17 $\pm$ 0.13	399.5	2811 $\pm$ 13	7.04
0.105	24.81 $\pm$ 0.23	29.11 $\pm$ 0.17	397.8	3198 $\pm$ 16	8.04
0.146	24.93 $\pm$ 0.23	29.06 $\pm$ 0.12	396.4	3490 $\pm$ 15	8.80
0.196	25.03 $\pm$ 0.20	28.98 $\pm$ 0.13	394.3	3842 $\pm$ 17	9.74
0.255	25.14 $\pm$ 0.26	28.84 $\pm$ 0.19	391.1	4248 $\pm$ 17	10.86

Heats of mixing: The heat of mixing of n_1 mole fraction of lithium chlorate and n_2 mole fraction of lithium nitrate was calculated as the difference between the observed and calculated values of heat contents at $401.0^\circ K$ (mp of lithium chlorate), i.e. $\triangle H^M = \triangle H_{obs} - \triangle H_{calc}$. The observed heat content was defined as:

$$\triangle H_{obs} = \triangle H_f \text{ (mixt.)} + \int_{T_f}^{401.0} C_p(\ell)dT$$

where $\triangle H_f$ (mixt.), T_f and $C_p(\ell)$ refer to the heat of fusion, freezing temperature and molar heat capacity in the liquid state of the mixture. The calculated heat content was obtained according to the equation:

$$\triangle H_{calc.} = n_1 \triangle H_f(1) + n_2 \triangle H_f(2)$$

where $\triangle H_f(1)$ and $\triangle H_f(2)$ are the molar heats of fusion of lithium chlorate and lithium nitrate at $401.0^\circ K$. $\triangle H_f(2)$ was in turn obtained using the relation[110]

$$\triangle H_f(2) = \triangle H_f(p) + \int_{401.0}^{T_p} \triangle C_p dT$$

where $\triangle H_f(p)$ is the heat of fusion of lithium nitrate at its melting point T_p and $\triangle C_p$ is the difference between the molar heat capacities of solid and liquid lithium nitrate, i.e. $\triangle C_p = C_p^{solid} - C_p^{liquid}$. It is assumed that C_p of lithium nitrate does not alter with temperature. The

isothermal heats of mixing at $401.0^\circ K$ are given in Table XXVII.
The heats of mixing values are correct to $\pm\ 2\%$.

Heat of transition: The heat of the transition,

$$\alpha\ LiClO_3 \rightleftharpoons \beta\ LiClO_3$$

was obtained as the difference between the differential heats
of solution of α and β forms of lithium chlorate at a given
concentration. The heat of solution was calculated by standard
techniques, viz., values of $\dfrac{\leqq \Delta H_i}{\leqq x_i}$ were plotted against $\leqq\ x_i$
where ΔH_i and x_i are the heat change and molarity at the
end of each addition. Three or four additions of lithium
chlorate were made. Table XXVIII gives the results of the
heats of solution experiments on the two forms of lithium
chlorate. Fig. 29 illustrates the results graphically.

Activities and free energies of mixing: The equation
(cf. page 20),

$$\ln a = \frac{\Delta H_f}{R}\left(\frac{1}{T} - \frac{1}{T_f}\right) + \frac{\Delta C_p}{R}\left(\ln\frac{T_f}{T} - \frac{T_f - T}{T}\right)$$

was used to calculate the activity of lithium chlorate in
the mixture. The values of T and T_f were those of Campbell,
Kartzmark and Nagarajan[68], whereas ΔH_f and ΔC_p were
obtained in the present investigation. The free energy of
mixing is given by the relation:

$$\Delta F^M = RT \ln a$$

TABLE XXVII

Heats of Mixing in Lithium Chlorate-Lithium Nitrate System at $401.0^{\circ}K$

n_2 = mole fraction of lithium nitrate

n_2	Heat content (calculated) $\Delta H_{calc.}$ Cal mole^{-1}	ΔH_f of sample cal mole^{-1}	$\int_{T_f}^{401.0} C_p(l)dT$ Cal mole^{-1}	Heat content (observed) $\Delta H_{obs.}$ Cal mole	ΔH^M cal mole^{-1}	$\Delta H^M/n_2$ cal mole^{-1}
0.050	2648	2811	43.8	2855	+ 207	+ 4150
0.105	2843	3198	93.2	3291	+ 448	+ 4264
0.146	2989	3490	133.7	3624	+ 635	+ 4351
0.196	3167	3842	194.2	4036	+ 869	+ 4432
0.255	3377	4248	285.5	4533	+ 1156	+ 4534

$\Delta H_{calc.} = n_1 \Delta H_f^1 + n_2 \Delta H_f^2$ $\Delta H_f^1 = 2470$ cal mole^{-1} $\Delta H_f^2 = 6060 + \int_{401.0}^{528.1} C_p^2 \, dT$

$\Delta H_{obs.} = \Delta H_f + \int_{T_f}^{401.0} C_p(l) \, dT$ $\Delta C_p^2 = -0.276$ cal deg^{-1} mole^{-1}

TABLE XXVIII

Heats of Solution of α and β Lithium Chlorate

No. of moles sample added to one litre of solution x_i	Heat change during each addition $\triangle H_i$ cal.	Total concentration Σx_i mole litre^{-1}	Total heat change per mole $\triangle H_{soln.}$ cal mole^{-1}
α-form			
0.238	+ 88.1	0.238	+ 369.6
0.289	+ 102.1	0.527	+ 362.1
0.268	+ 91.5	0.795	+ 354.9
β-form			
0.195	- 49.4	0.195	- 253.2
0.117	- 28.2	0.312	- 248.8
0.198	- 46.2	0.510	- 242.8
0.223	- 48.5	0.733	- 235.1

$\triangle H_{soln}(\alpha)$ extrapolated to infinite dilution = + 375.7

$\triangle H_{soln}(\beta)$ extrapolated to infinite dilution = - 258.7

Heat of transition α LiCLO$_3$ $\rightleftharpoons$ β LiCLO$_3$ = + 634.4 cal mole^{-1}

Entropy of transition = $\triangle S_{trans}$ = 1.70 cal deg^{-1} mole^{-1}

FIG·29 HEATS OF SOLUTION OF α & β LiClO$_3$

-270

β form

-250

230

580

α form

560

0·2   0·4   0·6   0·8

CONCENTRATION   mole litre^{-1}
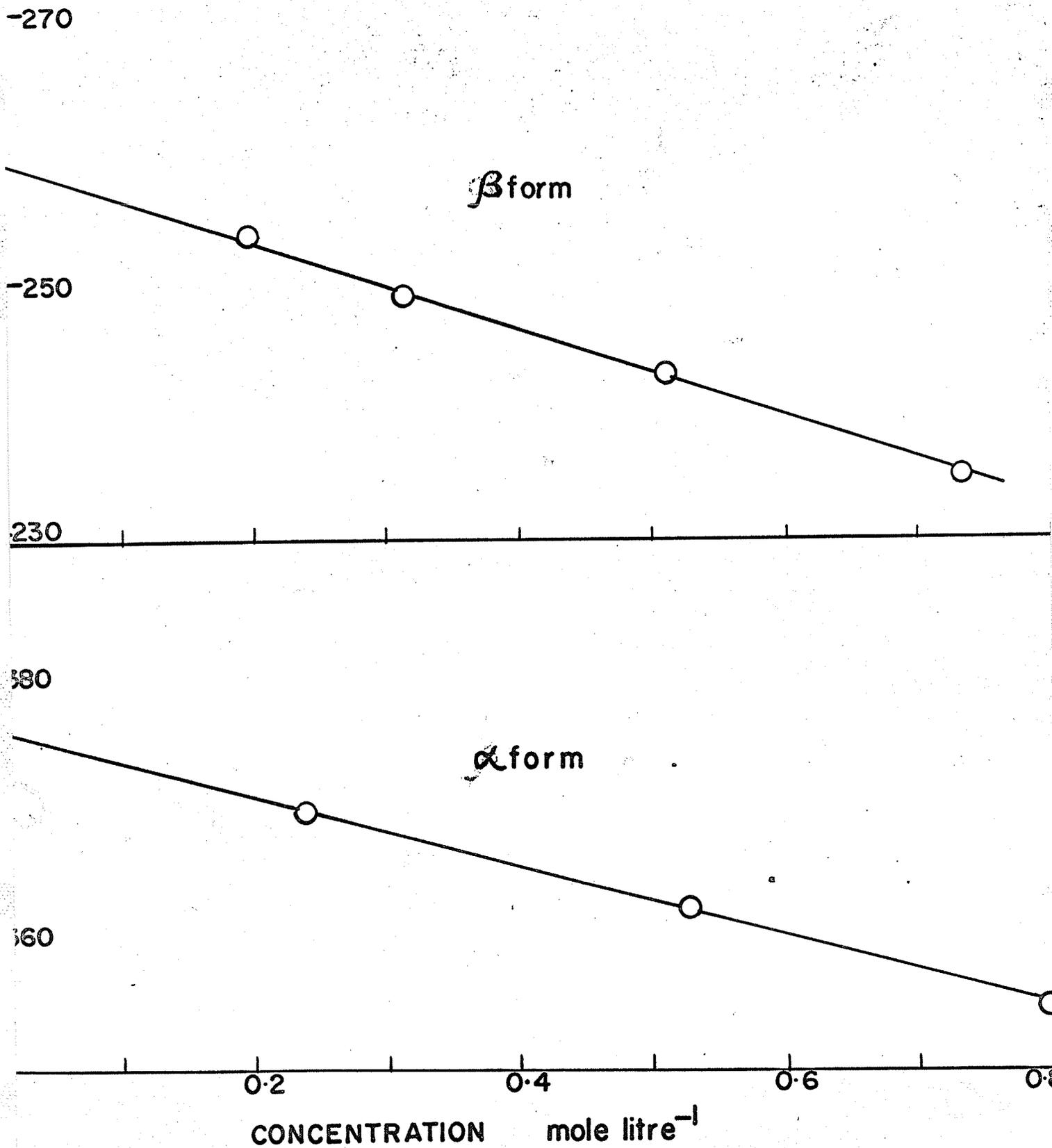
The values of activity and free energy of mixing are tabulated in Table XXIX. Employing the well known equation,

$$\Delta F^M = \Delta H^M - T \Delta S^M$$

and the values of ΔH^M given in Table XXIX, the entropy of mixing, ΔS^M, was obtained. Table XXX lists the values of free energy, enthalpy and entropy of mixing (at different concentrations of lithium nitrate) at $401.0^\circ K$. The ideal entropies of mixing,

$$\Delta S^M (ideal) = - R \ln n_1$$

were also calculated and are shown in the last column of Table XXX. Fig. 30 shows the dependence of ΔF^M, ΔH^M and $T \Delta S^M$ on n_1. The ideal and observed entropies of mixing are plotted, in Fig. 31, as functions of composition.

DISCUSSION

The value of the entropy of fusion for lithium chlorate, 6.16 cal deg^{-1} mole^{-1}, is higher than most salts which give rise to an ionic melt (cf. Table A1, Appendix), and falls in the general region of salts which are predominantly covalent. The entropy of the transition at $99.1^\circ C$, 1.70 cal deg^{-1} mole^{-1}, must be added to the entropy of fusion, when discussing the latter. The total entropy change is therefore 7.86 cal deg^{-1} mole^{-1}. As pointed out earlier (cf. page 16) the abnormally low melting point of lithium chlorate probably results from

TABLE XXIX

Free Energies of Mixing in Lithium Chlorate-
Lithium Nitrate System

n_1 = mole fraction of lithium chlorate

n_1	n_2	$T_f (^oK)$	Activity of Lithium Chlorate a	$\triangle_F^M$ = $RT_f \ln a$ cal mole-1
1.000	0.000	401.0	1.000	–
0.950	0.050	399.5	0.988	– 9.3
0.854	0.146	396.4	0.964	–28.6
0.725	0.275	390.2	0.919	–65.8
0.640	0.360	384.1	0.875	–102.4
0.585	0.415	379.5	0.841	–130.2
0.536	0.464	373.9	0.803	–160.9

TABLE XXX

Free Energy, Enthalpy and Entropy of Mixing in Lithium Chlorate-Lithium Nitrate System at $401.0^\circ K$

n_1 = mole fraction of lithium chlorate

n_1	ΔF^M cal mole^{-1}	ΔH^M cal mole^{-1}	$T\Delta S^M$ cal mole^{-1}	ΔS^M cal deg^{-1}mole^{-1}	ΔS^M (ideal) cal deg^{-1}mole^{-1}
1.000	0.000	0.000	0.000	0.000	0.000
0.950	-9.3	+207.5	+216.8	+0.541	+0.102
0.895	-20.8	+447.7	+468.5	+1.168	+0.221
0.854	-28.6	+635.3	+663.9	+1.656	+0.314
0.804	-40.9	+868.7	+909.6	+2.268	+0.433
0.745	-58.9	+1156.2	+1215.	+3.030	+0.585

NOTE: F^M values obtained by interpolation from Fig. 33

FIG·30 $\Delta F^M, \Delta H^M$ & $T\Delta S^M$ AS FUNCTIONS OF COMPOSITION
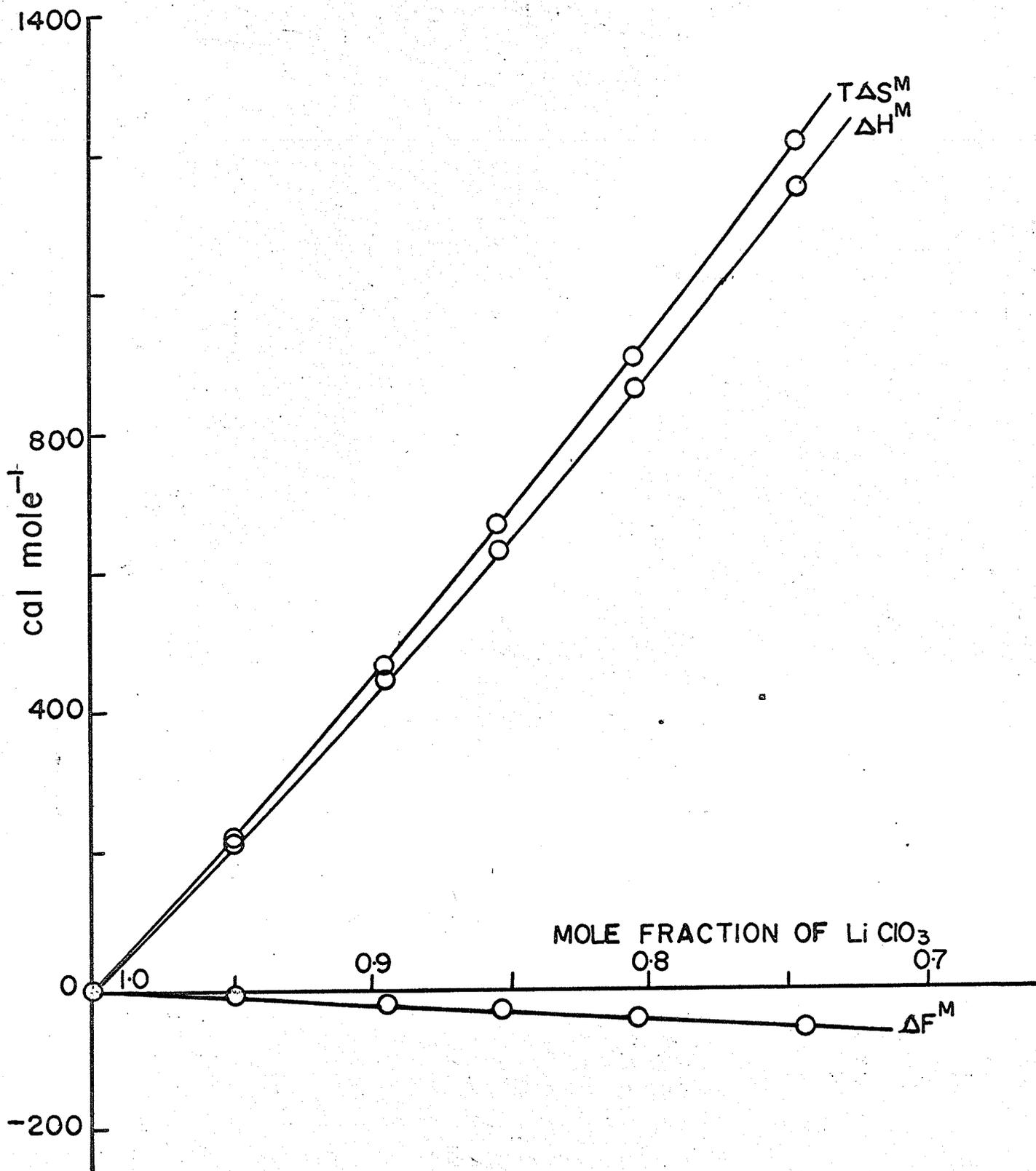
# FIG31 IDEAL & OBSERVED ENTROPY OF MIXING
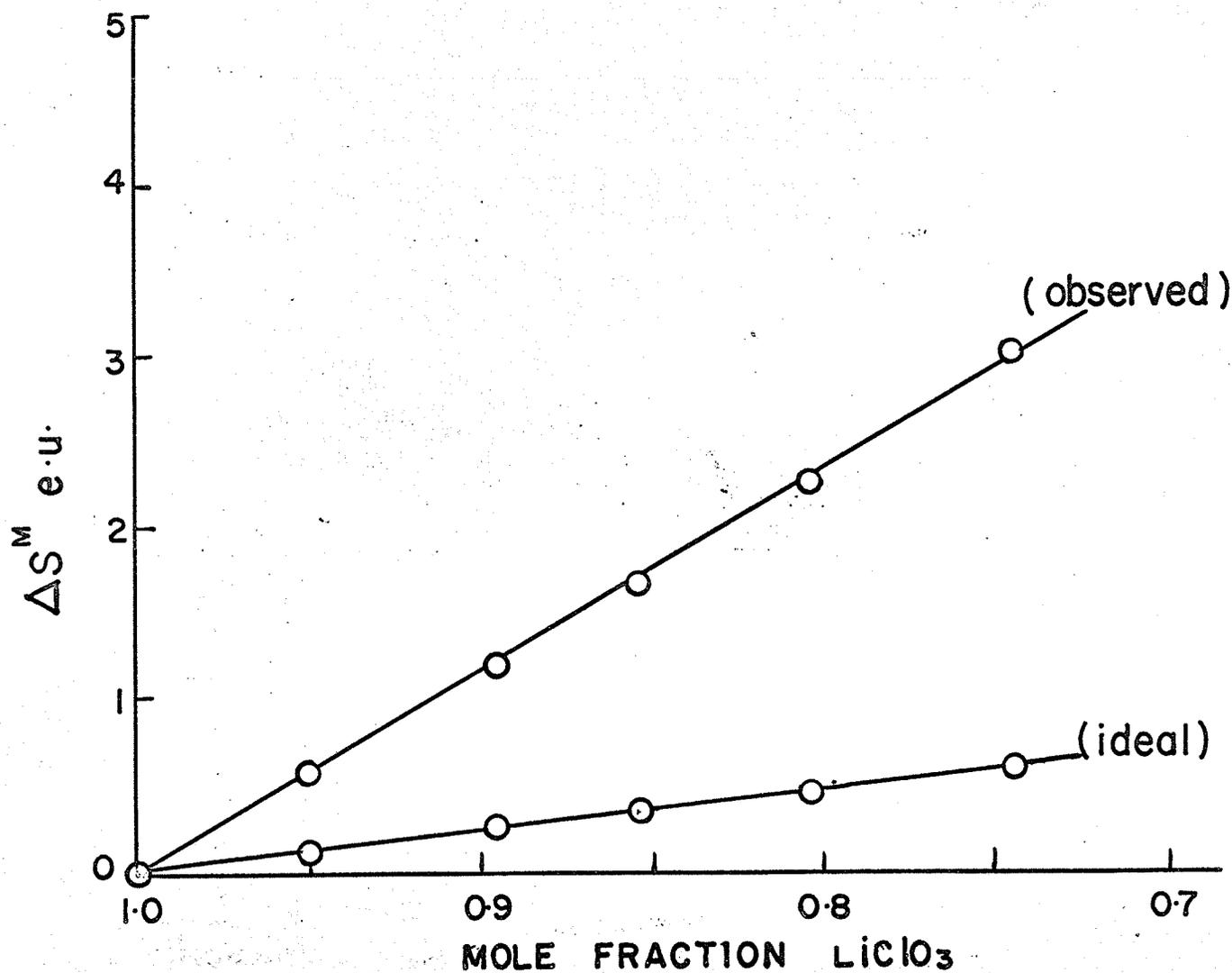
entropy contributions from sources other than positional changes, to total entropy of fusion. It is probable that particular low energy configurations occur in molten lithium chlorate and hence contribute an additional term (ΔS_{assoc}) to the total entropy of fusion. The molar heat capacity of molten lithium chlorate, 29.20 cal deg^{-1} $mole^{-1}$, compares favourably with those obtained for molten alkali nitrates (cf. Appendix). It is generally agreed[42] that ''association'' of some sort occurs in molten alkali nitrates. Therefore, it is probable that molten lithium chlorate also exhibits similar characteristics.

The entropy of fusion of lithium chlorate-lithium nitrate mixtures increases sharply with increasing concentration of lithium nitrate (e.g. from 6.16 e.u. at n_2 = 0 to 10.86 at n_2 = 0.255). Although the entropy of fusion of lithium nitrate itself is very high (viz. 10.86 e.u.), the increase in entropy of fusion of mixtures of lithium chlorate and lithium nitrate is much more than that predicted by a simple arithmatic mean value (e.g., at n_2 = 0.255, the mean value of $\Delta S_f = n_1 \Delta S_f(1) + n_2 \Delta S_f(2) = 7.51$ e.u.; whereas that observed is 10.86 e.u.). The sharp increase in entropy of fusion, on addition of lithium nitrate, may arise from some kind of interaction of nitrate ion with the chlorate lattice which results in an increased entropy value. The possibility of such an interaction has already been pointed out in Chapter IV. The change in molar heat capacity of lithium

chlorate-lithium nitrate mixtures also supports this view. The values of C_p are given as a function of composition in Fig. 32. The ideal values of C_p were obtained using the relation $C_p(mixt) = n_1 C_p(1) + n_2 C_p(2)$ and are also shown in Fig. 32. The observed molar heat capacities of lithium chlorate-lithium nitrate exhibit a positive deviation from ideality, in both solid and liquid states. The deviation is more pronounced in the liquid state than in the solid state. Since the differences are small (< 1%) and the experimental error is almost of the same order of magnitude as the deviations, no attempt to interpret these deviations on the lines suggested under Densitometry or Viscometry has been made, but the positive deviation from ideality indicates that the nitrate ion (or the chlorate lattice) does not exist as such, but is a part of the structural unit resulting from a possible inter-action of nitrate ion with the chlorate lattice. The formation of a more complex ''cluster'' than that presumably present in pure molten lithium chlorate, perhaps by a process of ''bridging'' by the nitrate ion, would account for the positive deviation of C_p from ideality, as well as the sharp increase in entropy of fusion.

The heat of mixing in the molten lithium chlorate-lithium nitrate system, at $401.0^\circ K$ (m.p. of lithium chlorate), is positive and increases with further additions of lithium nitrate. This is in agreement with the findings of Kleppa and Meschel[51], that in all the anion mixtures studied by them,

FIG·32 MOLAR HEAT CAPACITY AGAINST COMPOSITION
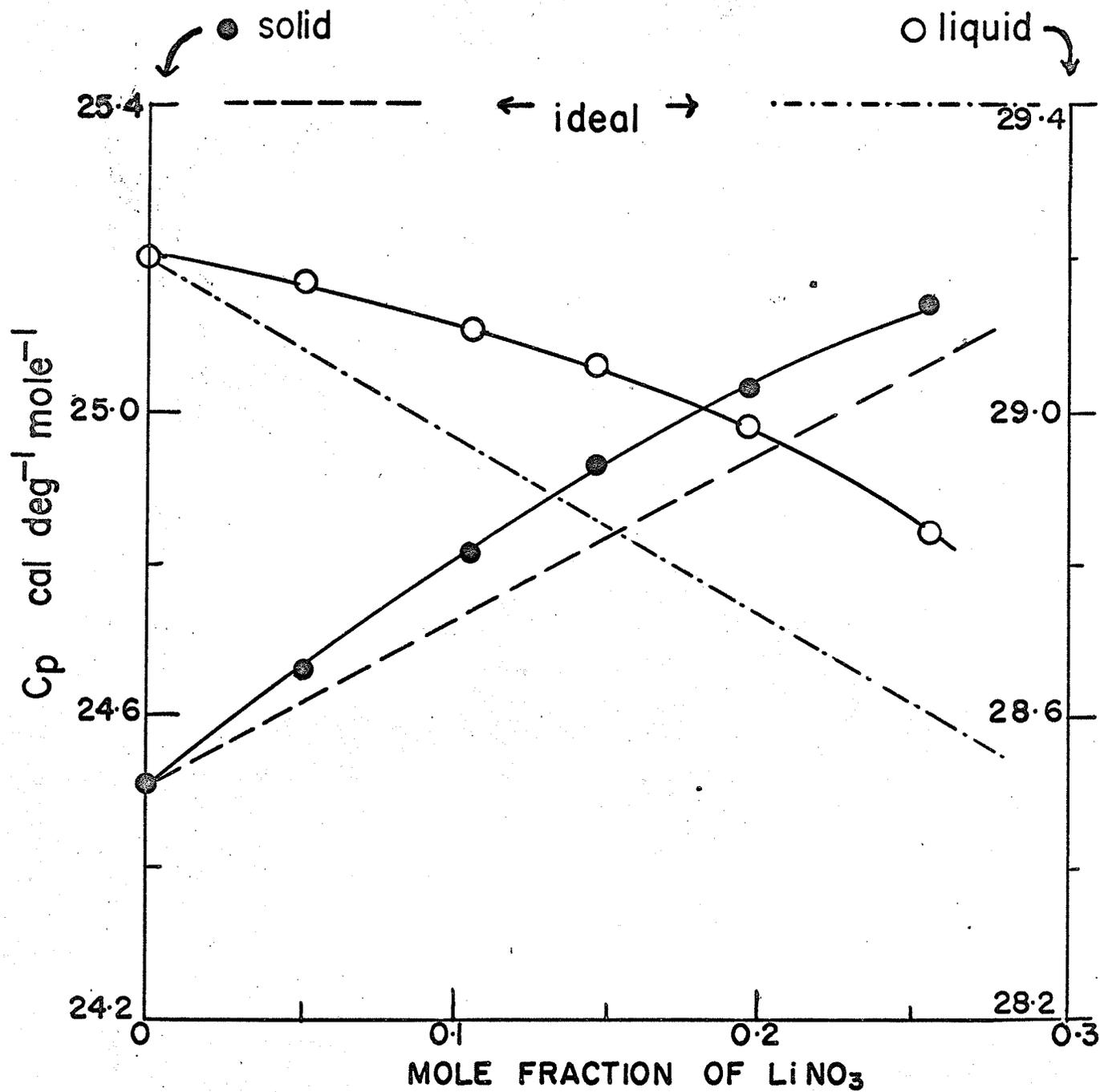
the heat of mixing is positive. Kleppa and Meschel[51] find it useful to plot $\Delta H^M/n_2$ against n_2, the mole fraction of lithium nitrate. They found that their thermal data on a number of systems satisfied the relation:

$$\Delta H^M/n_2 = \Delta H_f(t) + a(1 - n_2)$$

where the ''interaction parameter'', a, is a constant. The limiting value of $\Delta H^M/n_2$ at $n_2 = 0$, according to Kleppa and Meschel, represents the partial molal enthalpy associated with the transfer of one mole of the second component from the pure crystalline state into 'pure' liquid state of the first component at the temperature of the mixture. They consider this value to be formally composed of two terms: (a) the enthalpy change, $\Delta H_f(t)$, associated with the fusion of the second component at the temperature of the mixture, t; (b) the enthalpy change associated with the solution of this supercooled liquid in the pure first component.

The value of $\Delta H^M/n_2 = \Delta H_f(t) + a$, at $n_2 = 0$, therefore, must represent the above two quantities. The factor 'a' thus represents the effect of any possible interaction between the first and second components.

The values of $\Delta H^M/n_2$, listed in Table XXVII, are plotted against n_2 in Fig. 33. The data were found (by a least squares technique) to satisfy the linear relation:

$$\Delta H^M/n_2 = (4.060 + 1.93\, n_2) \text{ k cal}$$

FIG·33 PLOT OF $\Delta H^M/n_2$ vs n_2

MOLE FRACTION OF $LiNO_3$
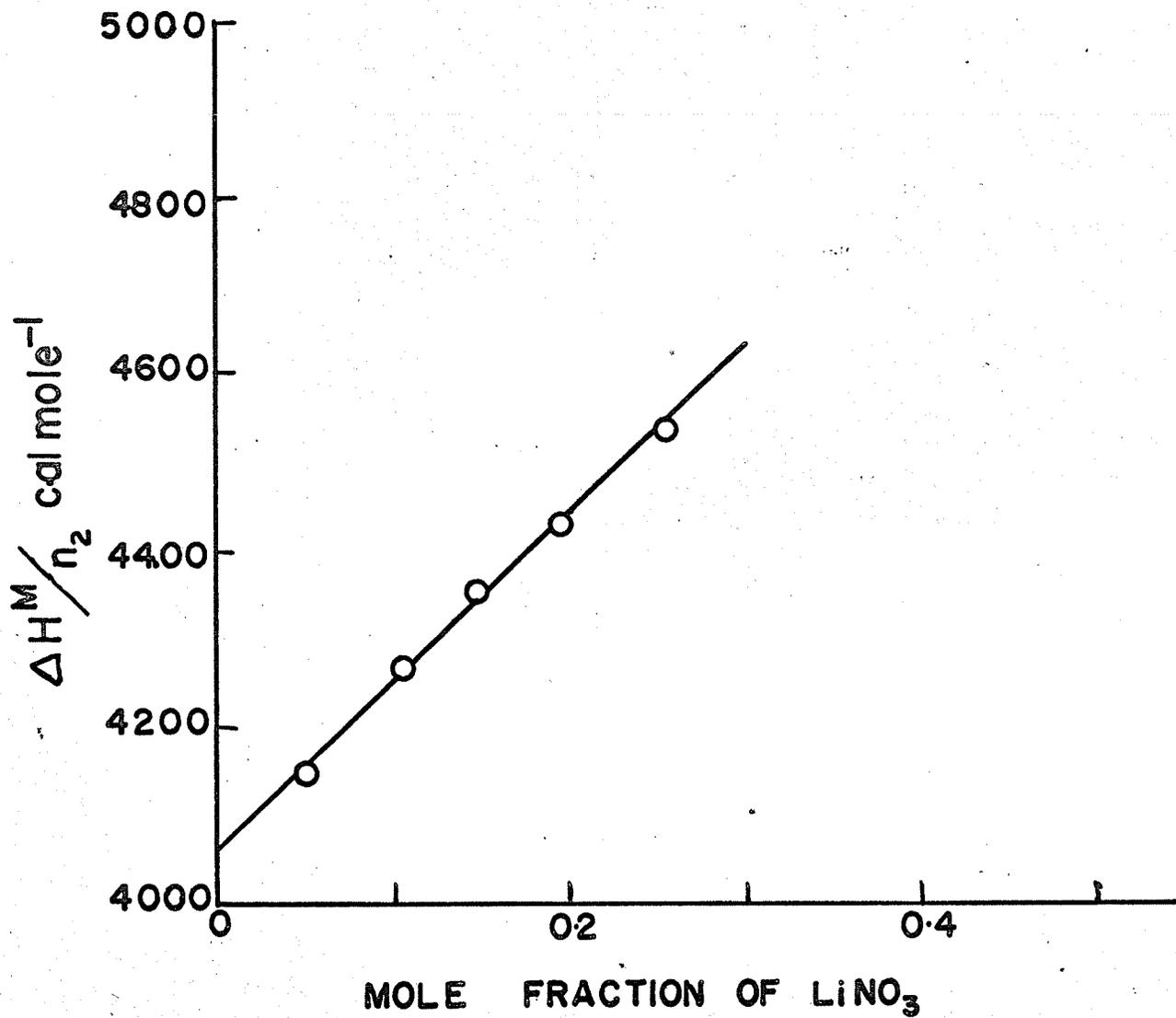
Therefore,

$$\triangle H_f(t) + a = 4.060 \text{ k cal}$$

$$a = -1.93 \text{ k cal}$$

and $\triangle H_f(t) = 5.990 \text{ k cal}$

The value of $\triangle H_f(t)$ is given by the expression:

$$\triangle H_f(t) = \triangle H_f(\text{m.p.}) + \int_{401.0}^{T_p} \triangle C_p \, dT$$

where $\triangle H_f(\text{m.p.})$ is the heat of fusion of pure lithium nitrate at its melting point T_p; $C_p = C_p(\text{solid}) - C_p(\text{liquid})$, for lithium nitrate. Using the value of 6060 cal mole^{-1} for $\triangle H_f$ (m.p.), the value of $\triangle C_p$ (assumed to be constant in the temperature region 401.0 to T_p) is -0.55 cal deg^{-1} mole^{-1}. The value of $\triangle C_p$ calculated from the data in the literature[101] is -0.22 cal deg^{-1} mole^{-1}.

The interaction parameter, a, in the present case is negative and large. Kleppa and Meschel[51] found that the value of 'a' is a small positive number ($\sim$ +0.2 to +0.4) in the alkali nitrate-chloride systems studied by them, but has considerable negative values for the systems $AgNO_3$ - Ag Cl and $AgNO_3$ - AgBr (-1.13 k cal and -2.17 k cal respectively). They explain the small positive values of 'a' as due to the anion-anion (i.e. second nearest neighbour) core repulsion in addition to the coulombic and van der waals forces. They conclude, however, that the large negative values obtained in

silver salt systems cannot be explained on the basis of their second nearest neighbour interaction concept. They suggest that "the large interaction parameters for silver salts must be considered as evidence for a certain degree of chemical interaction in the mixture". The large negative interaction parameter (a = -1.93 k cal) for lithium chlorate-lithium nitrate system probably reflects some kind of interaction between the nitrate ion and the chlorate lattice. Since 'a' is a measure of the enthalpy change associated with the solution of undercooled lithium nitrate in molten lithium chlorate at $401.0^{\circ}K$ (see page 108), a negative value of 'a' indicates a negative enthalpy change for the possible interaction of nitrate ion with the chlorate lattice.

Although the free energy of mixing given in Table XXIX is only approximate and subject to a number of assumptions, it gives additional support to the arguments presented above. The fact that the interaction between nitrate ion and chlorate lattice is possible is indicated by the negative free energy of mixing. The data presented in Table XXX and the Fig. 30, shows that in spite of a very large positive enthalpy of mixing ($\triangle H^M$), the mixing process is spontaneous ($\triangle F^M$-ve) since $T\triangle S^M$ is also large. The fact that the entropy of mixing plays such an important role in this system is indicative of pronounced structural effects. The large positive deviation of $\triangle S^M$ from ideality (cf. Fig. 31) suggest that

more stable, low energy configurations, of some kind, result
on the addition of nitrate ion to chlorate lattice. It is,
therefore, suggested that the extra contribution to the
ideal entropy of mixing is due to some kind of interaction
between the nitrate ion and chlorate lattice and the resultant
low energy particular configurations.

Chapter VI

GENERAL DISCUSSION

Nature of molten lithium chlorate: It is generally agreed that
molten salt systems with varying degrees of ionic and covalent
characters are possible.   Ubbelohde and coworkers[42] have
demonstrated a possible relationship between low melting point
and strong covalent character in the melt of a salt.   Almost
all the low melting inorganic salts possess an unsymmetrical,
complex anion.   No x-ray crystallographic data on lithium
chlorate are available in the literature.   In the absence of
such data, it is reasonable to assume that chlorate ion will
resemble nitrate ion and hence is, probably, non-spherical.
The data obtained by me, particularly the viscosity and ΔS_f,
suggest a very strong covalent character in lithium chlorate
melts.   In addition, the data obtained by Mr. D. F. Williams
on molten lithium chlorate also support the above view.   The
equivalent conductance has been found by him to lie between
those of predominantly ionic and strongly covalent melts.
The value 4.965 mho at 131.4°C is closer to those of strongly
covalent melts.

The surface heat content of molten lithium chlorate
(118 ergs cm^{-2}), based on surface tension measurements of
Mr. D. F. Williams, also suggests a strong covalent character

in lithium chlorate melts, since the value of $H_{surface}$ for lithium chlorate is closer to those of strongly covalent melts than predominantly ionic melts. The value of E_Λ/E_{vis}, (1.27) suggests a much larger configurational change associated with viscous flow than with ionic migration. Since the lithium ion is much smaller than the chlorate ion, it is reasonable to assume that the lithium ion is chiefly responsible for electrical migration. Mr. D. F. Williams has found that the volume of hole, activation energy for electrical conductance and degree of ionization do not alter much with temperature. The abnormally high viscosity of lithium chlorate melt bears a certain resemblance to those of molten silicates and oxides. In addition, E_{vis} diminishes noticeably with temperature. These two factors suggest the existence of some kind of 'network' of neutral lithium chlorate molecules. In the light of the forgoing observations it is suggested that molten lithium chlorate consists of 'clusters' or groupings, molecules and some ions. Increase of temperature, probably causes the breaking down of some of the 'clusters', and, in all probability, does not alter the concentration of free ions.

From his x-ray radial distribution curves of molten alkali nitrate, Furukawa[37] suggested the possible existence of certain preferred groupings of nitrate and alkali metal ions. Studies[111] on molten zinc chloride showed an abnormally high viscosity and this has been interpreted as possible evidence

for the presence of a 'network' structure in the melt. In molten lithium chlorate, these preferred groupings may be very considerable. It is probable that molten lithium chlorate exhibits very similar characteristics compared to molten alkali nitrates, but these are magnified many times, by its very low melting point (approx. 170° below the melting point of $NaNO_3$). In the absence of a reliable standard state for the comparison of properties of various salts, it is not possible to make generalizations regarding the nature of molten salts.

Nature of molten lithium chlorate-lithium nitrate melts:
In addition to the results obtained by me, the following data obtained by Mr. D. F. Williams are also relevant: (a) the equivalent conductance of molten mixtures of lithium chlorate and nitrate increases only very slightly with increasing concentration of lithium nitrate; (b) E_Λ remains practically constant over the range of concentration (of lithium nitrate) studied; (c) the surface heat content, the degree of ionization and volume of hole do not alter appreciably with composition. The above three statements indicate that the increase in the concentration of ions in molten mixtures is only small. The small decrease in the values of α, with increasing concentration of lithium nitrate (cf. Table VIII), probably reflects this slight increase in ionization. The volume, viscosity and

thermal data obtained by me indicate that the melt remains very largely covalent even at 0.3 mole fraction of lithium nitrate. In particular, the viscosity and thermal data suggest a possible interaction between nitrate ion and the strongly covalent chlorate lattice. The large structural contributions to molar volume and viscosity, the sharp increase in the value of ΔS_f with increasing concentration of lithium nitrate, the large negative interaction parameter 'a', and the considerable positive deviation of entropy of mixing support the possibility of such an interaction.

The work of Kleppa and Meschel[51], as already pointed out indicate the possibility of some kind of interaction between a dissimilar anion neighbour and a predominantly covalent silver halide lattice. Byrne, Fleming and Wetmore[112] found a very large increase in molar volume and other abnormal properties in the $AgNO_3$-$NaNO_3$ system. It is therefore very probable that molten silver salt systems also exhibit pronounced interactions.

Molten lithium chlorate-lithium nitrate mixtures can be considered to be composed of 'clusters' of lithium chlorate, more complex 'clusters' or combination of 'clusters' (low energy particular configurations, with possible bridging by means of nitrate ion), lithium chlorate molecules and lithium and chlorate ions. In addition, some free molecules of lithium nitrate and nitrate ions presumably exist, but no evidence either for or against this supposition has been obtained

in this work. Temperature has a marked effect on molten lithium chlorate-lithium nitrate mixtures. This probably means that the complex 'clusters' tend to break up more readily than the simple 'clusters'.

The structural changes resulting from the interaction in the melt are probably related to the changes in viscosity and molar volume of molten lithium chlorate-lithium nitrate melts. The 'structural contributions' of viscosity and molar volume (η_s and V_s), to the total change in viscosity and molar volume of the reference state lattice (viz., pure lithium chlorate melt at $401.0^{\circ}K$), are plotted as functions of ΔS_f and ΔS^M in Figs. 34 and 35 respectively. The values of η_s, V_s, ΔS_f and ΔS^M refer, in each case, to a particular composition and were obtained by interpolations. η_s and V_s vary linearly with ΔS_f and ΔS^M, according to the following equations:

$$\eta_s = 1.96 - 0.64 \, \Delta S^M$$

$$\eta_s = -4.54 - 0.41 \, \Delta S_f$$

$$V_s = -0.416 - 0.196 \, \Delta S^M$$

$$V_s = 3.42 - 1.25 \, \Delta S_f$$

The linear dependance of η_s and V_s on ΔS_f and ΔS^M indicate that η_s and V_s do reflect the change in order of the melt with varying composition. Thus the arbitrary choice of

FIG·34 PLOTS OF V_s & η_s AGAINST ΔS_f

FIG·35 PLOTS OF Vs & ηs AGAINST $\triangle$S^M

$\triangle$S^M e·u·
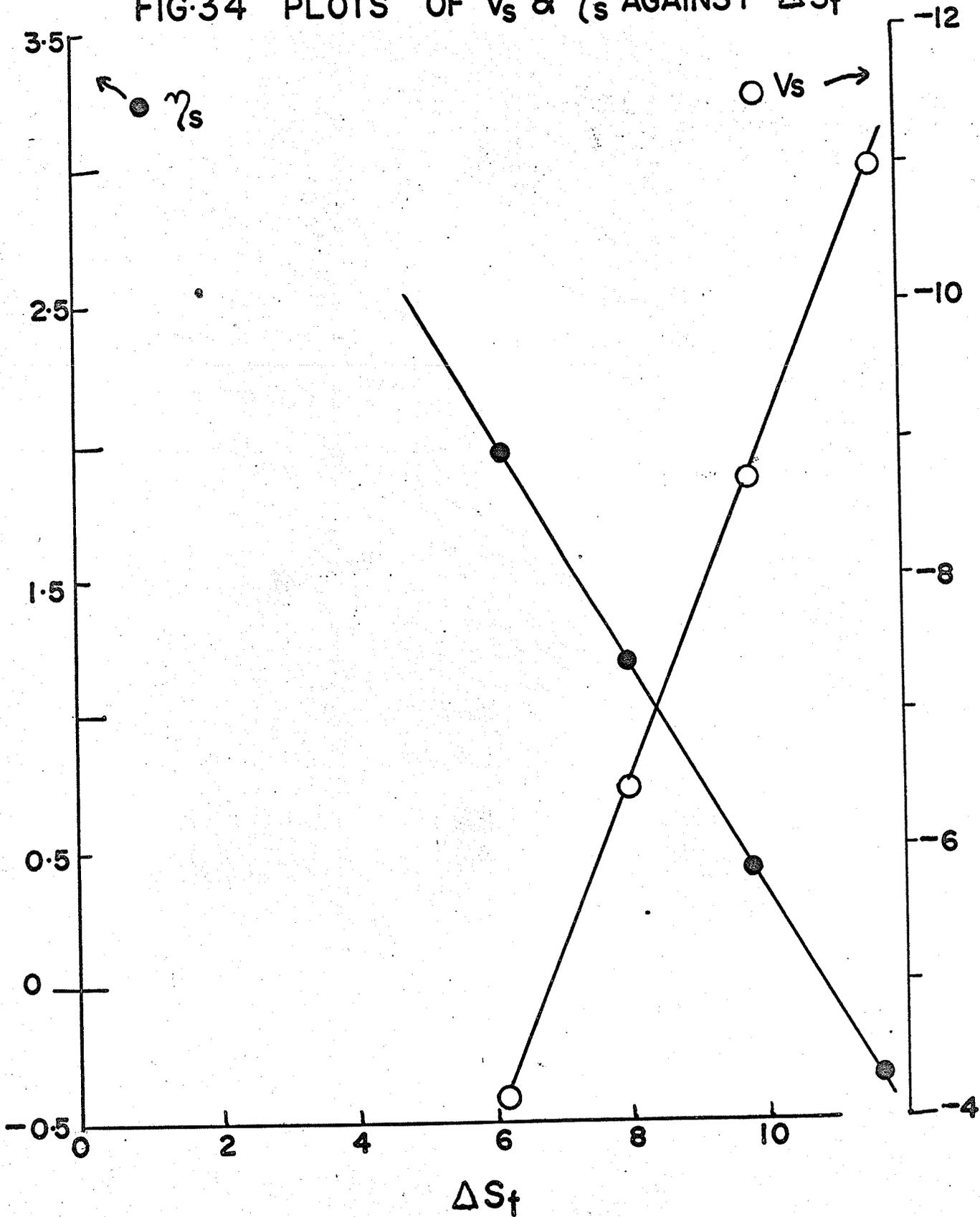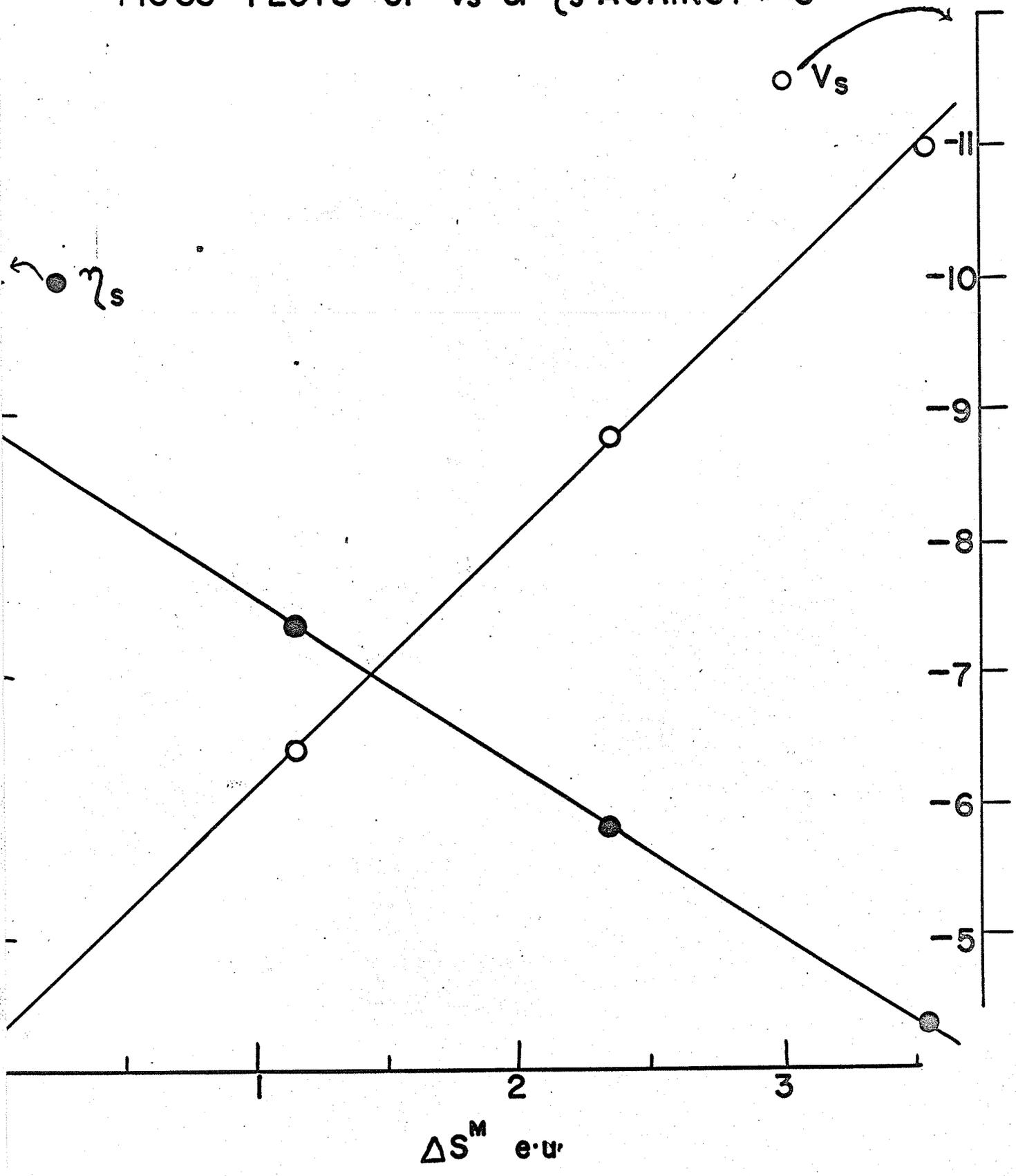
reference state (page 57) is at least partially justified.
But the above equations, beyond stating the fact that structural
contributions of viscosity and molar volume are directly
related to the changes in order on melting and on mixing, give
no further information on the mechanism of the structural
changes.

SUMMARY AND CONCLUSIONS

Densities of molten mixtures of lithium chlorate were determined by a dilatometric method, in the concentration range 0-30 weight percent lithium nitrate and over the temperature range 130° - 170°C. The molar volume showed a positive deviation from ideality. The coefficient of thermal expansion decreased slightly with increasing concentration of lithium nitrate. The data indicated strong covalent character in the lithium chlorate melt, diminishing only slighty with increasing concentration of lithium nitrate.

Viscosities of molten mixtures of lithiumchlorate and lithium nitrate were determined by a flow method in the concentration and temperature ranges quoted above. Viscosity isotherms showed considerable positive deviation from ideality. The activation energy for viscous flow was practically independent of composition and temperature. An interpretation of the data suggested the possible existence of 'clusters' or preferred groupings of molecules, in addition to free molecules and ions, in the lithium chlorate melt. Some kind of interaction between the nitrate ion and the chlorate lattice was also indicated.

Heats of fusion and molar heat capacities (both in solid and liquid state) were determined calorimetrically, using the method of mixtures. The entropy of fusion, of mixtures of lithium chlorate and lithium nitrate, increased with

increasing concentration of lithium nitrate, far more sharply than a simple additive relationship predicts. The molar heat capacity of mixtures also exhibited a similar increase.

A discussion of these data provided some additional evidence for some kind of interaction between the nitrate ion and the chlorate lattice. Heats of mixing at $401.0^\circ K$ were calculated from the thermal data and were found to be positive. A detailed interpretation of heats of mixing also indicated possible interaction between nitrate ion and chlorate lattice resulting in the formation of more complex 'clusters' with possible 'bridging' by the nitrate ion between two or more clusters. Free energies of mixing were calculated using the thermal data and the phase diagram of the system lithium chlorate-lithium nitrate and were found to be negative. Entropies of mixing, calculated from the free energies and heats of mixing data, were found to be positive. The observed entropy of mixing was more than that calculated for an ideal system.

On the basis of these results a probable model for molten chlorate has been put forward, viz., the melt consists of 'clusters' of molecules (i.e. low energy particular configuration), molecules and ions. The addition of lithium nitrate gives rise to some kind of interaction between the nitrate ion and the chlorate lattice, resulting in the formation of more complex 'clusters', possibly by 'bridging' of 'clusters' by

nitrate ions. These complex 'clusters' are more temperature

sensitive than the simple 'clusters'.

BIBLIOGRAPHY

1. a) Lorenz R., Die Electrolyse geschmolzener Salze, Halle (1905).

   b) Lorenz R. and Kaufler F., Handbuch der angew. Physik.

   chem., Leipzig, 11, 1 (1909).

2. Goodkin H. M. and Mailey R. D., Phys. Rev. 25, 469 (1907),

   26, 28 (1908).

3. Drossbach P., Electrochemic geschmolzener Salze, Berlin (1938).

4. Antipin L. N., Alabyshev, and Barzakovski, Electrochemistry

   of fused salts, U.S.S.R. (1937).

5. Ellis R. H., Chem. Eng. News, Oct. 10 (1960).

6. a) Warburg, Ann. Phys. Chim. 21, 622 (1884).

   b) Ostroumov, J. Gen. chem. U.S.S.R. 19, 363 (1949).

   c) Bockris J. O'M., Kitchener J. A., Ignatowicz S. and

   Tomlinson J., Trans. Farad. Soc. 48, 75 (1952).

7. Lark-Horowitz K. and Miller E. P., Phys. Rev. 49, 418 (1936).

   51, 61 (1937).

8. Johnson J. W., Agron P. A. and Bredig M.A., J. Am. Chem.

   Soc. 77, 2734 (1955).

9. Harris R. L., Wood R. E. and Ritter H. L., J. Am. Chem.

   Soc. 73, 3151 (1951).

10. Danilov V. I. and Krasnitskii, Doklady, Akad. Nauk SSR,

    101, 661 (1955).

11. Levy H. A., Agron P. A., Bredig M. A. and Dansford, Ann.

    N.Y. Acad. Sci., 79, 762 (1960).

12. Lennard-Jones J. E. and Devonshire A. F., Proc. Roy. Soc.

    A 163, 53 (1937); A 165, 1 (1938).

13. Hill T. L., Statistical Mechanics (McGraw-Hill Book Co. Inc., New York, 1956), Chap. 8.

14. Lennard-Jones J. E. and Devonshire A. F., Proc. Roy. Soc. A 169, 317 (1938).

15. Stillinger F. H., Kirkwood J. G. and Wojtowicz P. J., J. Chem. Phys. 32, 1837 (1960).

16. Debye P. and Huckel E., Phys. z. 24, 185, 305 (1923).

17. McQuarrie D. A., J. Phys. Chem. 66, 1508 (1962).

18. Dahler J. S., Hirschfelder J. O. and Thachet H. G., J. Chem. Phys. 25, 249 (1956).

19. Eyring H., J. Chem. Phys. 4, 283 (1936).

20. Frenkel J., Acta Physico chim 3, 633, 913 (1935).

21. Alter W., J. Chem. Phys. 5, 577 (1937).

22. Furth R., Proc. Camb. Phil. Soc. 37, 352 (1941).

23. Bockris J. O'M. and Richards N. E., Proc. Roy. Soc. A 241, 44 (1957).

24. Bockris J. O'M., Ed. Modern aspects of electrochemistry, No. 2, Butterworths Sci. Publications, London (1959), page 200.

25. Borucka A. Z., Bockris J. O'M. and Kitchener J. A., J. Chem. Phys. 24, 1282 (1956).

26. a) Cernuschi F. and Eyring H., J. Chem. Phys. 7, 547 (1939).
    b) Rowlinson J. S. and Curtiss C. F., J. Chem. Phys. 19 1519 (1951).
    c) Peek H. M. and Hill T. L., J. Chem. Phys. 18, 1252 (1950).

27. a) Mayer J. E. and Careri G., J. Chem. Phys. 20, 1001 (1952).

    b) Levine H. B., Mayer J. E. and Aroeste H., J. Chem. Phys. 26, 201, 207 (1957).

28. Blomgren G. E., J. Chem. Phys. 34, 1307 (1961).

29. Zaraycki J., J. Physique Rad. 19, 13A (1958).

30. Eyring H., Ree T. and Hirai N., Proc. National Acad. Sci. 44, 683 (1958).

31. Carlson C. M., Eyring H. and Ree T., ibid. 46, 333 (1960).

32. Ree T. S., Ree T and Eyring H., ibid. 48, 501 (1962).

33. Carlson C. M., Eyring H. and Ree T. ibid. 46, 649 (1960).

34. Thomson T. R., Eyring H. and Ree T., ibid. 46 336 (1960).

35. Kirkwood J. G., J. Chem. Phys. 3, 300 (1935); 7, 919 (1939); 14, 80 (1946).

36. a) Bernal J. D., Nature 183, 141 (1959); 185, 68 (1960).

    b) Bernal J. D. and Mason, Nature 188, 910 (1960).

37. Furukawa K., Disc. Farad. Soc. No. 32, 53 (1962).

38. Levy H. A., Ann. N.Y. Acad. Sci. 47, 1881 (1961).

39. Temken M., Acta Physiochim U.R.S.S. 20, 411 (1945).

40. Richards N.E., Brauner E. J. and Bockris J. O'M., British J. Applied Phys. 6, 387 (1955).

41. Bockris J. O'M. and Richards N.E., Proc. Roy. Soc. A 241, 44 (1957).

42. Ubbelohde A. R. ''Melting Mechanisms of Ionic Crystals'', in ''The Structure of Electrolytic Solutions'', John Wiley and Sons, N.Y. (1959).

    also   Proc. Chem. Soc., 332 (1960).

43. Flood H., Disc. Farad. Soc. 32, 168 (1961).

44. Papousek D. and Kucirek J., J. Phys. Chem. (U.S.S.R.) 34
168 (1960).

45. Fischmeister H. F., Acta Cryst. 9, 416 (1956).

46. a) Laity, R. W., J. Am. Chem. Soc. 79, 1849 (1957).

b) Braunstein J. and Blander M.,J. Phys. Chem. 64, 10
(1960) and subsequent papers.

47. Aukrust E., Bjorge B., Flood H. and Forland T., Ann. N.Y.
Acad. Sci. 79, 831 (1960).

48. Murgulescu I. G. and Sternberg S., Z. Physik Chemie 219,
114 (1962).

49. Kleppa Ø. J. and Hersh L. S., J. Chem. Phys. 34, 351 (1961).

50. Forland T., ''On the properties of some mixtures of fused
salts'' (N.T.H. Trykk, Trondheim, Norway, 1958).

51. Kleppa O. J. and Meschel S. V., J. Phys. Chem. 67, 668 (1963).

52. Blander M., J. Chem. Phys. 36, 1092 (1962).

53. Toguri J., Flood H. and Forland T., unpublished, quoted in
ref. 43.

54. Hildebrand J. H. and Salstrom E. J., J. Am. Chem. Soc. 54
4257 (1933).

55. Fowler R. and Guggenheim E. A., ''Statistical Thermodynamics'',
Camb. Univ. Press, New York, N.Y. (1939) Ch. VIII.

56. Panish M. B., Blankenship F. F., Grimes W. R., and
Newton R. F., J. Phys. Chem. 62, 1325 (1958);
63, 668 (1959).

57. Flood H., Forland T. and Grjotheim K., Z. Anorg. Allgem.
chem. 276, 289 (1954).

58. Bloom H. and Welch quoted in ref. 24.

59. Blander M., J. Phys. Chem. $\underline{63}$, 1262 (1959).

60. Blander M. and Braunstein J., Ann. N.Y. Acad. Sci. $\underline{79}$, 838 (1960).

61. Frame J. P., Rhodes E. and Ubbelohde A. R., Trans. Farad. Soc. $\underline{55}$, 2039 (1959).

62. Janz G. J. and McIntyre J. D. E., Ann. N. Y. Acad. Sci. $\underline{79}$, 790 (1960).

63. Plester D. W., Rogers S. E. and Ubbelohde A. R., Proc. Roy. Soc. $\underline{A\ 235}$, 469 (1956).

64. Ubbelohde A. R., Proc. Chem. Soc. (Lond.), 332 (1960).

65. Campbell A. N. and Griffiths J. E., Can. J. Chem. $\underline{34}$, 1647 (1956).

66. Scatchard G., Prentiss S. S. and Jones P. T., J. Am. Chem. Soc. $\underline{56}$, 805 (1934).

67. Campbell A. N., Kartzmark E. M. and Williams D. R., Can. J. Chem. $\underline{40}$, 890 (1962).

68. Campbell A. N.,Kartzmark E. M. and Nagarajan M. K., Can. J. Chem. $\underline{40}$, 1258 (1962).

69. Kraus C. A. and Burgess W. M., J. Am. Chem. Soc. $\underline{49}$, 1226 (1927).

70. Williams D. R., Ph.D. Thesis, The University of Manitoba, Winnipeg (1963).

71. Klotschko M. A. and Grigorjew I. C., English translation of paper in Akad. Wiss (U.S.S.R.) Nacht. Abt. Physik-Chem. Analyse 21, 288 (1950).

72. Janz G. J. and Lorenz M. R., Rev. Sci. Instr. $\underline{31}$, 18 (1960).

73. Boardman N. K., Dorman F. H. and Heymann E., J. Phys. Colloid Chem. $\underline{53}$, 375 (1949).

74. Potilitzin A., J. Russ. Phys.-Chem. Soc. $\underline{16}$, 840 (1883).

75. Selected from Smithsonian Tables, Handbook of Chemistry and Physics, Chemical Rubber Publishing Co., 43rd Edn. 2157 (1961-62).

76. Rhodes E. and Ubbelohde A. R. Trans. Farad. Soc. $\underline{55}$, 1075 (1959).

77. Batchinski A. J., Z. Physik. Chem. $\underline{84}$, 643 (1913).

78. Higgs R. W. and Litovitz T. A., J. Acoust. Soc. Am. $\underline{32}$, 1108 (1960).

79. Marchessault J. G. and Litovitz T. A., J. Acoust. Soc. Am. $\underline{34}$, 616 (1962).

80. deGuzman, Anal. Fis. Quim. $\underline{9}$, 353 (1913).

81. Andrade E. N. da C., Phil. Mag. (7), $\underline{17}$, 698 (1934).

82. Frenkel J., The kinetic theory of liquids, Oxford Univ. Press (1946).

83. Brush S. G., Chem. Rev. $\underline{63}$, 513 (1962).

84. Glasstone S., Laidler K. J. and Eyring H., The Theory of Rate Processes, McGraw-Hill Pub. Co. (1941).

85. Ewell R. H., J. Appl. Physics $\underline{9}$, 252 (1938).

86. Harrap B. S. and Heymann E., Chem. Rev. $\underline{48}$, 45 (1951).

87. Bloom H. and Heymann E., Proc. Roy. Soc. $\underline{188\ A}$, 392 (1947).

88. Harrap B. S. and Heymann E., Trans. Farad. Soc. $\underline{51}$, 259 (1955).

89. Dantuma R. S., Z. anorg. chem. <u>175</u>, 1 (1928).

90. Frame J. P. Rhodes E. and Ubbelohde A. R., Trans. Farad. Soc. <u>55</u> 2039 (1959).

91. Andrade E. N. da C., ''Viscosity and Plasticity'', Chemical Publishing Co., New York, N.Y. (1951).

92. Andrade E. N. da C., Nature <u>170</u>, 794 (1952).

93. Campbell A. N., Debus G. H. and Kartzmark E. M., Can. J. Chem. <u>33</u>, 1508 (1955).

94. International Critical Tables Vol. V, 10, (1929).

95. Handbook of Chemistry and Physics, Chemical Rubber Publishing Co., 43rd Edn. 2156 (1961-62).

96. Yaffe I. and Van Artsdalen E. R., J. Phys. Chem. <u>60</u>, 1125 (1956).

97. Harrap B. S. and Heymann E., Trans. Farad. Soc. <u>51</u>, 259 (1955).

98. Janz G. J. and Goodkin J., J. Phys. Chem. <u>63</u>, 1975 (1959).

99. Kleppa O. J. and Meschel S. V., J. Phys. Chem. <u>67</u>, 668 (1963).

100. Kraus C. A. and Burgess W. M., J. Am. Chem. Soc. <u>49</u>, 1226 (1927).

101. Kelley K. K., U. S. Dept. Commerce. Bur. Mines Bull. 371 (1934).

102. White W. P., The Modern Calorimeter, Am. Chem. Soc. Monograph Series N O 42 (1928).

103. Goodkin J., Solomons C. and Janz G. J., Rev. Sic. Instr. <u>29</u>, 105 (1958).

104. Kleppa O. J., J. Phys. Chem. <u>64</u>, 1937 (1960).

104a. Gilbert R. A., J. Phys. Chem. <u>67</u>, 1143 (1963).

105. Campbell A. N., Kartzmark E. M. and Friesen H., Can. J. Chem. $\underline{39}$, 735 (1961).

106. Lutz B. C. and Wood J. H., Can. J. Research $\underline{A\ 26}$, 145 (1948).

107. Campbell A. N. and Kartzmark E. M., Can. J. Chem. $\underline{34}$, 1428 (1956).

108. Ref. 75, p. 2085.

109. Pyrex Catalogue, 4 (1960).

110. Solomons C., Goodkin J., Gardner H. J. and Janz G. J., J. Phys. Chem. $\underline{62}$, 248 (1958).

111. MacKenzie J. D. and Murphy W. K., J. Chem. Phys. $\underline{33}$, 366 (1960).

112. Byrne J., Fleming H. and Wetmore F. E. W., Can. J. Chem. $\underline{30}$, 922 (1952).

TABLE Al

Substance	T_f (°K)	V_f/V_s (%)	$\alpha \times 10^4$	E_η (Kcal)	E_η/E_λ	ΔH_f (Kcal)	ΔS_f (Kcal)	Class of Liquid
Ar	83.6	14.4	---	---	---	0.280	3.35	Molecular
H$_2$	14	12.2	---	---	---	0.028	2.0	(inert)
Na	371	2.5	---	---	---	0.63	1.70	Metallic
Hg	234	3.6	---	---	---	0.58	2.48	
Salts								
NaCl	1073	25	5.01	9.4	6.1	7.22	6.7	Predominantly
KBr	1003	22	5.58	7.96	3.1	5.93	5.9	ionic
LiNO$_3$	528	---	3.76	4.23	0.94	6.06	10.86	Predominantly
NaNO$_3$	581	11	4.23	3.95	1.4	3.86	6.6	covalent
KNO$_3$	607	---	4.28	3.66	1.05	2.84	4.7	
AgNO$_3$	483	0.7	---	3.08	0.70	2.76	5.7	
NaClO$_3$	533	---	---	4.23	0.94	5.4	10.1	
KClO$_3$	629	---	---	4.04	---	---	---	
MgCl$_2$	987	---	2.46	--	---	10.3	10.4	Strongly
ZnCl$_2$	548	---	---	--	---	5.5	10.0	Associated